# Avian Sleep: Examining Age-Related Variations and Local Sleep in Zebra Finches

**Hamed Yeganegi**

Graduate School of Systemic Neurosciences

LMU Munich

**Dissertation for the Graduate School of Systemic Neurosciences**
**Ludwig-Maximilians-Universität München**
2 October 2024

First supervisor:

Dr. Janie Michelle Ondracek

Chair of Zoology. Technical University of Munich. Liesel-Beckmann-Straße 4. 85354 Freising-Weihenstephan.

Second supervisor:

Prof. Dr. Harald Luksch

Chair of Zoology. Technical University of Munich. Liesel-Beckmann-Straße 4. 85354 Freising-Weihenstephan.

| | |
|---|---|
| First Reviewer: | Dr. Janie Michelle Ondracek<br>Technical University of Munich |
| Second Reviewer: | Dr. Daniela Vallentin<br>Max Planck Institute for Biological Intelligence |
| External Reviewer: | Dr. Nicolas Giret<br>Université Paris-Saclay |

Date of Submission: 2 October 2024

Date of defense: 6 March 2025

# Table of contents

**Chapter 1: General Introduction**

Sleep architecture and brain oscillations of sleep ..... 4

Common NREM characteristics in mammals ..... 6

Slow Oscillations ..... 7

Delta oscillations ..... 8

Contribution of subcortical structures to slow waves ..... 8

Common REM characteristics in mammals ..... 9

Theta rhythm ..... 9

Ponto-geniculo-occipital waves ..... 10

Gamma oscillations ..... 10

Sleep oscillations and brain metabolism ..... 11

An overview of the regulation of sleep in the avian brain ..... 12

A primer to the avian brain ..... 12

Neural signature of sleep in avian species ..... 13

Sleep ontogeny ..... 16

Brain lateralization ..... 17

Focus of the thesis ..... 19

**Chapter 2: Multi-channel recordings reveal age-related differences in the sleep of juvenile and adult zebra finches**

Abstract ..... 21

Introduction ..... 22

Results ..... 23

Discussion ..... 38

Methods ..... 43

References ..... 51

Supplementary data one: ANOVA tables ..... 59

Supplementary data two: supplementary figures ..... 65

**Chapter 3: Local sleep in songbirds: Different simultaneous sleep states across the avian pallium**

Summary ..... 75
Introduction ..... 75
Methods ..... 78
Results ..... 84
Discussion ..... 94
References ..... 97
Supplementary data ..... 104

**Chapter 4: General Discussion**

Local aspects of sleep: interpretations and outlooks ..... 113
Development of neural lateralization ..... 116
IS sleep and development ..... 118
Linking together sleep oscillations, memory function of sleep, and local aspects of sleep ..... 119
Speculations on the origin of two-stage sleep ..... 121

**References** 124

**Acknowledgment** 134

**List of publications** 135

**Author Contributions** 135

**Affidavit** 136

**CV** 137

# Chapter 1

# General Introduction

In this Ph.D. thesis, we report on multi-channel recordings in the brain of an avian species, the zebra finch (*Taeniopygia guttata*), during sleep. Using these recordings, we studied age-related changes in sleep structure (manuscript one), and local differences in the neural activity across the brain (manuscript two). Before we report on these findings, we review some main aspects of the neural control of sleep in this chapter.

## Sleep architecture and brain oscillations of sleep

Sleep is considered to be a homogenous state of rest. However, as early electroencephalography (EEG) recordings in humans revealed, sleep consists of two primary stages: rapid eye movement (REM) sleep, characterized by rapid jerky eye motility, and non-rapid eye movement (NREM) (1) (see Fig. 1A). During each stage of sleep, brain activity measured by EEG differs markedly too. During REM sleep in humans, theta (4-8 Hz) and gamma rhythms (~30-90 Hz) dominate scalp EEG; during NREM sleep, oscillations below 4 Hz prevail (2, 3) (see Fig. 1B). In humans, NREM sleep can be further divided into three stages, based on the appearance of specific EEG waves. As such, awake states, REM sleep, and different stages of NREM sleep are all viewed as discrete 'states' of the brain. However, recent discoveries challenge the notion of treating sleep stages as discrete and unitary events.

The neural oscillations which delineate the distinct stages of sleep are non-uniform across the cortex. That is, region-specific variations have been observed across cortical sites, uncovered by the recent multichannel EEG recordings and other whole-brain imaging techniques (4-6). For example, low-frequency oscillations typical of NREM sleep are also observed during wake or REM sleep (4, 6).

The duration and proportion of sleep stages also change with age (7, 8). For example, during the first years of life, delta activity during NREM sleep increases to a maximum

before puberty. Afterward, it gradually decreases during adolescence into adulthood (8, 9). These changes in sleep oscillations might reflect structural changes within the brain. For instance, the above-mentioned decrease in delta oscillations is paralleled by massive synaptic remodeling (10) and a decline in gray matter during adolescence (9).

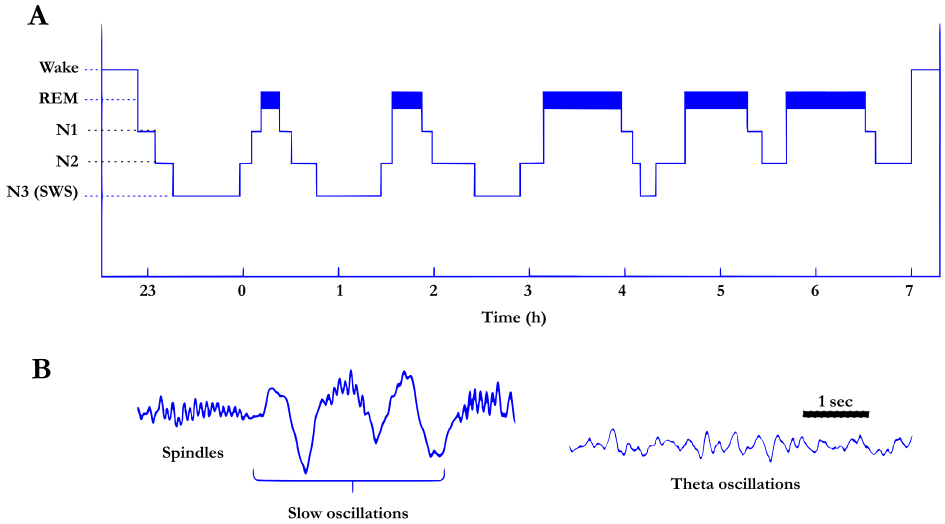


**Figure 1 Sleep stages and examples of EEG waves during sleep.** (**A**) Sleep in humans consists of NREM and REM phases. NREM is further divided in to three stages, N1-N3. Similarly, in all mammals and birds sleep time could be broken down into two principal phases, i.e., NREM and REM sleep. (**B**) Sleep in mammals and birds is characterized by specific EEG oscillations. Slow oscillations are among the waves observed during SWS. Theta waves appear during REM sleep. Spindles are observed only in mammals. Modified, with permission, based on (11).

Surprisingly, two phases of sleep is not unique to humans and is observed across the vertebrate taxa, despite the marked differences in the brain structures. In fact, some form of two stage of sleep with distinct neural oscillations has been observed in other mammals (12-14), birds (15-17), non-avian reptiles (18, 19), fish (20), and cephalopods (21). However, whether sleep oscillations vary across the brain sites (5, 6, 22) and are impacted by age (23) is not yet established in the taxa other than mammals. In fact, our current understanding of these changes in sleep architecture predominantly comes from studies in human and rodents. Consequently, the extent to which these dynamic aspects of sleep are indispensable across animal kingdom, in animals other than human or rodents, is not clear.

Our current knowledge concerning the mechanistic neural control of sleep comes almost exclusively from studies in rodents. Sleep studies in avian taxa are mainly limited to descriptions of sleep, i.e., characteristics of sleep stages, the presence of unihemispheric sleep, etc., in a few avian species. How the control of sleep in birds is regulated, and how it may differ from mammals, is not known. Therefore, it is informative to have a basic understanding of the general pattern of sleep control in the

mammalian system. Our assumption is not that the neural control of sleep in the avian brain follows that of the mammalian system. However, since the known sleep-related brain areas in the mammalian brain, such as the basal forebrain and hypothalamus, are shared structures across vertebrates, it is fair to assume that the avian brain shares some of the neural circuitry of sleep control with the mammalian system. As such, we start by reviewing the distinct oscillations associated with NREM and REM sleep in the mammalian system. Then we review some of the brain areas known to be either sufficient or necessary for triggering NREM and REM sleep.

After reviewing the neural circuitry of sleep (originating from mammalian studies), we review the main findings in the avian sleep literature. Here, we emphasize the similarities and differences between avian and mammalian sleep. Finally, as an introduction to the first manuscript, where we report on the age-related changes in the sleep architecture of zebra finches, we end by briefly reviewing the current knowledge on the topic of sleep ontogeny and brain lateralization.

## Common NREM characteristics in mammals

While the discrete classification of sleep into stages, referred to as "sleep scoring" or "sleep staging", has been criticized for being somewhat arbitrary and overlooking the inter-individual differences(24), it remains a prevailing practice in both clinical and scientific contexts to partition sleep time into distinct stages. In humans, the commencement of sleep, characterized by diminished responsiveness to external stimuli, a decline in body temperature, stabilization of heart rate, and the absence of rapid eye movement, is denoted as NREM sleep. The prevailing standard for sleep scoring in humans, as outlined by the American Academy of Sleep Medicine in 2007, divides the NREM period into three specific stages, namely N1–N3 (25).

The N1 stage denotes the transition from wakefulness to closed eyes, distinguished by the emergence of cortical alpha waves (8–11 Hz), succeeded shortly thereafter by theta waves (4.0–7.5 Hz). Next, the presence of sleep spindles marks the onset of N2. (A sleep spindle is a brief burst of activity usually with a frequency in the range of 10–15 Hz that lasts less than 1.5 seconds (26)). Lastly, the N3 stage is marked by substantial slow oscillations (<1 Hz) and delta waves (0.5–4 Hz).

In rodent studies, NREM sleep is identified by predominant, distinctive delta oscillations (0.5–4 Hz), occasionally interspersed with irregular spindles (27). In rodent research, the classical approach involves treating NREM sleep as a singular stage (27) or occasionally further dividing it into a mixed-frequency intermediate stage (IS) and

slow-wave sleep stages (SWS) (28). The IS usually consists of brief periods of time that collectively account for a mere 2% of sleep time (28), and as such, in rodent research, NREM and SWS are used interchangeably. In the following, we describe the neural oscillations typical of the mammalian NREM sleep.

## Slow Oscillations

The N3 sleep stage exhibits oscillations ranging from 0.5 to 4 Hz, encompassing distinct components—slow oscillations, which are characterized by frequencies below 1 Hz, and delta waves, ranging from 1 to 4 Hz (29). Here we elaborate on the dynamics of these waves.

Slow oscillations concur with fluctuations in the resting membrane potentials of thalamic and cortical neurons, transitioning between depolarized 'UP' and hyperpolarized 'DOWN' states (29). This cyclic shift between UP and DOWN states gives rise to a slow oscillatory pattern at frequencies below 1 Hz. This phenomenon is observable through both EEG and LFP electrodes placed across thalamocortical structures (30).

Several lines of evidence implicate the cortex in the formation of slow oscillations. Following the removal of the thalamus (thalamectomy), slow oscillations persist within the neocortex (31), implying the sufficiency of the cortex for the genesis of slow oscillations. Furthermore, slow oscillations arise in the cortex after pharmacological suppression of thalamic activity (32), and in isolated cortical segments (33). These oscillations cease within the thalamic region in decorticated cats, further underscoring the essential role of the cortex in the formation of slow oscillation (34).

Beside the role of cortex in generating slow waves, experimental evidence also demonstrates the involvement of midline and dorsal thalamic structures in generating slow waves (35, 36). Lesioning (37) and pharmacological blockade (32) in thalamus leads to a transient elimination of slow waves in neocortical areas, although it is followed by the subsequent reappearance of slow waves. These investigations suggest that slow waves emanate from cortical regions, thalamic regions, or a combination thereof.

Though the neural mechanisms that underlie the genesis of slow waves encompass extensively synchronized activity patterns among neuronal populations (the UP and DOWN states), multichannel recordings have demonstrated that slow waves exhibit regional selectivity and are not a pervasive and uniform cortical phenomenon (4, 6, 38). These observations suggest that slow waves are similar to propagating waves and originate from discrete cortical areas primarily situated in the frontal cerebral region (5,

39). Moreover, they tend to propagate along the frontoparietal axis and traverse the cingulate pathways in felines (40) and humans (41). Only a minor fraction of these waves reach the posterior cortices (42).

## Delta oscillations

Delta waves, ranging from 1 to 4 Hz, manifest prominently during the N3 stage of NREM sleep in human subjects. Similar to slow oscillations, both cortical and thalamic structures are involved in the genesis of delta oscillations. Within cortical neurons, an intrinsic delta oscillation exists, as evidenced by observations in both isolated forebrain (through midbrain transection)(31) and cortical slices (38). On the other hand, thalamus projections to cortical sites has an essential role in the formation of delta waves: suppression of midline and dorsal thalamic neurons through optogenetic manipulation reduces the amplitude of delta oscillations across cortical regions (35).

## Contribution of subcortical structures to slow waves

Analogous to cortical regions, subcortical structures exhibit an assortment of distinct neural activities upon the onset of NREM sleep. In humans, for instance, hippocampal sleep spindles appear before the initiation of NREM sleep in the neocortex (43). At the same time, oscillations resembling neocortical slow waves are detectable in the thalamus (44). Preliminary investigations into the neural circuitries underpinning the initiation of NREM sleep, subsequently named the 'sleep switch' (2), implicated sleep-active neurons within the hypothalamus (the ventrolateral preoptic area and median preoptic nucleus of hypothalamus), which release either GABA or galanin, in both human and rodent models. Notably, activation of these brain areas using pharmacogenetics to induce sleep caused a concomitant decrease in body temperature, mirroring the temperature reduction observed during natural NREM sleep in mammals (43). This suggests a potential dual functionality for these hypothalamic cells, i.e. initiating (NREM) sleep and reducing body temperature.

Beyond the hypothalamus, specific clusters of cells within other subcortical structures have been implicated in the regulation of NREM sleep. This includes GABAergic neurons in the brainstem parafacial zone (44), cells expressing adenosine receptors in the nucleus accumbens of the basal forebrain (45), neurons within the zona incerta beneath the thalamus (46), as well as groups of glutamatergic or GABAergic neurons in the midbrain (47) and brainstem (48), which all have roles in NREM sleep regulation. In summary, the activation of numerous subcortical cell groups can initiate sleep. The interplay between these 'switches' and the cortical factors governing NREM sleep are still an active area of research.

## Common REM characteristics in mammals

REM sleep is also termed paradoxical sleep. During REM sleep, cortical EEG patterns resemble those of wakefulness, thus justifying the term "paradoxical." REM sleep EEG is characterized by theta and gamma oscillations (27), swift and irregular eye movements, the relaxation of muscle tone, heightened brain temperature, and irregularities in respiration and heart rate (27, 49).

Notably, REM sleep has traditionally been associated with the dream phase of sleep (1), and the eye movements during REM sleep are thought to be linked to dream content (50). However, recent observations have revealed that dreams occur in both REM and NREM sleep stages and are controlled by different mechanisms (51, 52). In addition, the term "desynchronized," which was previously employed to describe brain activity during REM sleep is becoming obsolete due to the observation of synchronized theta and gamma oscillations in the hippocampus during this sleep phase (53). In the following, we review the most common oscillations observed during REM sleep.

### Theta rhythm

The "theta rhythm" is a hallmark of hippocampal activity during REM sleep in mammals (12, 54). Theta oscillations, which are also observed during awake cognitive activities, are coupled with gamma oscillations during REM sleep (55). Beyond hippocampal theta activity, smaller-scale theta oscillations (diminished in amplitude compared to those in the hippocampus), have been documented in the prefrontal cortex (56) and amygdala (57) in both rodents and humans (58) during periods of wakefulness and REM sleep.

Regarding the generation of theta activity, the basal forebrain medial septum (along with its major projections to the hippocampal formation), has been shown to have a critical role in formation of the hippocampal theta rhythm (59). GABAergic neurons within the medial septum exhibit rhythmic firing at theta frequencies, and are synchronized with the hippocampal theta rhythms during REM sleep (59). In contrast, cholinergic neurons within the medial septum have a slower firing pattern in comparison to the GABAergic neurons (60). As such, it is believed that their role is to fine-tune the amplitude of the hippocampal theta rhythm, rather than its initiation. They have the capacity to enhance the hippocampal theta rhythm or diminish peri-theta oscillations, such as slow waves (<4 Hz) and beta-frequency (~12-30 Hz) waves (60).

Lastly, a subset of the glutamatergic neurons in the medial septum spontaneously exhibit theta-frequency firing, similar to the GABAergic neurons within the same region (61). These glutamatergic neurons also project to the hippocampus, where they have a critical role in driving the theta rhythm.

Beyond the influence of the medial septum, there are supplementary inputs originating from the entorhinal cortex, posterior hypothalamus, and brainstem circuits that all have a role in modulating REM sleep theta oscillations (27). Remarkably, theta oscillations exhibited during REM sleep possess a phasic and transient nature, which is closely linked to the transient waves of pontine origin (53), referred to as REM sleep ponto-geniculo-occipital (PGO) waves. These PGO waves are associated with heightened synchrony in the theta-band within the hippocampus (53). We briefly elaborate further on PGO waves in the following subsection.

### Ponto-geniculo-occipital waves

REM sleep pontine waves, conventionally termed PGO waves, appear as substantial phasic waves in the pontine local field potential during the occurrences of eye saccades within REM sleep (62). In feline recordings, it was shown that these waves originate from synchronized bursts of action potentials within the pontine reticulum. This firing triggers the activation of specific subsets of cholinergic neurons within the pons, namely, the pedunculopontine tegmentum and laterodorsal tegmentum (63, 64). The activation of these cholinergic neurons is followed by the activation of the lateral geniculate nucleus (in the thalamus) and the occipital cortex (63, 64), thereby leading to the designation of "ponto-geniculo-occipital." Progressively, the influence of PGO waves extends to a range of downstream targets, including the amygdala as well as hippocampal and thalamocortical systems (57, 64, 65).

### Gamma oscillations

Gamma oscillations are prominent during periods of wakefulness and REM sleep across diverse regions of the neocortex, hippocampus, amygdala, striatum, thalamus, and hypothalamus in both humans and rodents (66). These oscillations often exhibit a coupled relationship with lower frequency oscillations (67). REM sleep gamma oscillations are phasic in nature, which arises from the coordinated interplay between neuronal excitation and inhibition (61).

In contrast to slow waves, gamma rhythms typically concur with stochastic firing patterns of individual neurons (67). Consequently, the frequency of gamma oscillations displays considerable variability depending on the specific underlying neural circuitry (67). In elucidating the formation of these oscillations, multiple models have been proposed, with a shared emphasis on the important role of inhibitory interneurons (67).

One such model highlights the reciprocal connections linking excitatory cortical pyramidal cells and the delayed feedback stemming from inhibitory interneurons (67). According to this theory, a certain threshold of synaptic strength must be attained to initiate and sustain gamma oscillations. Further, the oscillation frequency was found to be determined by the extent of phase delay present in the feedback loop formed by the interneurons (67).

## Sleep oscillations and brain metabolism

The brain oscillations that arise during sleep can also be examined in consideration of brain energetics. Research into cerebral blood flow (CBF) and cerebral metabolic rate (CMR) during different stages of sleep using brain imaging techniques has revealed significant insights into the brain dynamics underlying EEG activity (68). For example, stage N2 of (NREM) sleep is marked by a moderate decrease in both global CBF and CMR, ranging from 3-10% below awake levels. Similarly, during SWS, i.e. stage N3, CBF and CMR plummet by 25-44% (68, 69). Interestingly, during REM sleep CBF and CMR are similar to awake levels (68).

Given that CBF and CMR reflect cortical synaptic activity, the profound reduction in these metrics during SWS sleep suggests that there is around a 50% decrease in overall cortical synaptic activity compared to wakefulness (68). In addition, research into brain metabolism during sleep indicates that glucose utilization and the concentrations of several brain metabolites consistently change across the sleep-wake cycle (70). Lactate, a product of glycolysis that is involved in synaptic plasticity, has emerged as a good biomarker of brain state (70).

Collectively, these findings indicates that activity-induced changes in the concentration of several neuroactive substances, including neurotoxic waste products (71), in the brain blood supply (70) and the interstitial space (72) might shift the neural synchronization dynamics, leading to formation of slow oscillations observed during sleep. Indeed, computer simulation and in vitro experiments verifies that changes in extracellular potassium concentration, a product of neural activity, lead to the emergence of a synchronized pattern of neural activation akin to that of slow oscillations (73, 74).

# An overview of the regulation of sleep in the avian brain

## A primer to the avian brain

Our current understanding of the network properties underlying the genesis and propagation trajectories of sleep oscillations, specifically slow waves and gamma activity, relies almost exclusively on intra-cortical recordings from a few mammalian species (75). Birds also exhibit alternating patterns in their sleep EEG, similar to the NREM and REM sleep activity in mammals (15, 76-78), despite the fact that the cytoarchitecture of the avian brain differs from that of the mammalian neocortex (79-81).

During development, the dorsal part of the pallium (see Fig. 2) gives rise to the neocortex in mammals and the hyperpallium in birds (82). In all extant mammalian taxa, i.e., monotremes, marsupials and placentals, the cortex exhibits a six-layered laminar structure, presumably inherited from their common therapsid ancestor more than 200 million years ago (83). However, the avian hyperpallium has a unique organization that has so far been found only in birds (79). The avian hyperpallium consists of semi-layered subdivisions and might have evolved more recently than the mammalian six-layered cortex, as birds evolved approximately 50–100 million years after mammals (80). Although most of the hyperpallium is homologous to the primary visual cortex in mammals, it differs from the mammalian neocortex in its cytoarchitecture (79, 80, 84). Specifically, the mammalian cortex contains pyramidal cells with apical dendrites spanning multiple layers, which presumably play an important role in the formation of the oscillations observed in EEG (85), whereas the avian hyperpallium is composed of small, densely packed stellate neurons (86) organized in "pseudo-layers" which are connected via axonal projections (87, 88).

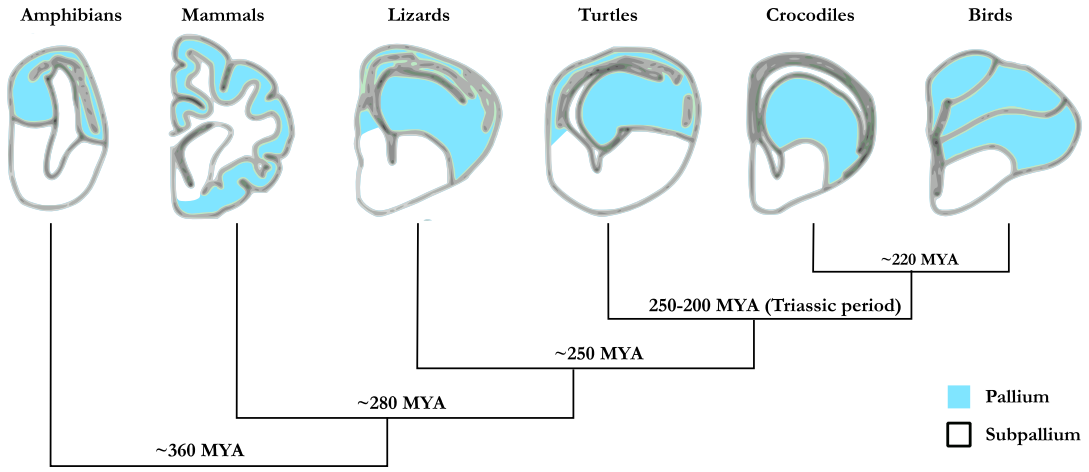


**Figure 2 Pallial areas across the vertebrate lineage.** Schematics show transverse sections of the anterior part of right hemisphere; left is medial, up is dorsal. Pallial areas are colored pale blue. The pallium in (large) mammals is thin and folded. In contrast, the major part of pallium of non-avian and avian reptiles, below the lateral ventricle, is nuclear and thick. The pallium in birds is further divided to three main subdomains, which are called, from dorsal to ventral, Hyperpallium, Mesopallium, and Nidopallium. MYA, million years ago. (redrawn after (89) with permission)

## Neural signature of sleep in avian species

Despite the differences in the neuronal cytoarchitecture between the mammalian and avian brain, numerous similarities exist between the two taxa with regard to brain activity during sleep. During NREM sleep (also commonly referred to as SWS in the context of avian sleep literature) EEG recordings in birds display prominent, high-amplitude slow waves similar to those observed in mammals. Much like their mammalian counterparts, these avian slow waves appear to mirror the gradual oscillation of neuronal membrane potentials, transitioning between "On-states" marked by neural depolarization, and "Off-states" characterized by neuronal inactivity (90). Moreover, similar to mammals, slow waves propagate as traveling waves throughout the avian pallium (91).

One shared characteristic of sleep between birds and mammals is the homeostasis of NREM sleep. In songbirds, EEG slow-wave activity (SWA), that is EEG activity below 4 Hz (comparable with the combination of slow wave oscillation and Delta waves in the mammalian sleep), is most pronounced at the onset of the night and diminishes progressively with the duration of total NREM sleep (77, 92). This pattern implies a resemblance to the homeostatic regulation commonly observed in mammals. Regarding the homeostasis of SWA, although an early study in pigeons did not observe an elevation in SWA following 24 hours of sleep deprivation (93), a more recent work

has demonstrated the homeostatic regulation of SWA in pigeons after a shorter, eight-hour, sleep deprivation (94).

Similar to mammals, SWS in birds also shows activity-dependent local regulation. In humans and other mammals, SWA increases locally in a cortical area in response to specific stimulations caused by wake-time activity (5). Similarly, recent research has shown that the heightened SWA observed after sleep deprivation in birds also depends on the level of visual stimulation during wakefulness. Pigeons that were kept awake for eight hours and exposed to a visual stimulus with only one eye showed an increase in SWA during the NREM periods of the subsequent sleep. Importantly, this increase of SWA was observed exclusively in a visual part of the pallium (i.e. hyperpallium), and only in the hemisphere that was receiving input from the stimulated eye (i.e., contralateral to the exposed eye) (76).

Another similarity shared between mammals and birds is the origin of delta waves. As mentioned earlier in the section on delta oscillations, thalamic input has an important role in the generation of slow waves and delta oscillations. In cats, the UP-state of slow waves, starts in layer five (40), a layer that along with layer four receives input from the thalamus (95). Similarly, intracerebral recordings in the hyperpallium and thalamus in naturally sleeping pigeons showed that slow waves tend to appear first in the thalamic-recipient layers of the hyperpallium (96).

A highly synchronized wave in mammals is the hippocampal sharp wave ripple (SWR), a mixed wave consisting of a sharp deflection (sharp wave) and bursts of fast oscillations (ripples) (97, 98). Recently, SWRs has been found in the avian hippocampus (99), and surprisingly, outside of avian hippocampus, across mesopallium, a pallial subdivision ventral to hyperpallium (100). However, it is unknown whether the avian hippocampal and mesopallial SWRs share a common origin or are independent events. Nevertheless, the presence of SWR in the avian brain is surprising, since the formation of SWR in the mammalian hippocampal is thought to rely on the specific anatomy of the hippocampus (98). However, unlike the mammalian hippocampus, cells are less clustered in the avian hippocampus, and dendrites are not strictly aligned in parallel (101-103).

Avian and mammalian REM sleep also exhibit numerous shared features. In both groups, REM sleep is characterized by a low-amplitude, high-frequency EEG activity akin to patterns observed during wakefulness (15, 77, 92). During these phases of EEG activation, some avian species display behavioral indications of reduced muscle tone, exemplified by a gradual lowering of the head (104, 105). Comparable to mammals, responses related to thermoregulation, such as shivering are suspended during REM

sleep, likely due to the decrease in muscle tone (106). Furthermore, this 'paradoxical' stage of sleep (regarding the wake-like EEG activity of REM sleep) is indeed linked to the occurrence of rapid eye movements (except in species with limited eye movements, like owls) and occasional muscle twitches (17, 77).

A vital function of sleep, i.e., clearing neurotoxic waste products that accumulate in the awake central nervous system (107), is also shared between mammals and birds. In mice, this clearing process occurs during sleep and is marked by an increase in the cerebrospinal fluid (CSF) flow (71) (this study did not classify sleep stages). Furthermore, a study in humans shows that EEG delta waves are coupled to and precede CSF oscillations, marking the role of NREM sleep in the waste removal (108). Similar to this function of NREM sleep in mammals, a recent study in sleeping pigeons demonstrated that the ventricular CSF flow increases during NREM sleep, compared to wakefulness, and drops during REM sleep (109).

When discussing the parallels between mammalian and avian NREM sleep, it is also important to acknowledge the differences. Notably, sleep spindles which are a hallmark of N2 sleep in mammals, are neither observed in surface EEG recordings (77) nor in intracerebral recordings in the avian hyperpallium or thalamus (96). In addition, the brain activity during REM sleep also shows differences between the two taxa. Firstly, as we mentioned earlier, in the section on PGO waves, in mammals the thalamic lateral geniculate nucleus shows increased activity during REM sleep. Such an activation of the lateral geniculate nucleus is not present in sleeping pigeons (109). Instead, during REM sleep, the nucleus rotundus is activated in pigeons. However, it is worth mentioning that similar to the lateral geniculate nucleus, the nucleus rotundus is also a thalamic relay for visual information.

Unique to birds are several ecologically-specific sleep modifications that push the definition of sleep beyond the conventional mammalian understanding. For example, many migratory birds engage in non-stop flights that could last up to several weeks (110). An EEG recording in frigatebirds flying over the ocean provided clear evidence that birds do sleep during the flight (110). Of note, the flying frigatebirds sleep only 7.4% of the time they spend sleeping on land. Such an adaptive reduction of sleep time is not particular to flying periods and has been also observed on land. The male pectoral sandpipers, are forced to greatly reduce their sleep time during a three-week period of intense male-male competition for access to fertile females (111). A similar EEG study in female chinstrap penguins, which are constantly exposed to an egg predator and aggression from other penguins, demonstrated the flexibility of sleep in birds. To keep their vigilance, the penguins slept in very short bouts (4 seconds on average), but

numerous (>10000) times per day. Such observations demonstrate that sleep occur in many diverse forms.

## Sleep ontogeny

Sleep architecture, specifically the proportion and duration of NREM and REM sleep, undergoes dynamic changes throughout an animal's lifespan. During early stages of development, neonatal mammals are thought to spend up to 90% of their sleep in a state similar to an immature manifestation of adult REM sleep (13). This nascent form of REM sleep is characterized by frequent muscle twitches, rapid ocular movements, and irregular respiratory cycles (13). However, an alternate theory suggests that the presence of REM sleep is not evident at birth, but rather that these behavioral patterns could result from spontaneous activity generated from an underdeveloped nervous system (112). In fact, it appears that all mammals early in development exhibit spontaneous brain activity that progressively becomes organized into distinct REM and NREM sleep stages.

With respect animal studies, a comprehensive classical study investigated the ontogeny of sleep in infant rats, kittens, and infant guinea pigs, during their first month of postnatal life (13). In all three species, paradoxical sleep declined rapidly during the first postnatal month of development. However, recordings in (13) were not performed longitudinally in each individual. Instead, each individual was recorded for a certain period of time. A new longitudinal study in rats (113), during postnatal days 14-27 showed that the percentage, duration, and number of REM episodes indeed decreased by age, confirming the previous findings in (13).

In humans the duration of SWS declines during childhood and adolescence. A comprehensive analysis of existing literature revealed a statistically significant inverse correlation between the proportion of SWS and age (23). Similarly, a longitudinal study encompassing the childhood and adolescence phases of life has shown a strong decline in NREM delta and theta activity around the age of 10, continuing until approximately 16 years (8). Furthermore brain scans in humans reveal a correlation between the reduction in slow-wave activity and the diminution of gray matter during the trajectory of cortical maturation throughout adolescence (9).

Among the mammalian species studied for their sleep, ferrets have a special position; Ferrets appear to show two distinct stages of REM sleep, both characterized by high-frequency EEG, but with low amplitude (REM1) and high amplitude EEG (REM2) , and the proportion of REM sleep (REM1 and REM2 together) is exceptionally high

(40% of sleep) (114, 115). A longitudinal polysomnographic recording in ferret kits, starting from postnatal day 30, revealed that REM sleep levels slightly decreased over the following two weeks, while wakefulness and NREM sleep durations increased. Besides, NREM delta power also increased with age.

Sleep ontogeny in avian species is relatively less explored, and the findings of the few existing studies are inconsistent (16, 104, 116); A more recent investigation in a large population (n=66) of young barn owls demonstrated a linear reduction in the duration of NREM episodes and the percentage of REM sleep as a function of age (117). However, in that study, statistical analysis did not show evidence for age-dependence change in the percentage of NREM and duration of REM sleep episodes. Owls are night-active predators, and this circadian factor might play a role in their sleep architecture. Therefore, to enhance our knowledge of how sleep develops in avian species, further research is required. In this thesis (the first manuscript), we examine the neural changes in the sleep patterns of zebra finches.

## Brain lateralization

In the second chapter (first manuscript), we will report on an interesting asymmetry in the functional connectivity between hemispheres that forms in juvenile zebra finches. Brain lateralization is a large topic on its own and goes beyond sleep. Here, we briefly overview some of the essential key concepts in lateralization of the brain and behavior. Related to the topic of this thesis, as we see in the following, song birds have a unique position in studies that revealed lateralities in the brain.

Brain lateralization is characterized by the different functional specializations of the left and right brain hemispheres (118). For more than a century, brain lateralization has been considered a human trait related to complex cognitive functions, such as language (119). Mark Dax and, thirty years later, Paul Broca (120) independently demonstrated that the lesions in specific regions of the left hemisphere, but not the right, were coincident with deficits in language production, thus suggesting left hemisphere dominance for speech. In the last fifty years, study of asymmetric behavioral preferences and their underlying neural asymmetries in other species suggests that brain lateralization is a common trait across animal kingdom (118).

The first system in which nonhuman behavioral and neural lateralization was demonstrated is that of singing behavior in songbirds (121-123). Lateralization has been demonstrated in both song production and song perception systems. The vocal organ of a songbird, the syrinx (equivalent to the mammalian larynx), is a paired

bilateral structure (124). Transecting the nerve that connects brain stem motor areas to the left syrinx disrupts singing almost completely, while denervation of the right nerve leads to the loss of merely 10% of syllables (121, 122) (Fig 3).

Later investigations revealed that song control is also lateralized in the brain. In the songbirds' brain, HVC (formerly, Hyperstriatum Ventrale, pars Caudalis, now sometimes referred to as the "higher vocal center") is a nucleus necessary for song learning and song production (125). Lesions of the left HVC disrupt singing more severely than lesions of the right HVC (126).

Similarly, song perception is also performed preferentially by the left hemisphere. For example, lesions in HVC, or lesions to auditory pathways, disrupt song discrimination more severely when made on the left side compared to the right side (127, 128). Thus, similar to humans, production and perception of vocal signals is lateralized in songbirds.

The emergence of lateralization in the brain could be explained by the evolutionary benefits of lateralized behaviors. We will briefly discuss the advantages and disadvantages of a lateralized brain later in the Discussion.

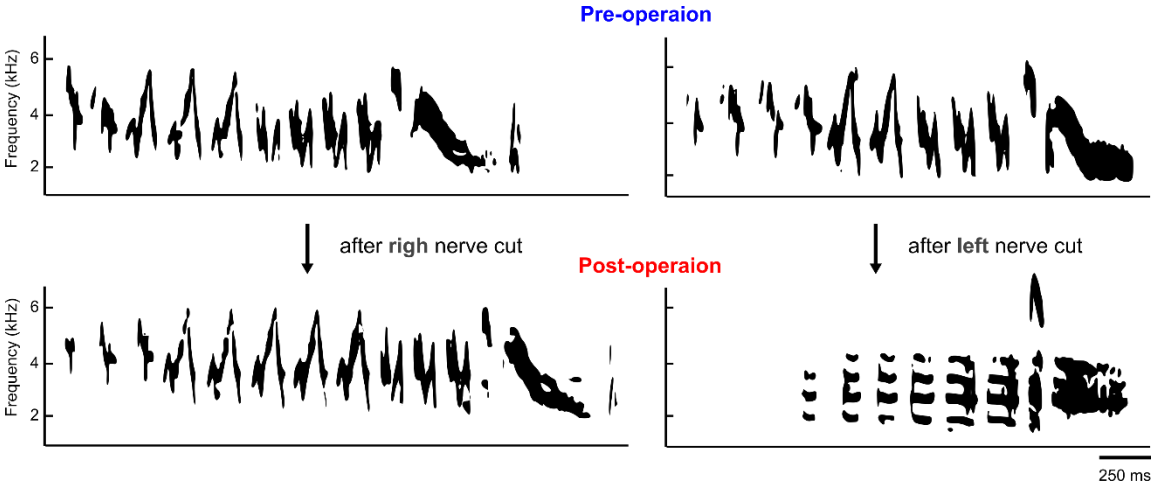


**Figure 3 Song control in songbirds is lateralized. (Upper panels)** Left and right panels show the songs of two adult chaffinches. Both birds shared the same song. **(Lower panels)** Cutting the nerve that connects brain stem motor areas to the syrinx (the hypoglossus nerve), disrupts singing almost completely if performed on the left nerve, but has minimal consequences, if performed on the right nerve. This work, (121), published in 1971, is an iconic study of bird song that expanded brain lateralization to non-human species. Redrawn after (121) with permission.

## Focus of the thesis

The focus of this thesis is on two aspects of neural signature of sleep in the avian brain, that is, sleep ontology and local sleep. We collected data by conducting electrophysiological recordings in zebra finches (*Taeniopygia guttata*). The results are presented in two manuscripts.

In the first manuscript we have investigated the age-related variations in brain dynamics of sleep in juvenile finches. Notably the recordings are conducted when they underwent the critical song learning period. As such, the findings broadly contribute to our understanding of the interactions between sleep and learning.

In the second manuscript we turn our attention to the local variations in brain dynamics across the pallium. Previous studies have characterized the local differences by recording from either the surface of the brain; i.e., EEG, or intracortically, i.e., LFP. We have recorded the neural activity simultaneously on the surface and inside the avian pallium. Our data suggests that oscillations associated with sleep stages vary largely across pallial sites, as opposed to being a brain-wide phenomenon. These findings impact our current understanding of sleep stages as being unitary whole-brain states. Collectively, our findings help to expand our understanding of brain dynamics in the avian system and sleep characteristics in general.

# Chapter 2

# Multi-channel recordings reveal age-related differences in the sleep of juvenile and adult zebra finches

**Summary**

Despite their phylogenetic differences, mammals and birds exhibit similar sleep EEG patterns, with distinct REM and SWS stages. Sleep organization undergoes age-related changes in humans and other mammals, but do these variations also occur in the avian brain? To find out, we recorded multi-channel sleep EEG in zebra finches of different ages. Adults showed more SWS and REM sleep, while juveniles spent more time in intermediate sleep (IS). Male juveniles engaged in vocal learning had more IS than female juveniles, suggesting its importance for vocal learning. Functional connectivity increased rapidly in young juveniles but stabilized as they aged. Synchronous activity during sleep was more prominent in the left hemisphere, and intra-hemispheric synchrony surpassed inter-hemispheric synchrony. Graph theory analysis revealed that adults had fewer but larger networks of highly correlated EEG activity, while juveniles had more numerous, albeit smaller, networks. In summary, our findings highlight significant age-related changes in sleep patterns in avian brains.

**The manuscript was published as**

Yeganegi, Hamed, and Janie M. Ondracek. "Multi-channel recordings reveal age-related differences in the sleep of juvenile and adult zebra finches." *Scientific Reports* 13.1 (2023): 8607.

## Multi-channel recordings reveal age-related differences in the sleep of juvenile and adult zebra finches

**Hamed Yeganegi[1,2] and Janie M. Ondracek[1]***

[1]Chair of Zoology, Technical University of Munich, Liesel-Beckmann-Str. 4, 85354 Freising-Weihenstephan, Germany

[2]Graduate School of Systemic Neurosciences, Ludwig-Maximilians-University Munich, Großhaderner Str. 2, 82152 Planegg, Germany

* Corresponding author

## Abstract

Despite their phylogenetic differences and distinct pallial structures, mammals and birds show similar electroencephalography (EEG) traces during sleep, consisting of distinct rapid eye movement (REM) sleep and slow wave sleep (SWS) stages. Studies in human and a limited number of other mammalian species shows that this organization of sleep into interleaving stages undergoes radical changes during lifetime. Do these age-dependent variations in sleep patterns also occur in the avian brain? Does vocal learning have an effect on sleep patterns in birds? To answer this question, we recorded multi-channel sleep EEG from juveniles and adult zebra finches for several nights. Whereas adults spent more time in SWS and REM sleep, juveniles spent more time in intermediate sleep (IS). The amount of IS sleep was significantly larger in male juveniles engaged in vocal learning compared to female juveniles, which suggest that IS sleep could be important for learning. In addition, we observed that the functional connectivity increased rapidly during maturation of young juveniles, and was stable or declined at older ages. Synchronous activity during sleep was larger for recording sites in the left hemisphere for both juveniles and adults, and generally intra-hemispheric synchrony was larger than inter-hemispheric synchrony during sleep. A graph theory analysis revealed that in adults, highly correlated EEG activity tends to be distributed across fewer networks that are spread across a wider area of the brain, whereas in juveniles, highly correlated EEG activity is distributed across more numerous, albeit smaller, networks in the brain. Overall, our results reveal significant changes in the neural signatures of sleep during maturation in an avian brain.

## Introduction

Sleep is a reversible state characterized by a reduced level of behavioral activity and responsiveness to the environment. Sleep - or a sleep-like state - has been observed across animal taxa, including early animals without a centralized nervous system, such as the cnidarian.[1,2]

Reconstructing the evolution of sleep across groups of amniotes has been a major thrust of comparative sleep research, and these investigations have usually provided 1) a description of the presence or absence of behavioral sleep, 2) a search for electrophysiological evidence of SWS and REM sleep, and 3) a final interpretation about what the presence or absence of certain features of sleep in an animal means to the evolution of sleep within amniotes.

As major features of sleep were first defined in mammals, the search for electrophysiological features of sleep in both avian and non-avian reptiles was heavily influenced by mammalian-like indicators of sleep, i.e., the presence of slow waves or delta power, (indicative of SWS in the mammalian cortex), and non-SWS characterized, by low amplitude brain activity, concomitant eye movement, and decreased muscle tone (measured using electromyogramy (EMG) and indicative of mammalian REM sleep).

Pigeons were one of the first non-mammalian animals whose sleep was investigated,[3,4] and it is now generally accepted that birds undergo behavioral sleep and show signs of both SWS and REM sleep. In birds, SWS is characterized by delta activity (1-4 Hz) with some tonic muscle tone, and REM sleep is generally characterized by low amplitude brain activity and conjugate and occasional non-conjugate eye movements. Additionally, birds show an intermediate stage (IS) of sleep, which has been compared to the early stages of mammalian non-REM (NREM) sleep and which can be considered a transitional stage of sleep.[5,6]

Despite these similarities, clear differences do exist between mammals and birds. For example, many birds remain vigilant during sleep, opening one or both eyes during SWS, and only closing both eyes during REM sleep.[7–9] Sleep spindles, a hallmark of mammalian NREM, have not been observed during avian sleep.[5,6,10] Furthermore, particular sleeping postures differentially affect nuchal muscle tone, creating difficulties in relying on clear differences in EMG as a definition of REM sleep versus SWS sleep states.[11,12] Finally, how should one interpret the behavior of migrating birds, which can fly continuously for days? Using a strict behavioral definition of sleep, flying birds cannot be sleeping (see [13] for an examination of how migrating birds sleep).

Although there are more than 10,000 species of birds,[14] electrophysiological signs of sleep have been investigated in only a handful of these animals: chickens and pigeons;[3] geese;[15] white-crowned sparrow;[16] zebra finch;[5] burrowing owl;[7] ostrich;[12] sandpiper;[17] and the tinamou,[18] to name a few. The sleep studies of birds so far have focused primarily on adult birds, and the few studies of immature birds [19–21] do not provide a comprehensive understanding of how aspects of sleep change as a function of aging - or learning.

Vocal learning in songbirds is one of the few innate learning models that can be used to study the effects of sleep on memory in birds. As a juvenile bird learns to sing, it must undergo a complex memory task that involves the formation of auditory memories, sequences of motor output, and associative higher-order representations of learned vocalizations.[22] The process of song learning is similar to speech learning in humans and consists of 1) auditory encoding of the song template during a sensory phase, and 2) the process of vocal imitation during the sensorimotor phase.[23,24] As soon as a juvenile bird is exposed to the song of another male bird (usually its father, the "tutor"), the young bird begins to imitate aspects of those songs in squeaky and noisy subsongs, which are often compared to the babbling of human babies.[25,26] Through a process of auditory feedback and motor learning, juvenile subsongs transition from acoustically simple songs to complex and stereotypical adult songs in a process known as crystallization.[27]

Considering the extensive alterations in sleep architecture that occur during development and across aging in mammals[28] as well as the paucity of information available about sleep in juvenile birds - and specifically juvenile birds engaged in vocal learning - it is of major interest to characterize sleep across different ages of birds to examine whether there are clear differences between sleep features in adult and juvenile zebra finches.

## Results

### Sleep traces are globally similar across electrode sites

In order to investigate the differences between sleeping brain activity in juvenile and adults, we chronically implanted 10 zebra finches (3 adults; 7 juveniles; see Table 1 for more information) with custom-designed electrodes to record supra-dural EEG from 16 sites over a wide area of the skull (approx. 7 mm × 8 mm; Fig. 1A). We recorded brain activity during 12-hour periods of natural sleep for 49 total nights across animals (more than

600 hours of data for all animals). During the tethered sleep recordings, animals assumed typical avian sleep postures, such as tucking the head in the feathers (Supplementary Fig. S1A, B). The body movement, as assessed with video recordings throughout the night, was generally low (Fig. 1B, Supplementary Fig. S1C).

For each night, we compared the structure of sleep in adults and juveniles by determining the ratio of low frequency oscillations to gamma oscillations, calculated as the ratio of the relative power of the delta ($\delta$) and theta ($\theta$) bands ($\delta+\theta$ = 1.5-8 Hz) to the gamma ($\gamma$) band ($\gamma$ = 30-49 Hz).This metric is analogous to those used in mammals[29,30] and reptiles[31] but accounts for the frequency bands prevalent in avian EEG.[5,32]

We observed that across animals, the $(\delta+\theta)/\gamma$ ratio generally varied on the order of tens of seconds (Fig. 1B, Supplementary Fig. S1C). We examined the raw EEGs at high, middle and low points of the $(\delta+\theta)/\gamma$ ratio. High ratio values corresponded to EEG patterns typical of SWS, and low ratio values corresponded to REM sleep (Fig. 1C; Supplementary Fig. S1D). Middle $(\delta+\theta)/\gamma$ values corresponded to an intermediate stage (IS) of sleep which has been compared to stage 1 and 2 of non-REM sleep in human.[6]

We examined whether the $(\delta+\theta)/\gamma$ ratio changed as a function of anatomical position by comparing the $(\delta+\theta)/\gamma$ traces for different quarters of the brain (Fig. 1D). We found that the $(\delta+\theta)/\gamma$ ratio captured global aspects of sleep and was largely similar across a wide range of electrode sites (Fig. 1D). The correlation between $(\delta+\theta)/\gamma$ traces computed across all electrodes for all birds was high (correlation coefficient = 0.64 ± 0.085; mean ± SD; see Supplementary Fig. S2A for individual correlations). Therefore, for the rest of the analysis in this work, we used electrode site 4 for all birds (Fig. 1A, black circle; Fig. 1C, black arrow).

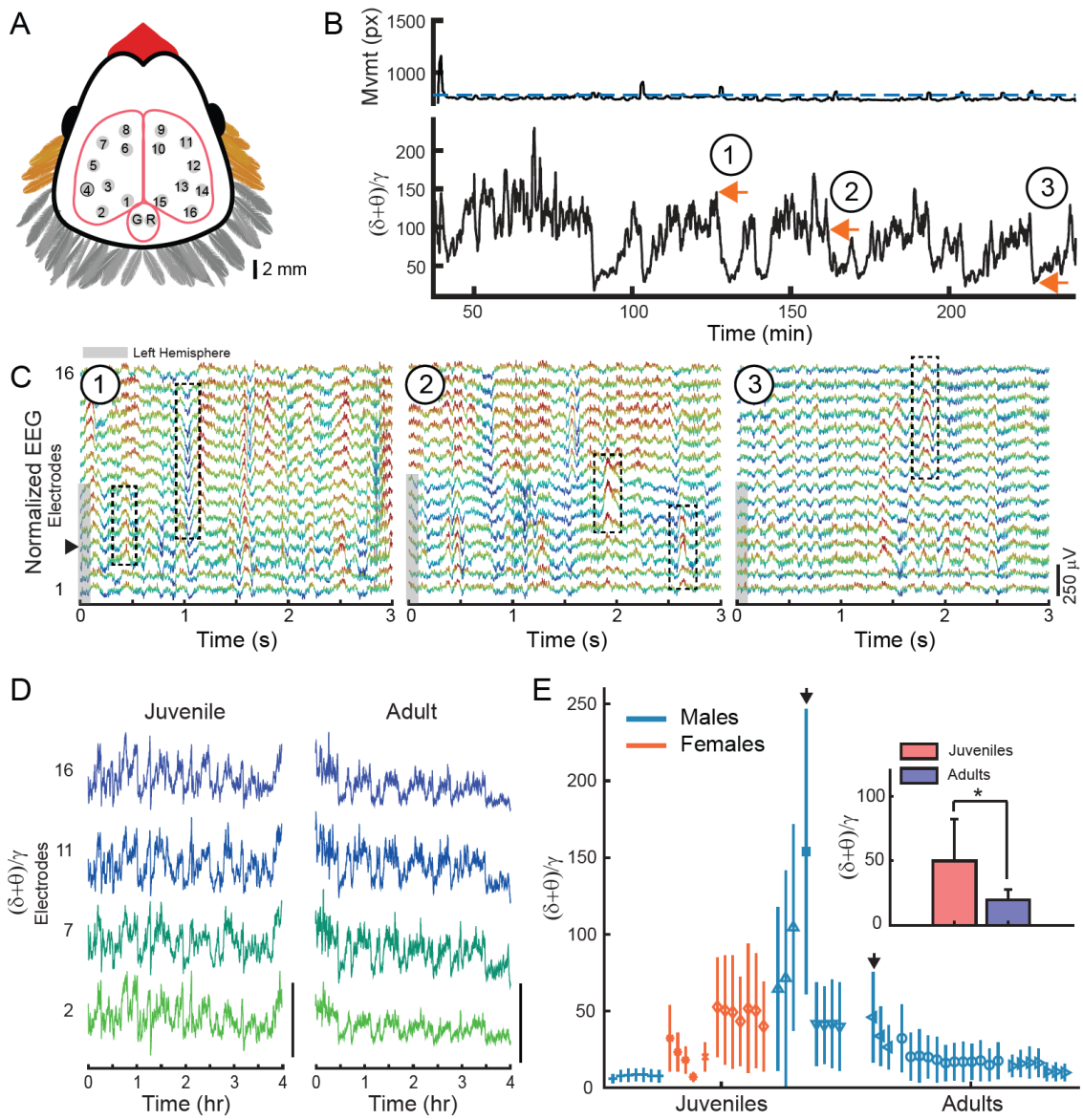


**Figure 1. Multichannel EEG recordings during sleep.** (A) Position of 16 EEG electrode sites on the surface of the skull: 8 electrode sites were located on each hemisphere and covered a wide area over the surface of pallium. Specific brain structures underlying each electrode are listed in Table 2. G, ground electrode; R, reference electrode. (B) Top: Bird movement extracted from the infrared video recording (px, pixels). Blue dashed line indicates the threshold delineating wake and sleep. Bottom: Corresponding $(\delta+\theta)/\gamma$ trace shows the oscillatory components of EEG, representing different sleep stages. Orange arrows 1, 2, and 3, correspond to EEG data in C. Movement and $(\delta+\theta)/\gamma$ traces are smoothed with a 30s window for visualization purposes. (C) 3s examples of simultaneous EEG recorded from the 16 different electrodes (bottom trace, electrode 1; top trace, electrode 16). Circled numbers correspond to orange arrows in B and indicate examples of SWS (1), IS (2), and REM sleep (3). Color scheme is for visualization purposes only. Gray shading on left indicates the electrodes that are located on the left hemisphere. Black dotted boxes highlight examples of local waves (see Fig. 3). Black arrow indicates electrode 4. (D) $(\delta+\theta)/\gamma$ traces are similar across electrode sites in a time scale of minutes. Traces are for a single juvenile (left) and adult (right); exact nights are indicated with black arrows in (E). Scale bar is 200 (unitless $(\delta+\theta)/\gamma$ ratio). (E) Median $(\delta+\theta)/\gamma$ values calculated across 12 hours of sleep in 3s bins, for all nights of

each bird (median ± interquartile). Each symbol represents a different bird, and different nights of sleep are presented sequentially. Teal lines indicate males; orange lines indicate females. $(\delta+\theta)/\gamma$ values are relatively consistent across nights within each individual bird, but large variability exists across different birds. Black arrows indicate animals and nights use in (D). Inset: $(\delta+\theta)/\gamma$ values averaged across all juveniles (red) and adults (blue). Error bars indicate the SD. A significant effect of age was present (p=0.032; two-way unbalanced ANOVA).

### $(\delta+\theta)/\gamma$ values are larger in juveniles compared to adults

We calculated the median $(\delta+\theta)/\gamma$ value for each 12-hour night of sleep for each bird (Fig. 1E). Interestingly, the variability around the median was largely similar for different nights of sleep within the same animal, but this variability differed widely across animals. This finding mirrors results from studies of human sleep, where distinct inter-individual differences in EEG have been observed in human.[33]

When comparing median $(\delta+\theta)/\gamma$ value of each night between adults and juveniles, we found that the $(\delta+\theta)/\gamma$ values in juveniles were larger compared to the adults (Fig. 1E inset; $(\delta+\theta)/\gamma$ = 49.9 ± 32.2 (mean ± SD) in juveniles versus 19.5 ± 8.4 in adults; n = 27 nights of sleep in juveniles and n = 22 nights of sleep in adults). To statistically assess the effect of age group, i.e. juvenile versus adult, as well as sex, we used an unbalanced analysis of variance (ANOVA). The ANOVA test revealed that the $(\delta+\theta)/\gamma$ values were significantly different across age groups (p=0.032, two-way unbalanced ANOVA). The ANOVA did not show a significant effect of sex on the $(\delta+\theta)/\gamma$ values (p=0.645, two-way unbalanced ANOVA); however, this is difficult to interpret as the adult group only consisted of male birds.

The larger $(\delta+\theta)/\gamma$ values that we observed in juveniles could be due to an increase in the low $\delta+\theta$ frequencies or a decrease in the $\gamma$ frequencies compared to adults. We examined the power in each of these bands separately (Supplementary Fig. S2B). Although the low $\delta+\theta$ frequencies were higher in juveniles compared to adults (Supplementary Fig. S2C; 0.088 ± 0.059 in juveniles versus 0.062 ± 0.080 in adults; mean ± SD), this difference was not significant (p=0.07, two-way unbalanced ANOVA). The $\gamma$ power was not significantly different between juveniles and adults (Supplementary Fig. S2D; 0.0040 ± 0.0050 in juveniles versus 0.0038 ± 0.0052 in adults; p=0.47, two-way unbalanced ANOVA). The 2-way ANOVA did not indicate a significant effect of sex on low or high frequency power (p=0.18 in both cases).

These findings likely result from the fact that there was large variability in the normalized $\delta+\theta$ or $\gamma$ frequencies across nights for some animals (see Supplementary Fig. S2B, adult bird symbol ‘right triangle’) which nevertheless resulted in stable and low $(\delta+\theta)/\gamma$ ratios (Supplementary Fig. S2E).

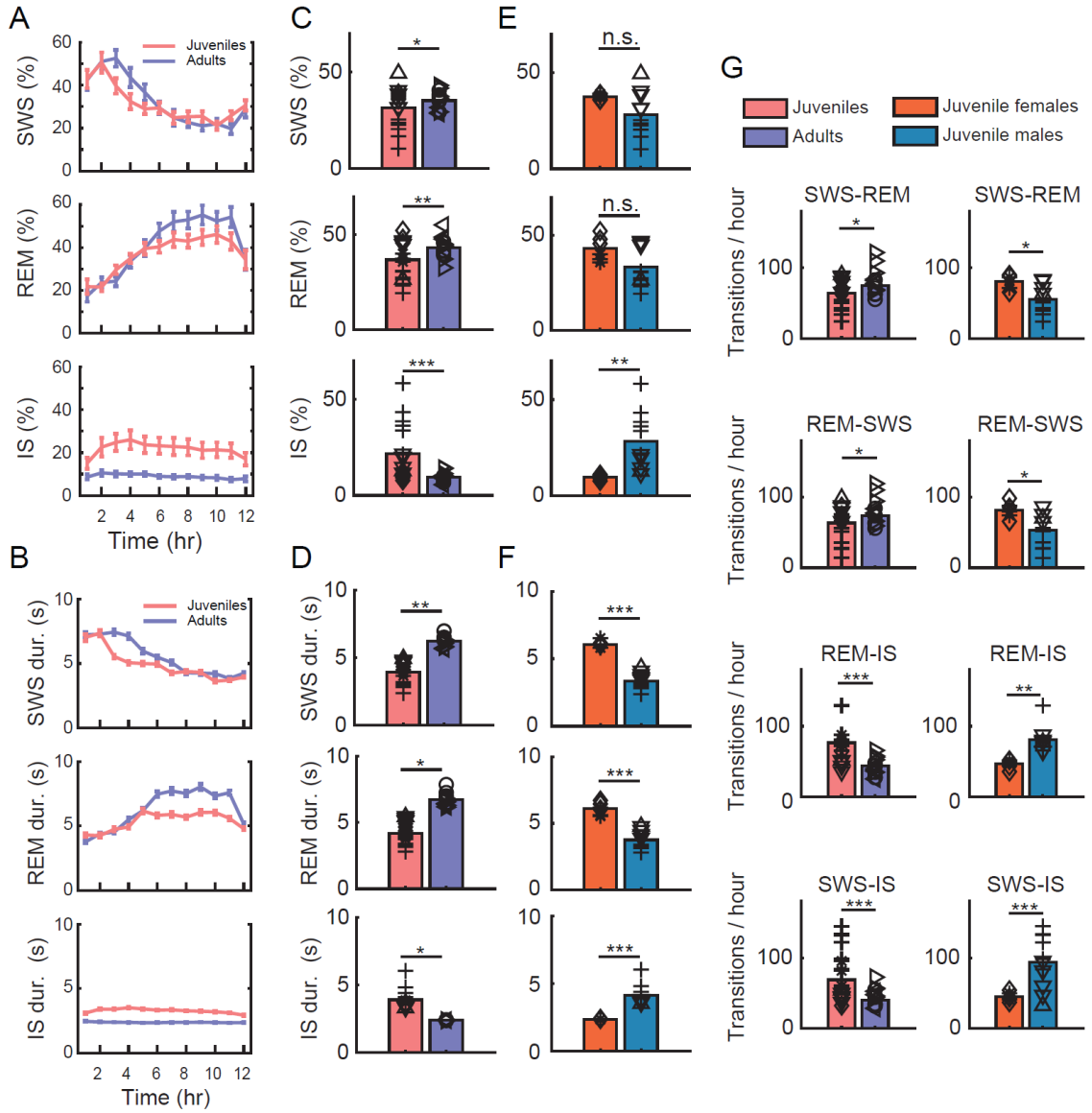


**Figure 2. Sleep stage percentages and transitions in juveniles and adults based on automatic sleep segmentation.** (A) Average percentage of SWS (top), REM (middle), and IS (bottom) for juveniles (red) and adults (blue) over 12 hours of sleep. Error bars indicate the s.e.m. Note how the early hours of the night are dominated by SWS, whereas the later hours of the night are dominated by REM for both adults and juveniles. (B) Duration of SWS, REM, and IS in juveniles and adults over 12 hours of sleep. Figure conventions same is in (A). (C) Mean percentages of SWS (top), REM (middle), and IS (bottom) pooled over all nights for juveniles (red) and adults (blue). Symbols indicate nights from individual animals (see Fig. 1E). Asterisks indicate significance (two-way ANOVA; * $p \leq 0.05$; ** $p \leq 0.01$; *** $p \leq 0.001$). (D) Mean durations for SWS (top), REM (middle), and IS sleep (bottom) pooled over all nights for juveniles (red) and adults (blue). Figure conventions same as for (C). (E) Percentages of SWS (top), REM (middle), and IS (bottom) pooled over all nights for female juveniles (orange) and male juveniles (teal). Figure conventions same as for (C). (F) Mean durations for SWS (top), REM (middle), and IS sleep (bottom) pooled over all nights for female juveniles (orange) and male juveniles (teal). Figure conventions same as for (C). (G) Mean number of transitions per hour for juveniles (red) and adults (blue) and juvenile females (orange) and juvenile males (teal). Figure conventions same as for (C).

**Adults spend more time in SWS and REM; male juveniles spend more time in IS sleep**

In order to quantify the amount of time spent in each sleep state, we used a clustering-based sleep scoring method[5,6] to categorize sleep into discrete bins of REM sleep, SWS, or IS sleep. This allowed us to calculate the proportion and duration of each sleep stage, including the IS stage. We analyzed n=32 nights of sleep in this manner - the clustering-based algorithm did not converge to a plausible solution for 17 out of the 49 nights (Supplementary Fig. S3; Supplementary Fig. S4; see Methods for details).

At the beginning of the night, both adults and juveniles spent the largest amount of time in SWS (Fig. 2A). After about 6 hours of sleep, the amount of time spent in REM sleep gradually increased. This pattern of more SWS at the beginning of sleep and more REM sleep at the end of sleep is similar to the patterns reported in other animals[34,35] including adult zebra finches[5] and budgerigars.[6]

Similarly, for both adults and juveniles, SWS durations tend to be longer in the early hours of the night, whereas the REM sleep durations tend to be longer in the later part of the night (Fig. 2B).

On average, adult birds spent a significantly higher percentage of the night in SWS and REM sleep compared to juveniles ($p=0.026$ for SWS; $p=2.7\times10^{-3}$ for REM; two-way ANOVA; Fig. 2C). In contrast, juvenile birds spent significantly more time in IS sleep compared to adults ($p=9.57\times10^{-6}$; Fig. 2C). SWS and REM sleep durations were also significantly longer in adults, whereas IS durations were significantly longer in juveniles (Fig. 2D; SWS duration $p=0.0018$; REM sleep duration $p=0.017$; IS sleep duration $p=0.014$; two-way ANOVA).

We also observed a significant effect of sex on the SWS, REM, and IS sleep percentages (see Supplementary ANOVA statistics for p values), so we analyzed the juvenile males and juvenile females separately. While there was no significant difference for the percentage of the night spent in SWS and REM sleep between juvenile males and juvenile females, we found that males spent a significantly higher percent of the night in IS sleep compared to females (Fig. 2E).

We also observed a significant effect of sex on the SWS, REM, and IS sleep durations (see Supplementary ANOVA statistics for p values). Interestingly, female juveniles had significantly longer bouts of SWS and REM sleep, whereas male juveniles had significantly longer bouts of IS sleep (Fig. 2F).

We did not observe a negative correlation between the amount of time spent in REM sleep and age for juvenile zebra finches (Supplementary Fig. S5A), as reported elsewhere for owlets.[21]

**Juveniles transition to IS stages more frequently than adults**

In addition to the amount of time spent in each sleep stage, we were curious as to whether there were differences in the transitioning patterns between sleep stages for juveniles and adults. Using the automatic sleep scoring method, we quantified all the SWS to REM sleep / REM sleep to SWS transitions as well as the SWS to IS sleep / REM sleep to IS sleep transitions (Fig 2G; see Supplementary Fig. S5B, C for transitions per hour). In general, adults transitioned significantly more frequently between SWS and REM sleep compared to juveniles ($p=0.035$ for both SWS to REM sleep and REM sleep to SWS transitions; two-way ANOVA), whereas juveniles transitioned significantly more to IS sleep stages (Fig. 2G; $p=1.3\times10^{-7}$ for SWS to IS sleep transitions; $p=1.3\times10^{-5}$ for REM sleep to IS sleep transitions; two-way ANOVA).

Similar to what we found for other sleep statistics, we also observed a significant effect of sex on the sleep transitions (see Supplementary ANOVA statistics for p values). We found that on average, female juveniles had significantly more transitions between SWS and REM sleep, whereas male juveniles had significantly more transitions to the IS sleep stages (Fig. 2G).

We also examined transitions using the continuous $(\delta+\theta)/\gamma$ traces (Supplementary Fig. S6A). We focused on the transitions from SWS (high $(\delta+\theta)/\gamma$ values) to REM sleep (low $\delta+\theta)/\gamma$ values; Supplementary Fig. S6B; see Methods for details).

For adult birds, the transition frequency from SWS to REM sleep was relatively constant at around 45 transitions per hour throughout the night (Supplementary Fig. S6C; blue bars). In juveniles, however, the transition frequency varied throughout the night: it ranged from approximately 45 transitions per hour at the beginning of the night to about 30 transitions per hour in the middle of night, and rose to over 50 transitions per hour in the last hours of sleep (Supplementary Fig. S6C; red bars). For the 4th, 5th, and 6th hours of sleep, juveniles transitioned significantly less frequently between SWS and REM sleep compared to adults (Supplementary Fig. S6C; Wilcoxon rank-sum test, $p=0.045$, 0.001, and 0.0005 respectively).

We found that in juveniles, the variable frequency of transitions during the night was linked to the variable duration of time spent in SWS and the IS sleep phases (Supplementary Fig. S6B). When we examined SWS-REM-SWS transitions using high $(\delta+\theta)/\gamma$ values versus low $(\delta+\theta)/\gamma$ values, the

average SWS cycle was significantly longer in juveniles compared to adults (Supplementary Fig. S6D; 92.86 s ± 121.41 s versus 82.84 s ± 102.80 s, unpaired t-test, $p=5.7\times10^{-12}$). Similarly, when we examined REM sleep cycles, the average inter-REM sleep interval was also significantly longer for juveniles compared to adults (92.88 s ± 115.07 s versus 82.74 s ± 99.15 s, unpaired t-test, $p=5.5\times10^{-13}$; Supplementary Fig. S6D).

Altogether, these results suggest that juveniles - and specifically male juveniles - may spend a longer period of time in IS sleep and transition to IS sleep compared to adults and female juveniles.

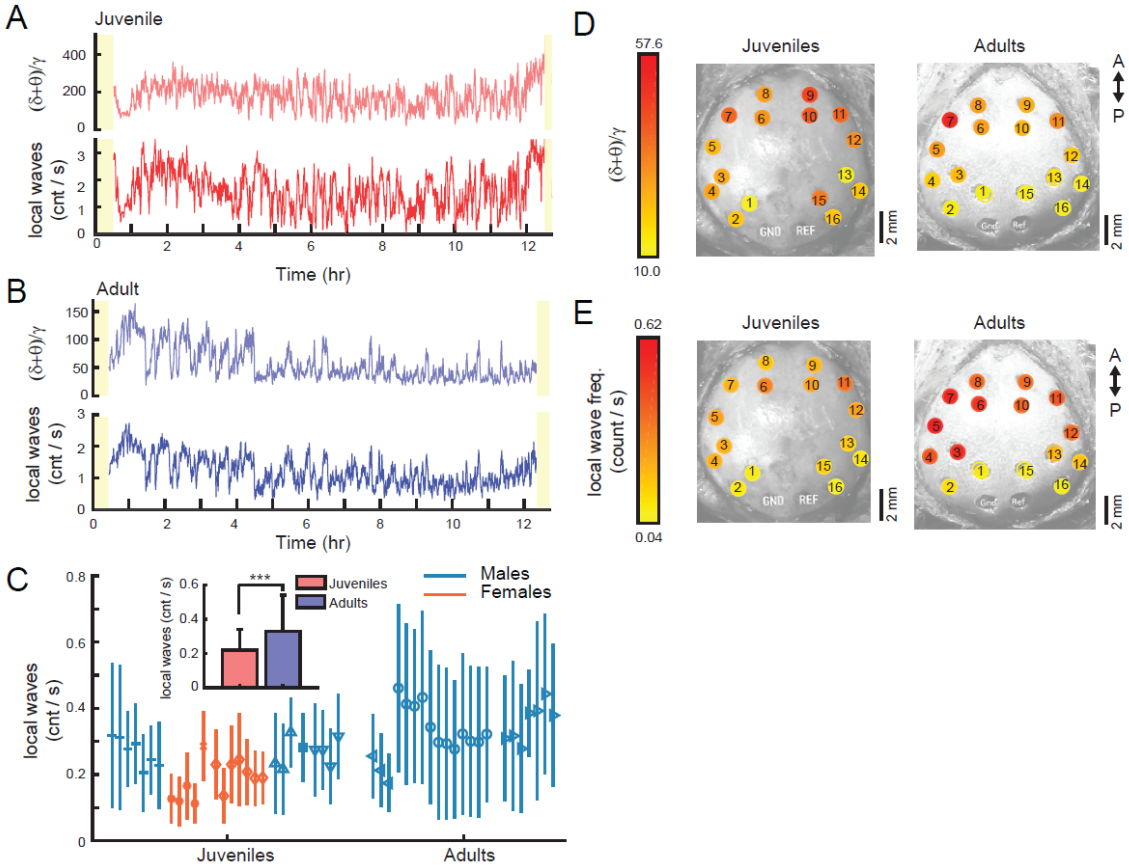


**Figure 3. Local waves have a higher incidence in adults and a posterior-anterior axis.** (A) An example of the (δ+θ)/γ trace for a juvenile bird (top, light red line) and the corresponding rate of occurrence for the local waves (bottom, dark red line) for a whole night of sleep (same juvenile as in Fig. 1D; black arrow in Fig. 1E). The occurrence of local waves was correlated with the (δ+θ)/γ ratio, i.e., local waves occurred more often during periods of high (δ+θ)/γ values. Note how this juvenile has a much larger median (δ+θ)/γ ratio compared to other juveniles and adults (see Fig. 1E), which may account for the large rate of local wave occurrence compared to the adult in (B). (B) An example of the (δ+θ)/γ trace for an adult bird (top, light blue line) and the corresponding rate of occurrence for the local waves (bottom, dark blue line) for a whole night of sleep (same adult as in Fig. 1D; black arrow in Fig. 1E). Data in (A) and (B) have been smoothed with a 30-s moving average filter for visualization purposes. (C) The average rate of occurrence for local waves across nights for all birds. Each symbol represents a different bird, and different nights of sleep are presented sequentially. Teal lines indicate males; orange lines indicate females. Vertical line

indicates the SD for the night. Inset: local waves occur significantly more frequently in the adult birds (blue bars) compared to juveniles (red bars; $p=6.7\times10^{-7}$; two-way unbalanced ANOVA) Error bars indicate SD. (D) Average $(\delta+\theta)/\gamma$ values computed at each electrode site across all juveniles (left) and all adults (right). $(\delta+\theta)/\gamma$ values are higher in anterior regions (red colors) compared to posterior sites (yellow colors). This anterior-posterior gradient is especially pronounced in adults. GND, ground electrode; REF, reference electrode; A, anterior; P, posterior. (E) Average rate of local waves computed at each electrode site across all juveniles (left) and all adults (right). Same figure conventions as for (D). An anterior-posterior gradient is also present for the local waves, such that anterior sites have a higher rate of local wave occurrence compared to posterior sites.

## Local waves occur more frequently during sleep in adults compared to juveniles

Sleep stages, such as REM sleep and SWS, are widespread events that are usually distinguishable based on their unique neural signatures.[3] In both adult and juvenile zebra finches, we observed that global aspects of sleep were highly similar across recording sites (e.g., Fig. 1D). However, we also observed short duration (10-100 ms) "local waves" that spanned a narrow range of EEG electrodes (see Fig. 1C, black dotted boxes, for examples). We defined local waves as oscillations that occurred on 25% to 75% of the electrodes at a given time (see Methods for details). Importantly, these local waves were distinct from unihemispheric SWS activity[39,40] in which patterns of slow waves are observed globally in one hemisphere but not the other and which typically have durations of tens of second or longer.

We quantified the occurrence of local waves relative to the $(\delta+\theta)/\gamma$ trace in both juveniles and adults (Fig. 3A, B). The occurrence of local waves was highly correlated with the $(\delta+\theta)/\gamma$ values; that is, we observed that periods of high $(\delta+\theta)/\gamma$ values corresponded to an increase in the number of local waves. The correlation between $(\delta+\theta)/\gamma$ values and the occurrence of local waves, calculated across all nights in 3-s bins was significant and relatively high for the adults ($0.52 \pm 0.14$; $p=1.5\times10^{-19}$; $n = 22$ nights; median ± interquartile interval, Pearson's correlation test). The correlation between the $(\delta+\theta)/\gamma$ values and the occurrence of local waves for juveniles, while lower, was also significant ($0.30 \pm 0.28$; $p=1.7\times10^{-4}$; $n = 27$ nights; Pearson's correlation test).

In juvenile birds, the rate of local wave occurrence ranged from 0.19 to 0.32 events/s (Fig. 3C). When averaged over all the nights for all juvenile birds, local waves occurred at a rate of $0.22 \pm 0.12$ events/s (mean ± SD), or about 1 local wave every 4.5 seconds. The rate of occurrence was slightly higher in adult birds, and ranged from 0.28 to 0.46 events/s (Fig. 3C). When averaged over all adult birds, local waves occurred at a rate of $0.33 \pm 0.21$

events/s, or about 1 local wave every 3 seconds. This difference was significant ($p=6.7\times10^{-7}$; two-way unbalanced ANOVA; Fig. 3C inset). Furthermore, we also observed a small but significant effect of the bird's sex on the local wave occurrence, such that local waves occurred significantly less frequently in females versus males (all males = 0.30 ± 0.19 events/s versus all females = 0.22 ± 0.14 events/s; p=0.013; mean ± SD; two-way unbalanced ANOVA).

**Local waves and slow waves are organized along an anterior-posterior axis during sleep**

It is known that there is an anterior-posterior axis for slow wave activity in humans, such that larger slow waves are typically recorded on anterior EEG sites compared to posterior sites.[36] We were curious to see if slow waves and local waves were similarly localized in the avian brain. Indeed, we observed that anterior EEG sites in both adult and juvenile zebra finches exhibited larger $(\delta+\theta)/\gamma$ values compared to posterior positions (Fig. 3D; red colors). We observed a similar trend for the local waves, which occurred more frequently in anterior sites compared to posterior sites, especially for adults (Fig. 3E; red colors).

The anterior electrode sites were located above the hyperpallium (electrodes 8, 9, 6, 10; Fig 3D, E) and the lateral end of the mesopallium (electrodes 7 and 11), whereas the posterior sites were located above the song nucleus HVC (electrodes 1 and 15 in males), the end of the arcopallium (electrodes2, and 16), or mesopallium (electrodes 3, 13). These findings suggest that there could be a developmental aspect to the localization of local waves to anterior sites, such that during the process of brain maturation and cortical specialization, the neuroanatomical development of the avian brain facilitates the spread of low-frequency oscillations (1.5-8 Hz) in anterior sites.

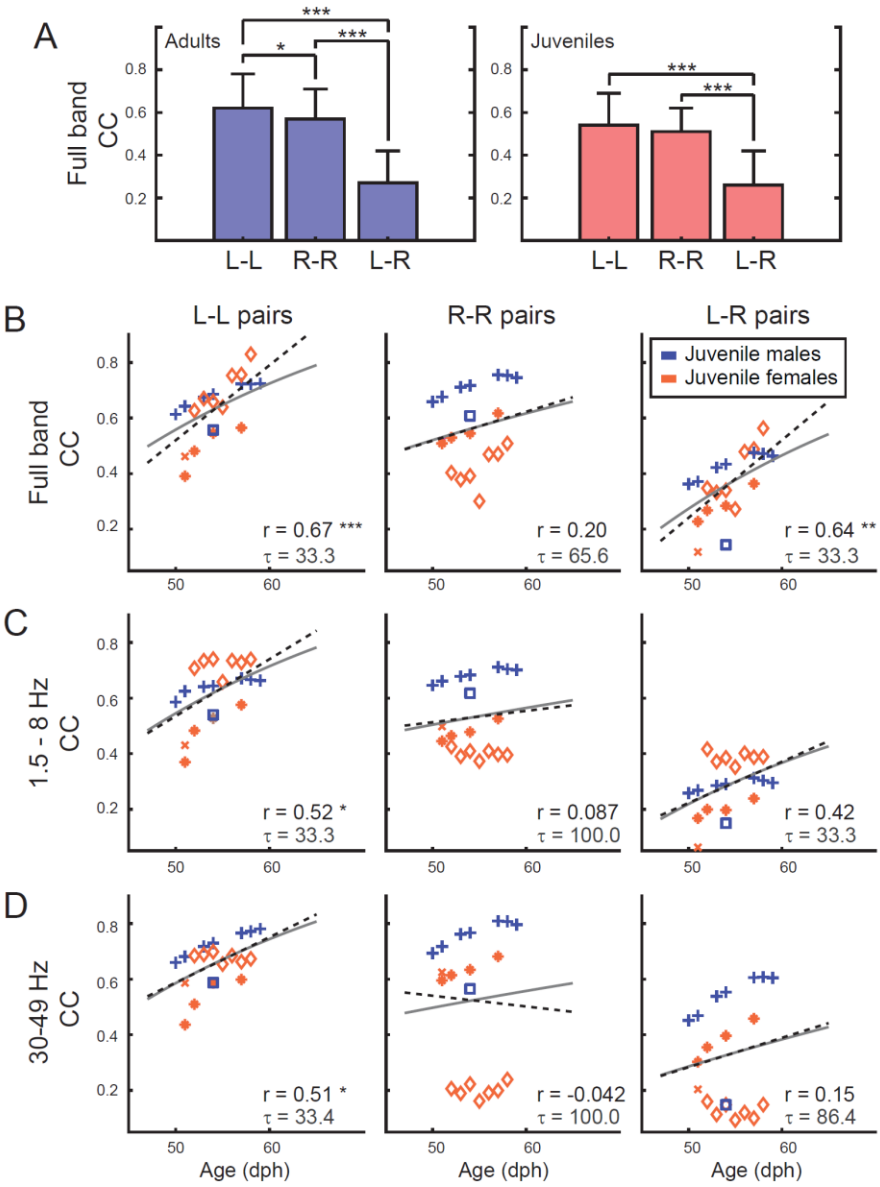


**Figure 4. Left intra-hemispheric functional connectivity increases linearly during early maturation in juveniles**

(A) Functional connectivity was calculated between pairs of electrodes using Pearson's correlation coefficient (CC) on the full band EEG signal. Pair-wise comparisons of electrodes located in the left hemisphere (L-L) were calculated separately from electrodes pairs located in the right hemisphere (R-R). In both adults and juveniles, L-L and R-R CCs were significantly larger than CCs calculated for inter-hemispheric electrode pairs (L-R). Furthermore, in adults, L-L CCs were significantly larger than R-R CCs. (B) Scatter plot depicts the average L-L, R-R, or L-R CCs calculated for each night as a function of the juvenile birds' age. Each symbol represents a different juvenile bird (same symbols as for Fig. 1E and Fig. 3C), and different nights of sleep are presented sequentially. Blue symbols indicate males; orange symbols indicate females. CCs were computed on the full band EEG signal (1.5 - 200 Hz). Black dotted line indicates the linear fit of the data, and the corresponding r value is located in the lower right corner. Asterisks indicate significant linear fits (* $p \leq 0.05$; ** $p \leq 0.01$; *** $p \leq 0.001$). Gray line indicates the exponential fit of the regressed data, and the corresponding time constant $\tau$ is located in the lower right corner. A significant linear trend

existed for L-L and L-R electrode pairs, but not R-R pairs. (C) Scatter plot depicts the average L-L, R-R, or L-R CCs calculated on the low frequency EEG band (1.5 - 8 Hz). Figure conventions same is in (B). For the low frequency band, only the L-L electrode pairs showed a significant linear increase in functional connectivity as a function of age. (D) Scatter plot depicts the average L-L, R-R, or L-R CCs calculated on the high frequency EEG band (30 - 49 Hz). Figure conventions same is in (B). For the high frequency band, only the L-L electrode pairs showed a significant linear increase in functional connectivity as a function of age.

## Functional connectivity is highest during SWS and lowest during REM in adults

Functional connectivity refers to the statistical (inter)dependence of neural activity in spatially distinct brain areas.[37] In particular, inter-areal synchronization of oscillations is thought to be important for normal brain function[38] and may facilitate the flow of neural information between different brain areas.[39] We explored the inter- and intra- hemispheric functional connectivity of juvenile and adult zebra finches using the between-electrode Pearson's correlation coefficient[38] (CC; Methods).

For adult birds, but not the juveniles, we found that the functional connectivity was significantly different as a function of sleep stage ($p=0.003$ in adults; and $p=0.66$ in juveniles; Friedman test). In adults, the functional connectivity was highest during SWS (CC = 0.52 ± 0.29; mean ± SD) and lowest during REM sleep (CC=0.49 ± 0.27) when averaged over all pairs of electrodes (n=2299 pairs).

## Left intra-hemispheric connectivity is higher during sleep in adults

During sleep in both adults and juveniles, we often observed strong synchrony of the EEG signal within a hemisphere, but also across hemispheres (see Fig. 1C; Supplementary Fig. S1D). We quantified this by comparing between-electrode CCs for all pairs of intra-hemispheric (L-L pairs and R-R pairs) and inter-hemispheric electrodes (L-R pairs) separately during the whole night of sleep.

For both adult and juvenile birds, the intra-hemispheric CCs were larger than the inter-hemispheric correlations. For adults, the average intra-hemispheric CC was 0.62 ± 0.16 for L-L pairs (mean ± SD) and 0.57 ± 0.14 for R-R pairs, whereas the average L-R inter-hemispheric CC was much smaller: 0.27 ± 0.15 (Fig. 4A, blue bars). This difference was significant across comparisons ($p=1.44e-53$; two-way ANOVA) and post-hoc tests revealed significant differences for all three comparisons (Fig. 4A, asterisks; see Supplementary ANOVA table for exact p values). Notably, in the adult group, the functional connectivity was significantly higher for electrode pairs in the left hemisphere compared to the right hemisphere ($p=0.040$, post-ANOVA Tukey-Kramer multiple comparison test).

The same trend was also true for juveniles (L-L = 0.54 ± 0.15; R-R = 0.51 ± 0.11; L-R = 0.26 ± 0.16 (Fig. 4A, red bars) and these differences were significant across comparisons (p = 9.64e-23; two-way ANOVA). However post-hoc tests revealed that only the inter-hemispheric comparisons were significant for juveniles (Fig. 4A, asterisks).

**Left intra-hemispheric functional connectivity increases linearly during early maturation in juveniles**

We observed that the average intra- and inter-hemispheric CCs were higher in sleeping adults compared to sleeping juveniles, and we wondered whether we could observe an increase in the functional connectivity as a function of maturation. For this analysis, we used the data from the younger juveniles in our study (age < 60 dph, n=5 out of 7 juveniles; see Supplementary Fig. S7A, B for the data from other birds). We did not observe a significant change in the functional connectivity as a function of age in adult birds (p>0.05; t-test).

We used two methods to look for an age-related increase in the functional connectivity in juveniles. First, we analyzed whether there was a linear relationship between the intra- and inter-hemispheric CCs and the age of the bird. Second, we regressed the intra- and inter-hemispheric CCs as a function of the birds' age (see Methods for details). To account for possible differences in the synchrony of the EEG oscillations at different frequencies, we computed the functional connectivity CCs for three different passbands: the full band (1.5-200 Hz; Fig. 4B), the low frequency band (1.5-8 Hz; Fig. 4C), and the high frequency band (30-49 Hz; Fig. 4D).

Interestingly, we observed that the functional connectivity increased linearly as a function of age for L-L electrode pairs in all frequency bands (Fig. 4C-D; R value asterisks), but that this was not true for R-R electrode pairs. Inter-hemispheric connectivity only increased as a function of age when computed for the full band, but not for the low or high bands individually.

When we examined the time constant $\tau$ arising from the regression model, values ranged from 33 to 100 days, demonstrating a fast increase of functional connectivity during maturation. We observed the highest rate of increase for the left hemisphere (L-L) pairs and for the inter-hemispheric (L-R) correlations.

These findings support the hypothesis that the juvenile zebra finch brain undergoes rapid changes in connectivity that stabilize in adulthood, and which is in line with observations in human studies.[40]

**Graph theory analysis reveals larger networks of correlated EEG activity in adults compared to juveniles.**

Although we observed broad differences in functional connectivity within and across hemispheres during sleep, we wanted to investigate functional connectivity at a finer spatial resolution. Borrowing methods from graph theory, (Fig. 5A; see Methods for details), we identified dominant co-active networks in juvenile and adults during SWS, REM sleep, and IS sleep. For each night, we considered each recording electrode as a "graph node" and analyzed 3-sec bins of EEG according to its putative sleep stage as determined by its $(\delta+\theta)/\gamma$ value. We connected a pair of electrodes with a link if their activity was significantly correlated. Then we extracted the sub-networks for which each electrode was highly correlated with all the other electrodes in the sub-network. We only analyzed the sub-networks that appeared at least in 10% of the bins throughout the night, for three separate nights (See Supplementary Fig. S8 for results using an appearance threshold of 5% and 15%; results are in line with those presented here). For simplicity we denote such a highly correlated sub-network as a "dominant network". Examples of these dominant networks are displayed in Fig. 5B (adult) and Fig. 5C (juvenile).

We analyzed the 8 out of 10 birds for which we had at least 3 nights of data (3 adults and 5 juveniles). In these birds, the size of dominant networks (the number of nodes; Fig. 5D), and their abundance (the number of dominant networks per bird; Fig. 5E), was used as an indication of overall connectivity.

On average, the dominant network size was significantly larger for adults compared to juveniles (Fig. 5D; 8.2 ± 2.9 electrodes (mean ± SD) for the adults and 4.2 ± 2.1 electrodes for the juveniles; $p=3.0 \times 10^{-8}$, Wilcoxon rank-sum test). On the other hand, the networks were more numerous in juveniles compared to adults (Fig. 5E; 7.3 ± 4.6 networks on average for adults and 10.6 ± 4.6 dominant networks in the juveniles).

The graph theory analysis reveals two distinct patterns in adults and juveniles: in adults, highly correlated EEG activity tends to be distributed across fewer networks that are spread across a wider area of the brain, whereas in juveniles, highly correlated EEG activity is distributed across more numerous, albeit smaller, networks in the brain.

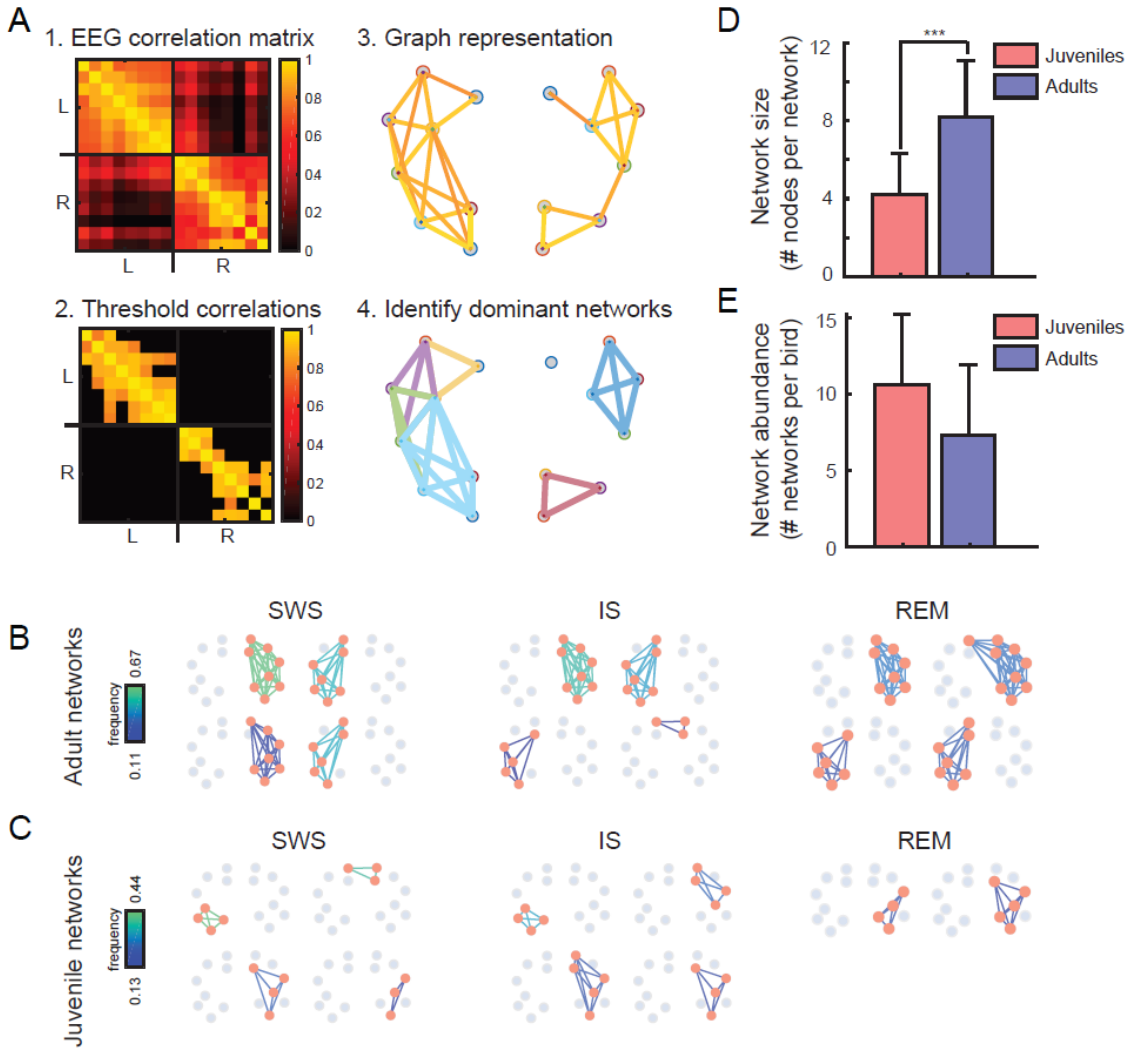


**Figure 5 Highly correlated EEG activity is distributed across a few large networks in adults and several small networks in juveniles.** (A) The main steps for the extraction of highly-correlated networks are illustrated (see Methods for more details). 1-The EEG correlation matrix was computed for each 3-sec bin. 2- Significantly correlated pairs were kept for further analysis, based on a statistical method[46]. 3- A graph representation of the significantly correlated pairs is constructed. To construct this graph, each EEG electrode was represented as a node, and a link connected two nodes in the case where the correlation between the corresponding EEG electrode was significantly high. 4. Using the Bron-Kerbosch algorithm from graph theory[41] we extracted the sub-networks for which all electrodes were highly correlated, the "dominant networks". (B) Dominant networks extracted from an adult during SWS, IS, and REM stages of sleep for 3 nights. A dominant network is indicated as a collection of orange nodes (the electrode sites) and the lines connecting them. Color coding of the lines represents the frequency of occurrence for each network across bins, i.e. the fraction of bins where the network appeared. Gray dots indicate nodes that are not included in the networks. In adults, dominant networks contain several nodes (are larger) but occur less frequently. (C) Dominant networks extracted from a juvenile during SWS, IS, and REM stages of sleep across all nights. Figure conventions same as in (B). In juveniles, dominant networks contain fewer nodes, but occur frequently. (D) Dominant network size was significantly larger for adults compared to juveniles. Error bars indicate the SD. (E) Dominant network abundance was lager for juveniles compared to adults, but not significantly different. Error bars indicate the SD.

## Discussion

In this study, we analyzed the sleep EEG recorded in 12 hour periods from 3 adult and 7 juvenile zebra finches, totaling more than 600 hours of recorded data for all animals. We analyzed differences in the sleep patterns between juveniles and adults using two main approaches: 1) we analyzed sleep as a continuous variable using the $(\delta+\theta)/\gamma$ ratio and 2) we categorized sleep into discrete stages using an automatic avian sleep clustering algorithm.[5,6] Whereas the former approach acknowledged the continuous nature of sleep-related dynamics, the latter approach allowed us to numerically characterize certain aspects of avian sleep and compare our results with other avian sleep studies.

We measured sleep EEG from 16 electrodes spanning the surface of the skull (Fig. 1A). We observed that across the electrode sites, $(\delta+\theta)/\gamma$ traces were globally similar in the time-scale of minutes (Fig. 1D). Although we observed an anterior-posterior organization of $(\delta+\theta)/\gamma$ values, such that anterior electrode sites tended to show larger $(\delta+\theta)/\gamma$ values than the posterior sites (Fig. 3D), these observations suggest that it is sufficient to use 1 or 2 (anterior) electrodes to measure sleep EEG, as many avian sleep studies have done.[5,6,12,13,18,21]

### Age-related differences in sleep between adults and juveniles: IS sleep and vocal learning

Vocal learning in songbirds is one of the few innate learning models that can be used to study sleep effects on memory. Although the link between REM sleep or SWS and vocal learning has not been investigated directly, behavioral experiments during song learning in juvenile zebra finches have highlighted a role for sleep.[42,43] Tutor song exposure causes a circadian pattern to develop in the vocalizations of the juvenile birds which continues into adulthood but does not exist prior to tutor song exposure. Experiments in another songbird, the starling, using an operant conditioning paradigm to train birds to discriminate between different auditory stimuli, showed that sleep supports the consolidation of recent auditory memories.[44]

The juveniles in these experiments were housed with their fathers. During the time of the recordings, juvenile males were engaged in vocal learning, and juvenile females were exposed to their father's songs and potentially engaged in auditory learning.[45,46]

We observed several differences in the sleep patterns between adults and juveniles. When we segmented sleep into SWS, REM sleep, and IS sleep, we found that adults spent a significantly larger percentage of the night in SWS and REM sleep compared to juveniles, whereas juveniles spent significantly more time in IS sleep compared to adults (Fig. 2C). When we examined male and female juveniles, we found that the male juveniles spent a significantly larger percentage of the night in IS sleep compared to female juveniles and that IS sleep bouts were longer in duration for juvenile males compared to females. Furthermore, juvenile males transitioned significantly more frequently to IS sleep stages compared to females. These results suggest that IS sleep could be an important aspect of vocal learning in juvenile males.

IS sleep is distinct from REM sleep, and it often occurs as a transition state between SWS and REM sleep. IS sleep typically contains a mix of low-amplitude delta and higher-frequency elements such as theta[6] (see Supplementary Fig. S3A for examples). As such, it is often not possible for human scorers to identify the onsets and offsets of IS sleep.[5,6] Indeed, analysis techniques that are reliant on human scorers to segment EEG data tend to categorize sleep into REM and NREM stages,[10,47] where NREM segments in this case contain both SWS and IS sleep, and the majority of the avian sleep literature focuses on REM versus NREM sleep.

Sleep is known to be important for learning, and specifically, SWS is known to have a critical role in the maintenance of memory in rodents[30,48,49] and humans.[50–52] However, it is unclear how to relate IS sleep to SWS. One commonality is that SWS and IS sleep are both characterized by large, slow oscillations, and it may be that slow oscillations, in general, have a similar role in memory consolidation in the avian brain.[53] Indeed, when we examined median $(\delta+\theta)/\gamma$ ratios, we found that the $(\delta+\theta)/\gamma$ ratios were significantly higher for juveniles compared to adults (Fig. 1E).

The role of slow waves and learning have not been thoroughly investigated in birds. One study in chicks observed a significant relationship between EEG theta oscillations that occurred during imprinting and memory consolidation during sleep, lending support to the idea that slow oscillations may have a role in avian learning.[54] Additional investigations in birds that leverage behavioral paradigms such as vocal learning[55–57] or spatial memory[58–60] could help us better understand the interplay between slow oscillations and different types of memory in the developing avian brain.

## Sleep ontogeny in birds and mammals

Newborn mammals are thought to spend as much as 90% of their sleep time in a state that resembles an immature form of adult REM characterized by frequent muscle twitches, rapid eye movements, and irregular respiratory cycles.[61] However, an alternative view suggested that REM sleep is actually not present at birth, but rather that these behavioral patterns could be spontaneous activity typical of an immature nervous system.[62]

In human development, children and adolescents spend more time in SWS. A meta-analysis of the literature showed that the percentage of SWS is significantly negatively correlated with age.[63] Similarly, a longitudinal study in children and adolescents revealed that NREM delta and theta activity drops sharply at the age of 10 and continues to decline until the age of 16.[64] In humans, the reduction of slow waves is linked with the reduction of gray matter during the course of cortical maturation in adolescence.[65] We speculate that the importance of SWS during human adolescence might be similar to the importance of IS sleep for male juvenile zebra finches, as both phases involve intense phases of learning and neural reorganization. However, more studies that examine the exact role of IS sleep during learning in birds are required to explore this idea in greater detail.

Sleep ontogeny has not been thoroughly investigated in birds. One study examined sleep in young barn owls aged 27-48 dph and found that the amount of time spent in REM sleep decreased linearly with age.[21] We did not find such a trend in our juvenile zebra finch data (Supplementary Fig. S5A). Rather, our work shows that adults have an increase in the amount of time spent in REM sleep and SWS and a decrease in IS sleep compared to juveniles. One obvious distinction between these two avian species is that juvenile zebra finches are engaged in vocal learning whereas juvenile barn owls are not. Similarly, zebra finches are daytime-active seed eaters, whereas owls are night-active predators. Such behavioral differences may account for the discrepancy in sleep patterns observed between these juvenile birds.

## The role of left hemisphere activity and brain lateralization in birds

Inter-areal synchronization of oscillations, also known as functional connectivity, is thought to facilitate the flow of neural information between different brain areas. We found that in adult zebra finches, the functional connectivity was significantly higher in the left hemisphere compared to the right hemisphere (Fig. 4A). Furthermore, we found that in our young juveniles (n=5/7 birds) the functional connectivity increased linearly as a

function of age for electrode pairs located on the left hemisphere (Fig. 4B). These results indicate an important role for neural synchronization of the left hemisphere. Indeed, several studies have already examined lateral asymmetry of the brain and behavior in the zebra finch and found left hemisphere dominance for both visual and auditory information processing related to courtship singing and visual displays. [66–68]

More generally, different cognitive tasks seem to be associated with different patterns of brain lateralization in birds.[69] Larger left hemisphere activation has been observed in pigeons engaged in visual discrimination tasks, whereas larger right hemisphere activation has been associated with animals engaged in spatial memory tasks.[70] In chickens, a task involving searching for food was associated with larger left hemisphere activation, while a predator avoidance task was associated with larger right hemisphere activation.[71] These results suggest that there is an advantage inherent in the lateralization of certain tasks in birds. We observed that intra-hemisphere synchrony was higher than inter-hemisphere synchrony in both adults and juveniles (Fig. 4A). The synchronous (re)activation of brain areas during sleep might be an important aspect of the stabilization of neural information during maturation and adulthood.

**An anatomical basis for reduced inter-hemispheric functional connectivity in birds**

In this work, we found that the inter-hemispheric functional connectivity was almost half of the intra-hemispheric connectivity for both juveniles and adults (Fig. 4A). This result is almost certainly a function of the reduced anatomical pathways connecting the left and right hemispheres in birds.

In mammals, the corpus callosum heavily interconnects the right and left cortical hemispheres. The inter-hemispheric connections in birds are far fewer, and the telencephalic pallium, sensory-motor, and associative regions receive limited input from the contralateral hemisphere.[72,73] The only inter-hemispheric pathways at the telencephalic level in birds consist of the anterior commissure and the much smaller hippocampal commissure.[72]

In addition, the great majority of pallial areas do not participate by themselves in inter-hemispheric exchange in the avian brain.[72] Instead, commissural exchange rests on a rather small arcopallial and amygdaloid cluster of neurons.[72] In comparison, in the eutherian mammals which includes humans and rodents, the cingulate cortex and most of isocortex are connected to the contralateral homotopic regions via abundant interhemispheric corpus callosum tracts.[74]

However, it is worth noticing that the lower inter-hemispheric connectivity in the avian brain is not necessarily a disadvantage compared with placental mammals. For instance, unihemispheric sleep, which is observed in many bird species,[8,9,75–77] including the zebra finch,[5] helps the bird overcome the problem of sleeping in a risky environment,[8] and might be facilitated through weaker inter-hemispheric connectivity. Another indication of more independent hemispheres that might be related to the absence of corpus callosum is independent eye movements enabling birds to scan 78 and focus [79] upon different environmental stimuli simultaneously.

Since maintaining a normal level of functional connectivity is essential for the brain to function properly,[80–82] we hypothesize that in birds, the evolution of brain connectivity took an alternative path in contrast with the emergence of corpus callosum in placental mammals; namely, that the left and right hemispheres developed stronger intra-hemispheric connectivity to compensate the lower inter-hemispheric connectivity while maintaining higher levels of hemispheric autonomy. However, more rigorous verification of this hypothesis would require further studies of functional connectivity in combination with brain stimulation to simultaneously measure effective connectivity, similar to human studies.[83,84] Further studies which examine functional connectivity in birds directly using non-invasive imaging techniques like functional MRI[85–87] would be a welcome addition.

**The effects of courtship on sleep: Potential confounds and prospects for future research**

In this study, juvenile and adult zebra finches were housed under different social conditions. We were not permitted to house animals in isolation, therefore, the 3 male adults were housed individually, but in visual and auditory contact with an adult female. In contrast, the male and female juvenile birds were housed individually, but in visual and auditory contact with their tutor father. Under these circumstances, the juvenile birds were exposed to the songs of their fathers and were assumed to be engaged in vocal learning (juvenile males) and/or auditory learning (juvenile females). In contrast, placing adult male birds in view of adult female birds might have induced courtship behavior.

This fundamental difference in the social housing conditions between adults and juveniles could have impacted the sleep in adults and juveniles differentially and could account for some of the differences we observed between juveniles and adults. For example, exposure to conspecifics of the other sex might modulate hormonal levels that affect arousal and activity during wakefulness, and which could in turn change aspects of sleep.

However, we observed that several aspects of adult male sleep matched the results from a previous sleep study in adult zebra finches,[5] including 1) a decrease in SWS as the night progresses and 2) an increase in REM sleep as the night progresses. Furthermore, the durations of SWS, REM sleep, and IS sleep states for our adult birds were all within range of those values previously reported.[5] This suggests that the differences we observed in sleep between adults and juveniles were not in fact due to differences in social housing. However further experiments, where for example the sleep EEG is recorded in adult females housed in visual and auditory contact with other adult females would help to clarify the potential effect of courtship behavior on sleep.

## Methods

### Ethical guidelines

All experiments were carried out in accordance with the principles of laboratory animal care and were conducted under the regulation of the current version of the German and European laws on Animal Experimentation (Approval # ROB-55.2-2532.Vet_02-18-108: J.M.O.), complying with ARRIVE guidelines. The study was approved by the ethics committee of the Government of Upper Bavaria (Regierung von Oberbayern; Committee following § 14.1 TierSchG (German animal welfare law)). Housing and breeding of animals were approved by the Veterinary Office of Freising, Germany (Approval # 32-568).

### Experimental animals

We used 3 adult and 7 juvenile zebra finches in these experiments. Zebra finches reach their sexual maturation at around 90 days post hatch (dph). The sex and the age of the birds at the first recording night are summarized in Table. 1.

| Name | symbol | sex | age (dph) | # of good electrodes |
|---|---|---|---|---|
| w009 | + | m | 50 | 15 |
| w016 | * | f | 50 | 13 |
| w020 | □ | m | 53 | 16 |
| w018 | X | f | 51 | 14 |
| w021 | ◊ | f | 52 | 13 |
| w043 | Δ | m | 69 | 15 |
| w041 | ∇ | m | 69 | 15 |
| 73-03 | < | m | 686 | 16 |
| 72-00 | ○ | m | 764 | 14 |
| 72-94 | > | m | 780 | 15 |

**Table 1 Description of experimental birds used in this study.** Bird name, symbol, sex, age in days post hatch (dph) at the first night of recording, and number of non-noisy electrodes recorded in the zebra finch is indicated. Table follows the same order as the data displayed in Fig. 1E.

Prior to experiments, birds were housed on site in aviaries and were kept on a 12:12-hr light: dark cycle. Finches received seed mix, millet, sepia bone, and water *ad libitum* and were given fresh salad and cooked egg supplements once a week.

### Behavior and video acquisition

Zebra finches were acclimated to the recording chamber for at least 5 days prior to the experiments. Experimental animals were kept together with a non-experimental female bird (adults) or the father tutor bird (juveniles) to prevent social isolation. Birds were separated from each other with a clear Plexiglas panel, such that animals could hear and see each other but could not interact physically.

In the recording chamber, finches received seed mix, millet, sepia bone, and water *ad libitum*. The recording chamber (total inner measurements: 120 cm x 50 cm x 50 cm) was equipped with LED lights, a UV bird light (Bird Systems, Germany), an infrared (IR) LED panel (850 nm), and had continuous air circulation. Video footage of the experimental animal was acquired with a near-IR sensitive camera (acA1300-60gm, Basler Ag, Germany) with custom-written software (ZR View, Robert Zollner) at a frame-rate of 20 fps, triggered with a pulse generator (Pulse Pal,[88] Sanworks, NY, USA).

### Electrode preparation and positioning

For each experiment, we constructed silver ball EEG electrodes from silver wire (254 µm bare wire diameter, Science Products GmbH, Hofheim, Germany) by melting the tip of the wire into a smooth ball of approximately 0.50 mm in diameter using a Bunsen burner (CFH Löt- und Gasgeräte GmbH, Offenau, Germany). 18 electrodes were implanted: 8 electrodes were implanted over each hemisphere, and 2 additional ground and

reference electrodes were implanted over the cerebellum (Fig. 1a). Electrode sites varied slightly across adult birds to avoid superficial blood vessels (variation less than 0.5 mm). The adult electrode map was rescaled for juveniles due to difference in head size, in order to maintain the relative electrode spacing. The brain structures underlying each electrode, according to the Nixdorf-Bergweiler zebra finch brain atlas[89] are listed in Table 2.

| Bilateral electrode pair | Underlying brain structures |
|---|---|
| 1, 15 | Medial end of HVc, Caudal end of Mesopallium |
| 2, 16 | Tractus dorso-arcopallialis, end of Arcopallium |
| 3, 13 | Lamina mesopallialis |
| 4, 14 | Lateral end of Lamina mesopallialis |
| 5, 12 | Hyperpallium apicale, lateral side of Lamina frontalis suprema |
| 6, 10 | Hyperpallium apicale, frontolateral side of Lamina frontalis suprema |
| 7, 11 | Lateral end of Mesopallium |
| 8, 9 | Frontal end of Hyperpallium apicale |

**Table 2 Position of the electrode relative to the underlying brain structures.**

## Anesthesia and Surgery

Zebra finches were anesthetized with isoflurane (1-3 %) mixed with oxygen generated with an oxygen concentrator (EverFlo OPI, Phillips, Netherlands) and administered using a vaporizer (Isotec 4, Groppler, Germany) through a small tube directly into the beak of the bird. Excess isoflurane was collected and filtered (Scavenger LAS, Groppler, Germany). The body temperature was monitored with an infrared thermometer (EVENTEK E300, ShenZhen ShengYa Hardware Products Co, China), and maintained at above 39.5°C through the use of a homoeothermic heating pad (Harvard apparatus, MA, USA).

Under anesthesia, the experimental animal was positioned in a small animal stereotaxic frame (Kopf Instruments, CA, USA). The scalp was anesthetized with xylocaine (Xylocain Pumpspray, Aspen Pharma Trading Limited, Ireland), the feathers were removed with forceps, and the scalp was resected along the midline. For each EEG electrode, a small hole was drilled above the forebrain with a high speed dental drill (Volvere i7, NSK Europe GmbH, Germany). EEG electrodes were placed in the sites and secured using dental cement (Paladur, Henry Schein Dental, Germany).

Following surgery, the animal was released from the stereotaxic frame and administered a dose of Metamizol (100-150 mg/kg, i.m.). The animal

remained on a heating pad until full recovery from anesthesia. An antibiotic (Baytril, 1025 mg/kg, i.m.) and an analgesic (Carprofen, 4 mg/kg, i.m.) were administered up to 3 days post-operatively. Following recovery from surgery, the animal returned to entirely normal feeding, sleeping, and singing behaviors as observed before surgery.

**Overnight electrophysiological recordings**

Recordings were started at the second night after the implantation. One hour before lights off (light off period: 9:00 PM - 9:00 AM), the animal was connected to the head-stage and custom-made lightweight tether cable and allowed to assume a natural sleep posture on a branch that had been placed on the floor of the chamber. The camera was positioned to allow for the best visualization of the animal during sleep. The animal was allowed to sleep naturally overnight, and was disconnected from the headstage and tether cable shortly after lights turned on. Data from the first night after surgery was not used in the analysis.

The EEG electrodes were connected to a preamplifier (Intan Technologies, RHD2132), which was connected to the data acquisition board via the tether cable. The implant (cement, omnetics connectors, and wires) weighed ~0.5-0.6 g. The preamplifier weighed 0.95 g. This combined weight of approximately 1.5 g was offset with an elastic string that was connected to the tether cable and was in the range of other impants and microdrives used in zebra finches.[90–92] Recordings were performed with an Open Ephys acquisition board[93] (Open Ephys Production Site, Portugal). Recordings were grounded and referenced against one of the reference wires. Signals were sampled at 30 kHz, wide band filtered (0.1-9987 Hz), and saved in a continuous format using the Open Ephys GUI.

**Anatomy**

After the period of recording was over, the animal was deeply anesthetized with an overdose of sodium pentobarbitol (250 mg/kg, i.m.) until the corneal reflex disappeared. Afterward, the animal was decapitated, the brain was removed from the skull and post-fixed in 4% paraformaldehyde in PBS for postmortem verification of electrode sites.

## Data Analysis

### Video Motion Extraction

We developed a program in MATLAB (The MathWorks Inc., Natick, MA, USA) to extract a single variable that represents the overall amount of frame-by-frame movements. For each 2 consequent frames ($m \times n$ matrices containing gray-scale pixel values), we first computed the absolute value of the difference (equation (1)).

$$diff(k)_{m,n} = \left| frame(k)_{m,n} - frame(k-1)_{m,n} \right| \qquad (1)$$

where $k$ represents the frame number. $diff(k)_{m,n}$ will have a non-zero value at any pixel that has changed from frame $k-1$ to frame $k$. Then we extract the weighted average of $diff(k)_{m,n}$ along the x and y axes separately. For example for the weighted average along the x axis, we sum up the $diff(k)_{m,n}$ values along the rows and then scale it by the vector $[1\ 2 \ldots n]$, the x vector, (equation (2)).

$$x = [1\ 2 \ldots n]', \quad S_{\mathrm{x}} = sum(diff(k)_{\mathrm{m.\,n}}, 1) \times x \qquad (2)$$

$S_y$ is acquired in the same way. At the end, using pythagoras formula, we merge Sx and Sy to achieve the total magnitude of movement (equation (3)).

$$Movement(k) = \sqrt{{S^2}_x + {S^2}_y} \qquad (3)$$

**EEG preprocessing and (δ+θ)/γ ratio analysis**

EEG was down-sampled by a factor of 64 (final sampling rate: 468.75 sps). The EEG signal from each electrode was normalized (using the MATLAB "z-score" function) to avoid inhomogeneities that might arise from changes in the impedance of electrodes over days and binned into 3-s windows.

Sleep was behaviorally defined based on movement extracted from the video data. Bins where the movement was above its median by 2 interquartile intervals were labeled as awake and consequently excluded from analysis. This automatic sleep/wake labeling was validated on one data set that was that was also labeled visually as ground truth. Additional bins were excluded for which the EEG amplitude was more than 4 interquartile intervals above the zero base line. In total, approximately 400, 3-s bins (or 20 minutes of data, or less than 3%) were discarded per night of recording due to artifact rejection. Finally, some electrodes were broken and were therefore excluded from all further analysis. The number of used electrodes for each bird is reported in Table 1.

We first assessed the sleeping brain dynamics not in discrete stages, but as a continuous variable, the (δ+θ)/γ ratio, defined as the ratio of power in delta and theta bands (δ+θ; 1.5 - 8 Hz) over the power in low gamma (γ; 30-49 Hz). Spectral power was computed using the Multitaper method with the time-halfbandwidth product equal to 1.25 and the number of DFT points equal to 2048.

### $(\delta+\theta)/\gamma$ correlation for electrode pairs

In order to determine which electrode to use for the analysis, we computed the $(\delta+\theta)/\gamma$ ratio in 3-s windows for each electrode separately for the first night of recording for each bird. The correlation coefficient between difference $(\delta+\theta)/\gamma$ ratios was calculated between each electrode pair and averaged, resulting in a single value for each bird (Supplementary Fig. S2A. The average $(\delta+\theta)/\gamma$ correlation for the different electrode pairs was quite high for each individual bird, and therefore we chose to use electrode 4 for our $(\delta+\theta)/\gamma$ ratio analysis for each animal.

### Sleep stage identification based on the $(\delta+\theta)/\gamma$ ratio

Previous research in zebra finch sleep shows that each stage of sleep, i.e. SWS, IS, or REM are computed based on their gamma- and delta-power content.[5] That means, for example, SWS bins contain the highest delta power, REM the lowest, and the IS bins stand in between. Therefore, in order to include samples from different stages of sleep, we first ordered the EEG bins according to their $(\delta+\theta)/\gamma$ values. The highest 10 percent were considered SWS, the lowest 10 were REM, and the 10 percent of the data encompassing the median $(\delta+\theta)/\gamma$ values formed the IS group.

### Stage transition detection

In order to detect the number of transitions from SWS to REM, we used a moving threshold calculated over 30-minute windows of the non-smoothed $(\delta+\theta)/\gamma$ values. The SWS threshold was defined as the moving average plus 0.4 × moving iqr (interquartile interval calculated over 30-minute windows), and the threshold for REM was defined as the moving average minus 0.4 × moving iqr.

### Clustering-based sleep staging

Apart from detection of SWS and REM, based on thresholding the L/G, as described above, we also adopted an automatic procedure to label each 3-second window of sleep as one of the IS, SWS, or REM stages. The algorithm we have used here is described previously[5,6] and has been used for segmenting sleep using budgerigar and zebra finch EEG. The main steps in this algorithms are as follows: 1. Sleep EEG data is binned into non-overlapping 3-sec windows, 2. Several stage-dependent EEG features, e.g. Delta power, are extracted, 3. Two clusterings for SWS vs non-SWS and REM vs non-REM are performed in parallel for all windows, and 4: The sleep stage label is decided based on the outputs of the two clustering algorithms from previous step. Finally, we visualized the sleep scoring labels along the EEG to verify if the automatically-assigned labels are conforming with the EEG patterns of each specific stage; in most of the cases (32 nights out of 49 recordings for n=5 juveniles and n=3 adults; see Supplementary Fig. S4

for more details) the sleep scoring with this method was valid and therefore used in this paper. On other nights the k-means clustering used in this scoring scheme converged to a numerical solution, which was a local minima of the cost function in k-means clustering, but did not yield acceptable scoring outputs (n=17 nights; see Supplementary Fig. S3 for examples of successful and unsuccessful clustering).

**Detection of local waves**

Normalized EEG data was filtered using a band-pass filter (0.5 - 20 Hz) to suppress the high frequency components that might affect the precise localization of wave peaks and troughs. Local wave detection consists of two steps: (1) detection of all the wave peaks or troughs across all the electrodes, and (2) extraction of the simultaneously-occurring waves.

All positive or negative peaks that were more than one inter-quartile interval away from median were detected. To prevent the double-detection of waves with a negative deflection following the positive peak, or vice versa, we set a minimum inter-wave period of 90 ms where subsequent peaks were not detected. We only considered peaks detected across different electrodes which occurred within a 10 ms time widow as simultaneous. Finally, in order to be considered a local wave, a wave needed to be present in only a subset of all the electrodes. Here we considered the simultaneous observation of peaks across the electrodes as a local wave if the peaks were present in at least 4 electrodes (25%) and not more than 12 electrodes (75%). This requirement was not constrained to a particular hemisphere, and indeed, some local waves were detected across hemispheres (see Fig. 1C for examples).

**Connectivity analysis**

In order to measure intra-hemispheric EEG correlation, we averaged the correlations between all pairs of right hemisphere electrodes (R-R; numbering 15, 21, or 28 pairs of electrodes, corresponding to 6, 7, or 8 non-noisy electrodes on the right hemisphere) and all pairs of left hemisphere electrodes (L-L; numbering 21 or 28 pairs of electrodes, corresponding to 7 or 8 non-noisy electrodes on the left hemisphere). The inter-hemispheric connectivity was computed as the average of the correlation between the pair of electrodes from opposing hemispheres (42-64 pairs, depending on the number of non-noisy electrodes). This correlation analysis was performed separately for the adult and juvenile group, and for 3 different frequency bands: low frequency (1.5-8 Hz), gamma (30-49 Hz), and full band (1.5-200 Hz).

## Regression Analysis

The juvenile CC values were fit with the following regression function:

Connectivity=A-B*exp$(-\text{age}/\tau)$,

where A and B are model parameters accounting for the initial point and the range of the exponential function and the time constant, $\tau$, represents the time it takes for the connectivity to reach 63 % of the maximum, an index of growth rate.

## Graph theory analysis

We explored the compartmentalization of brain activity by extracting dominant networks of activity using methods from graph theory. We define a dominant network as a subset of EEG electrodes wherein (1) each pair of electrodes are significantly correlated and (2) it has the maximum number of such electrodes, i.e., no other electrode could be added that correlates highly with the current electrode s. For example, if there are 4 EEG electrodes which are all highly correlated with each other, and no other electrode exists which is highly correlated with all of these 4 electrodes, then these 4 electrodes form a dominant network. Such a network is called a "clique" in graph theory literature.

We extracted dominant networks for each stage of sleep separately. First, we computed the pair-wise correlation matrix for each 3-second bin belonging to the given sleep stage (e.g., REM, SWS, or IS) for all electrodes. From the correlation matrix, the statistically significant correlated pairs of electrodes were extracted using a statistical inference technique.[94] A MATLAB implementation of this method was provided by the authors of [94]. Having the significantly correlated pairs of EEG, the cliques were extracted using a MATLAB implementation of the Bron-Kerbosch algorithm.[41] Among the obtained dominant networks, we discarded the ones involving fewer than 3 EEG electrodes and appearing in fewer than 10% of the bins for that sleep stage. In the end, for all the recording nights of a given bird, we kept the networks that were consistent across all the recording nights in a given sleep stage. The size of these dominant networks, i.e. number of EEG electrodes involved, and number of these networks were reported in Fig. 5D and Fig. 5E.

## Statistics

We have used two-way analysis of variance (ANOVA) to compare the $(\delta+\theta)/\gamma$ values in juvenile and adults, while accounting for age and sex independently. Furthermore, we used a one-way ANOVA to compared sleep statistics between male and female juveniles. Sometimes, for the sake of

brevity, some p values are reported only in the Supplementary Information ANOVA statistics. The complete table of statistics for each ANOVA test can be found in the supplementary information. In other cases, we use, t-tests, Wilcoxon ranksum test, or Friedman tests, where appropriate.

### Availability of Data and Materials

All data and analysis reported in this paper are available from the corresponding author (janie.ondracek@tum.de) upon request.

## References


1. Anafi, R. C., Kayser, M. S. & Raizen, D. M. Exploring phylogeny to find the function of sleep. *Nat. Rev. Neurosci.* **20**, 109–116 (2019).
2. Nath, R. D. *et al.* The Jellyfish Cassiopea Exhibits a Sleep-like State. *Curr. Biol.* **27**, 2984-2990.e3 (2017).
3. Klein, M., Michel, F. & Jouvet, M. Etude Polygraphique du Sommeil ches les Oiseaux. *C. R. Seances Soc. Biol. Fil.* **158**, 99–103 (1964).
4. Walker, J. M. & Berger, R. J. Sleep in the domestic pigeon (Columba livia). *Behav. Biol.* **7**, 195–203 (1972).
5. Low, P., Shank, S. S., Sejnowski, T. J. & Margoliash, D. Mammalian-like features of sleep structure in zebra finches. *Proc Natl Acad Sci U A* **105**, 9081–9086 (2008).
6. Canavan, S. V. & Margoliash, D. Budgerigars have complex sleep structure similar to that of mammals. *PLOS Biol.* **18**, e3000929 (2020).
7. Berger, R. J. & Walker, J. M. Sleep in the burrowing owl (Speotyto cunicularia hypugaea). *Behav. Biol.* **7**, 183–194 (1972).
8. Rattenborg, N. C., Lima, S. L. & Amlaner, C. J. Half-awake to the risk of predation. *Nature* **397**, 397–398 (1999).
9. Rattenborg, N. C., Amlaner, C. J. & Lima, S. L. Unilateral eye closure and interhemispheric EEG asymmetry during sleep in the pigeon (Columba livia). *Brain. Behav. Evol.* **58**, 323–332 (2001).
10. van der Meij, J., Martinez-Gonzalez, D., Beckers, G. J. L. & Rattenborg, N. C. Intra-“cortical” activity during avian non-REM and REM sleep: variant and invariant traits between birds and mammals. *Sleep* **42**, zsy230 (2019).

11. Rojas-Ramírez, J. A. & Tauber, E. S. Paradoxical sleep in two species of avian predator (Falconiformes). *Science* **167**, 1754–1755 (1970).
12. Lesku, J. A. *et al.* Ostriches sleep like platypuses. *PloS One* **6**, e23203 (2011).
13. Rattenborg, N. C. *et al.* Evidence that birds sleep in mid-flight. *Nat. Commun.* **7**, 12468 (2016).
14. Siegel, J. M. Do all animals sleep? *Trends Neurosci.* **31**, 208–213 (2008).
15. Dewasmes, G., Cohen-Adad, F., Koubi, H. & Le Maho, Y. Polygraphic and behavioral study of sleep in geese: Existence of nuchal atonia during paradoxical sleep. *Physiol. Behav.* **35**, 67–73 (1985).
16. Rattenborg, N. C. *et al.* Migratory sleeplessness in the white-crowned sparrow (Zonotrichia leucophrys gambelii). *PLoS Biol.* **2**, (2004).
17. Lesku, J. A. *et al.* Adaptive Sleep Loss in Polygynous Pectoral Sandpipers. *Science* **337**, 1654–1658 (2012).
18. Tisdale, R. K., Vyssotski, A. L., Lesku, J. A. & Rattenborg, N. C. Sleep-Related Electrophysiology and Behavior of Tinamous (Eudromia elegans): Tinamous Do Not Sleep Like Ostriches. *Brain. Behav. Evol.* **89**, 249–261 (2017).
19. Saucier, D. & Astic, L. [Polygraphic study of sleep in young chickens at hatching, evolution at third and fourth days]. *Electroencephalogr. Clin. Neurophysiol.* **38**, 303–306 (1975).
20. Szymczak, J. T. Distribution of sleep and wakefulness in 24-h light-dark cycles in the juvenile and adult magpie, Pica pica. *Chronobiologia* **14**, 277–287 (1987).
21. Scriba, M. F. *et al.* Linking melanism to brain development: expression of a melanism-related gene in barn owl feather follicles covaries with sleep ontogeny. *Front. Zool.* **10**, 42 (2013).
22. Margoliash, D. & Schmidt, M. F. Sleep, off-line processing, and vocal learning. *Brain Lang.* **115**, 45–58 (2010).
23. Konishi, M. Comparative neurophysiological studies of hearing and vocalizations in songbirds. *Z. Für Vgl. Physiol.* **66**, 257–272 (1970).
24. Konishi, M. The role of auditory feedback in birdsong. *Ann. N. Y. Acad. Sci.* **1016**, 463–75 (2004).
25. Brainard, M. S. & Doupe, A. J. What songbirds teach us about learning. *Nature* **417**, 351–8 (2002).
26. Aronov, D., Andalman, A. S. & Fee, M. S. A specialized forebrain circuit for vocal babbling in the juvenile songbird. *Science* **320**, 630–4 (2008).

27. Ondracek, J. M. & Hahnloser, R. H. R. Advances in Understanding the Auditory Brain of Songbirds. in *Insights from Comparative Hearing Research* (eds. Köppl, C., Manley, G. A., Popper, A. N. & Fay, R. R.) 347–388 (Springer New York, 2013). doi:10.1007/2506_2013_31.
28. Mander, B. A., Winer, J. R. & Walker, M. P. Sleep and Human Aging. *Neuron* **94**, 19–36 (2017).
29. Mukovski, M., Chauvette, S., Timofeev, I. & Volgushev, M. Detection of active and silent states in neocortical neurons from the field potential signal during slow-wave sleep. *Cereb. Cortex N. Y. N 1991* **17**, 400–14 (2006).
30. Siapas, A. G. & Wilson, M. A. Coordinated interactions between hippocampal ripples and cortical spindles during slow-wave sleep. *Neuron* **21**, 1123–8 (1998).
31. Shein-Idelson, M., Ondracek, J. M., Liaw, H., Reiter, S. & Laurent, G. Slow waves, sharp waves, ripples, and REM in sleeping dragons. *Science* **352**, 590–5 (2016).
32. Yeganegi, H., Luksch, H. & Ondracek, J. M. Hippocampal-like network dynamics underlie avian sharp wave-ripples. *bioRχiv* (2019) doi:http://dx.doi.org/10.1101/825075.
33. Siclari, F. & Tononi, G. Local aspects of sleep and wakefulness. *Curr. Opin. Neurobiol.* **44**, 222–227 (2017).
34. Tobler, I., Franken, P., Trachsel, L. & Borbély, A. A. Models of sleep regulation in mammals. *J. Sleep Res.* **1**, 125–127 (1992).
35. Trachsel, L., Tobler, I. & Borbely, A. A. Sleep regulation in rats: effects of sleep deprivation, light, and circadian phase. *Am. J. Physiol.-Regul. Integr. Comp. Physiol.* **251**, R1037–R1044 (1986).
36. Nir, Y. *et al.* Regional Slow Waves and Spindles in Human Sleep. *Neuron* **70**, 153–169 (2011).
37. Cao, J. *et al.* Brain functional and effective connectivity based on electroencephalography recordings: A review. *Hum. Brain Mapp.* **43**, 860–879 (2022).
38. Bastos, A. M. & Schoffelen, J.-M. A Tutorial Review of Functional Connectivity Analysis Methods and Their Interpretational Pitfalls. *Front. Syst. Neurosci.* **9**, (2016).
39. Womelsdorf, T. *et al.* Modulation of Neuronal Interactions Through Neuronal Synchronization. *Science* **316**, 1609–1612 (2007).

40. Smit, D. J. A. *et al.* The Brain Matures with Stronger Functional Connectivity and Decreased Randomness of Its Network. *PLOS ONE* **7**, e36896 (2012).
41. Bron, C. & Kerbosch, J. Algorithm 457: finding all cliques of an undirected graph. *Commun. ACM* **16**, 575–577 (1973).
42. Derégnaucourt, S., Mitra, P. P., Fehér, O., Pytte, C. & Tchernichovski, O. How sleep affects the developmental learning of bird song. *Nature* **433**, 710–6 (2005).
43. Margoliash, D. Song learning and sleep. *Nat. Neurosci.* **8**, 546–548 (2005).
44. Brawn, T. P., Nusbaum, H. C. & Margoliash, D. Sleep consolidation of interfering auditory memories in starlings. *Psychol. Sci.* **24**, 439–47 (2013).
45. Fujii, T. G., Coulter, A., Lawley, K. S., Prather, J. F. & Okanoya, K. Song Preference in Female and Juvenile Songbirds: Proximate and Ultimate Questions. *Front. Physiol.* **13**, 876205 (2022).
46. Liu, W., Landstrom, M., Schutt, G., Inserra, M. & Fernandez, F. A memory-driven auditory program ensures selective and precise vocal imitation in zebra finches. *Commun. Biol.* **4**, 1–9 (2021).
47. Rattenborg, N. C., Van Der Meij, J., Beckers, G. J. L. & Lesku, J. A. Local aspects of avian non-rem and rem sleep. *Front. Neurosci.* **13**, 1–16 (2019).
48. Barnes, D. C. & Wilson, D. A. Slow-Wave Sleep-Imposed Replay Modulates Both Strength and Precision of Memory. *J. Neurosci.* **34**, 5134–5142 (2014).
49. Oyanedel, C. N. *et al.* Role of slow oscillatory activity and slow wave sleep in consolidation of episodic-like memory in rats. *Behav. Brain Res.* **275**, 126–130 (2014).
50. Marshall, L. & Born, J. The contribution of sleep to hippocampus-dependent memory consolidation. *Trends Cogn. Sci.* **11**, 442–450 (2007).
51. Rasch, B., Büchel, C., Gais, S. & Born, J. Odor cues during slow-wave sleep prompt declarative memory consolidation. *Science* **315**, 1426–1429 (2007).
52. Mander, B. A. *et al.* β-amyloid disrupts human NREM slow waves and related hippocampus-dependent memory consolidation. *Nat. Neurosci.* **18**, 1051–1057 (2015).
53. Lesku, J. A., Vyssotski, A. L., Martinez-Gonzalez, D., Wilzeck, C. & Rattenborg, N. C. Local sleep homeostasis in the avian brain: convergence of sleep function in mammals and birds? *Proc. Biol. Sci.* **278**, 2419–2428 (2011).
54. Jackson, C. *et al.* Dynamics of a Memory Trace: Effects of Sleep on Consolidation. *Curr. Biol.* **18**, 393–400 (2008).

55. Gentner, T. Q. & Margoliash, D. Neuronal populations and single cells representing learned auditory objects. *Nature* **424**, 669–74 (2003).
56. Carouso-Peck, S. & Goldstein, M. H. Female Social Feedback Reveals Non-imitative Mechanisms of Vocal Learning in Zebra Finches. *Curr. Biol. CB* **29**, 631-636.e3 (2019).
57. Lipkind, D. & Tchernichovski, O. Quantification of developmental birdsong learning from the subsyllabic scale to cultural evolution. *Proc. Natl. Acad. Sci. U. S. A.* **108 Suppl 3**, 15572–15579 (2011).
58. Pravosudov, V. V. & Omanska, A. Dominance-related changes in spatial memory are associated with changes in hippocampal cell proliferation rates in mountain chickadees. *J. Neurobiol.* **62**, 31–41 (2005).
59. Shettleworth, S. J. & Krebs, J. R. Stored and encountered seeds: A comparison of two spatial memory tasks in marsh tits and chickadees. *J. Exp. Psychol. Anim. Behav. Process.* **12**, 248–257 (1986).
60. Ruploh, T., Kazek, A. & Bischof, H.-J. Spatial Orientation in Japanese Quails (Coturnix coturnix japonica). *PLoS ONE* **6**, e28202 (2011).
61. Jouvet-Mounier, D., Astic, L. & Lacote, D. Ontogenesis of the states of sleep in rat, cat, and guinea pig during the first postnatal month. *Dev. Psychobiol.* **2**, 216–239 (1970).
62. Frank, M. G. & Heller, H. C. The ontogeny of mammalian sleep: a reappraisal of alternative hypotheses. *J. Sleep Res.* **12**, 25–34 (2003).
63. Ohayon, M. M., Carskadon, M. A., Guilleminault, C. & Vitiello, M. V. Meta-Analysis of Quantitative Sleep Parameters From Childhood to Old Age in Healthy Individuals: Developing Normative Sleep Values Across the Human Lifespan. *Sleep* **27**, 1255–1273 (2004).
64. Campbell, I. G. & Feinberg, I. Longitudinal trajectories of non-rapid eye movement delta and theta EEG as indicators of adolescent brain maturation. *Proc. Natl. Acad. Sci.* **106**, 5177–5180 (2009).
65. Buchmann, A. *et al.* EEG Sleep Slow-Wave Activity as a Mirror of Cortical Maturation. *Cereb. Cortex* **21**, 607–615 (2011).
66. George, I., Hara, E. & Hessler, N. A. Behavioral and neural lateralization of vision in courtship singing of the zebra finch. *J. Neurobiol.* **66**, 1164–1173 (2006).
67. Lampen, J., McAuley, J. D., Chang, S.-E. & Wade, J. ZENK induction in the zebra finch brain by song: Relationship to hemisphere, rhythm, oestradiol and sex. *J. Neuroendocrinol.* **29**, (2017).

68. Rogers, L. J., Koboroff, A. & Kaplan, G. Lateral Asymmetry of Brain and Behaviour in the Zebra Finch, Taeniopygia guttata. *Symmetry* **10**, 679 (2018).
69. Güntürkün, O. The avian 'prefrontal cortex' and cognition. *Curr. Opin. Neurobiol.* **15**, 686–693 (2005).
70. Vallortigara, G. & Rogers, L. Survival with an asymmetrical brain: Advantages and disadvantages of cerebral lateralization. *Behav. Brain Sci.* **28**, 575–89; discussion 589 (2005).
71. Rogers, L. J., Zucca, P. & Vallortigara, G. Advantages of having a lateralized brain. *Proc. Biol. Sci.* **271 Suppl 6**, S420-422 (2004).
72. Letzner, S., Simon, A. & Güntürkün, O. Connectivity and neurochemistry of the commissura anterior of the pigeon (Columba livia). *J. Comp. Neurol.* **524**, 343–361 (2016).
73. Paterson, A. K. & Bottjer, S. W. Cortical inter-hemispheric circuits for multimodal vocal learning in songbirds. *J. Comp. Neurol.* **525**, 3312–3340 (2017).
74. Wyss, J. M., Swanson, L. W. & Cowan, W. M. The organization of the fimbria, dorsal fornix and ventral hippocampal commissure in the rat. *Anat. Embryol. (Berl.)* **158**, 303–316 (1980).
75. Tobler, I. & Borbély, A. Sleep and EEG spectra in the pigeon (Columba Livia) under baseline conditions and after sleep deprivation. *J. Comp. Physiol.* **163**, 729–738 (1988).
76. Ball, N. J., Weaver, G. & Amlaner, C. The Incidence of Hemispheric Sleep in Birds. in (1986).
77. Ball, N., Amlaner, C., Shaffery, J. & Opp, M. Asynchronous Eye-Closure and Unihemispheric Quiet Sleep of Birds. in 151–153 (1988).
78. Wallman, J. & Pettigrew, J. D. Conjugate and disjunctive saccades in two avian species with contrasting oculomotor strategies. *J. Neurosci. Off. J. Soc. Neurosci.* **5**, 1418–1428 (1985).
79. Schaeffel, F., Howland, H. C. & Farkas, L. Natural accommodation in the growing chicken. *Vision Res.* **26**, 1977–1993 (1986).
80. Krupnik, R., Yovel, Y. & Assaf, Y. Inner Hemispheric and Interhemispheric Connectivity Balance in the Human Brain. *J. Neurosci.* **41**, 8351–8361 (2021).
81. Lee, J. M., Kyeong, S., Kim, E. & Cheon, K.-A. Abnormalities of Inter- and Intra-Hemispheric Functional Connectivity in Autism Spectrum Disorders: A Study

Using the Autism Brain Imaging Data Exchange Database. *Front. Neurosci.* **10**, (2016).

82. Chang, X., Collin, G., Mandl, R. C. W., Cahn, W. & Kahn, R. S. Interhemispheric connectivity and hemispheric specialization in schizophrenia patients and their unaffected siblings. *NeuroImage Clin.* **21**, 101656 (2019).
83. Vink, J., Westover, M., Pascual-Leone, A. & Shafi, M. EEG functional connectivity predicts causal brain interactions. *Brain Stimul. Basic Transl. Clin. Res. Neuromodulation* **12**, 449 (2019).
84. Massimini, M. *et al.* Neuroscience: Breakdown of cortical effective connectivity during sleep. *Science* **309**, 2228–2232 (2005).
85. Behroozi, M. *et al.* Event-related functional MRI of awake behaving pigeons at 7T. (2020).
86. De Groof, G. & Van der Linden, A. Love songs, bird brains and diffusion tensor imaging. *NMR Biomed.* **23**, 873–883 (2010).
87. De Groof, G. *et al.* In vivo diffusion tensor imaging (DTI) of brain subdivisions and vocal pathways in songbirds. *NeuroImage* **29**, 754–763 (2006).
88. Sanders, J. I. & Kepecs, A. A low-cost programmable pulse generator for physiology and behavior. *Front. Neuroengineering* **7**, 1–8 (2014).
89. Nixdorf-Bergweiler, B. E. & Bischof, H. J. *A Stereotaxic Atlas of the Brain of the Zebra Finch, Taeniopygia Guttata: With Special Emphasis on Telencephalic Visual and Song System Nuclei in Transverse and Sagittal Sections*. *Brain* (University of Kiel, 2007).
90. Jovalekic, A. *et al.* A lightweight feedback-controlled microdrive for chronic neural recordings. *J. Neural Eng.* **14**, 026006 (2017).
91. Fee, M. S. & Leonardo, A. Miniature motorized microdrive and commutator system for chronic neural recording in small animals. *J. Neurosci. Methods* **112**, 83–94 (2001).
92. Long, M. A. & Fee, M. S. Using temperature to analyse temporal dynamics in the songbird motor pathway. *Nature* **456**, 189–94 (2008).
93. Siegle, J. H. *et al.* Open Ephys: an open-source, plugin-based platform for multichannel electrophysiology. *J. Neural Eng.* **14**, 045003 (2017).
94. Kramer, M. A., Eden, U. T., Cash, S. S. & Kolaczyk, E. D. Network inference with confidence from multivariate time series. *Phys. Rev. E* **79**, 061916 (2009).

## Author contributions

Conceptualization, J.M.O.; Methodology, J.M.O. and H.Y.; Software: H.Y. and J.M.O.; Validation, J.M.O.; Formal Analysis, H.Y.; Investigation, H.Y.; Writing – Original Draft, H.Y.; Writing – Review & Editing, J.M.O.; Funding Acquisition, J.M.O.; Resources, J.M.O.; Visualization, H.Y. and J.M.O.; Supervision, J.M.O.; Project Administration, J.M.O.

## Additional Information

The authors declare no competing interests.

## Acknowledgments

This research was funded by grants from the German Research Foundation (Deutsche Forschungsgemeinschaft; ON 151/1-1) and the Daimler and Benz Foundation (Postdoctoral scholarship) to J.M.O. The authors are grateful to B. Seibel and Y. Schwarz for technical assistance; C. Fink and E. Jochen for help with mechanical design, fabrication, and electronics; A. Schuhbauer for administrative assistance, and H. Luksch, U. Firzlaff, T. Fenzl, and M. Shein-Idelson, and two reviewers for feedback on previous versions of the manuscript.

# Supplementary data one: ANOVA tables

## Multi-channel recordings reveal age-related differences in the sleep of juvenile and adult zebra finches


## Hamed Yeganegi[1,2] and Janie M. Ondracek[1*]

[1]Chair of Zoology, Technical University of Munich, Liesel-Beckmann-Str. 4, 85354 Freising-Weihenstephan, Germany

[2]Graduate School of Systemic Neurosciences, Ludwig-Maximilians-University Munich, Großhaderner Str. 2, 82152 Planegg, Germany


### Analysis of Variance tables for the tests presented in the main text

Two-way ANOVA for **(δ+θ)/γ**, x1: age, x2: sex, using anovan MATLAB function

| Source | Sum Sq. | d.f. | Mean Sq. | F | Prob>F |
|---|---|---|---|---|---|
| X1 | 4138.6488 | 1 | 4138.6488 | 6.2945 | 0.032698 |
| X2 | 141.6964 | 1 | 141.6964 | 0.21551 | 0.64568 |
| Error | 30245.2729 | 46 | 657.5059 | | |
| Total | 34977.0134 | 48 | | | |

Constrained (Type III) sums of squares.

Two-way ANOVA for **(δ+θ)**, x1: age, x2: sex, using anovan MATLAB function

| Source | Sum Sq. | d.f. | Mean Sq. | F | Prob>F |
|---|---|---|---|---|---|
| X1 | 0.015669 | 1 | 0.015669 | 3.2951 | 0.076009 |
| X2 | 0.0084312 | 1 | 0.0084312 | 1.773 | 0.18957 |
| Error | 0.21874 | 46 | 0.0047553 | | |
| Total | 0.23547 | 48 | | | |

Constrained (Type III) sums of squares.

Two-way ANOVA for γ, x1: age, x2: sex, using anovan MATLAB function

| Source | Sum Sq. | d.f. | Mean Sq. | F | Prob>F |
|---|---|---|---|---|---|
| X1 | 1.3207e-05 | 1 | 1.3207e-05 | 0.51222 | 0.4778 |
| X2 | 3.5236e-05 | 1 | 3.5236e-05 | 1.3665 | 0.24843 |
| Error | 0.0011861 | 46 | 2.5784e-05 | | |
| Total | 0.0012218 | 48 | | | |

Constrained (Type III) sums of squares.

Two-way ANOVA for **REM percentage**, x1: age, x2: sex, using anovan MATLAB function

| Source | Sum Sq. | d.f. | Mean Sq. | F | Prob>F |
|---|---|---|---|---|---|
| X1 | 620.137 | 1 | 620.137 | 10.7135 | 0.0027508 |

| | | | | | |
|---|---|---|---|---|---|
| X2 | 372.7795 | 1 | 372.7795 | 6.4402 | 0.01679 |
| Error | 1678.6209 | 29 | 57.8835 | | |
| Total | 2380.5423 | 31 | | | |

Constrained (Type III) sums of squares.

Two-way ANOVA for **SWS percentage**, x1: age, x2: sex, using anovan MATLAB function

| Source | Sum Sq. | d.f. | Mean Sq. | F | Prob>F |
|---|---|---|---|---|---|
| X1 | 308.5916 | 1 | 308.5916 | 5.4826 | 0.026288 |
| X2 | 342.2265 | 1 | 342.2265 | 6.0801 | 0.019828 |
| Error | 1632.2957 | 29 | 56.2861 | | |
| Total | 2081.2443 | 31 | | | |

Constrained (Type III) sums of squares.

Two-way ANOVA for **IS percentage**, x1: age, x2: sex, using anovan MATLAB function

| Source | Sum Sq. | d.f. | Mean Sq. | F | Prob>F |
|---|---|---|---|---|---|
| X1 | 2243.3562 | 1 | 2243.3562 | 28.6299 | 9.573e-06 |
| X2 | 1344.5007 | 1 | 1344.5007 | 17.1586 | 0.0002715 |
| Error | 2272.3579 | 29 | 78.3572 | | |
| Total | 4809.4547 | 31 | | | |

Constrained (Type III) sums of squares.

Two-way ANOVA for **REM duration**, x1: age, x2: sex, using anovan MATLAB function

| Source | Sum Sq. | d.f. | Mean Sq. | F | Prob>F |
|---|---|---|---|---|---|
| X1 | 15.4459 | 1 | 15.4459 | 6.3213 | 0.017732 |
| X2 | 13.1744 | 1 | 13.1744 | 5.3917 | 0.027459 |
| Error | 70.8609 | 29 | 2.4435 | | |
| Total | 90.6333 | 31 | | | |

Constrained (Type III) sums of squares.

Two-way ANOVA for **SWS duration**, x1: age, x2: sex, using anovan MATLAB function

| SourceSum | Sq. | d.f. | Mean Sq. | F | Prob>F |
|---|---|---|---|---|---|
| X1 | 14.0336 | 1 | 14.0336 | 11.7447 | 0.0018455 |
| X2 | 14.2408 | 1 | 14.2408 | 11.918 | 0.0017279 |
| Error | 34.6518 | 29 | 1.1949 | | |
| Total | 54.1352 | 31 | | | |

Constrained (Type III) sums of squares.

Two-way ANOVA for **IS duration**, x1: age, x2: sex, using anovan MATLAB function

| SourceSum | Sq. | d.f. | Mean Sq. | F | Prob>F |
|---|---|---|---|---|---|
| X1 | 14.4968 | 1 | 14.4968 | 6.7135 | 0.014823 |
| X2 | 11.7487 | 1 | 11.7487 | 5.4409 | 0.026817 |
| Error | 62.6208 | 29 | 2.1593 | | |
| Total | 80.7874 | 31 | | | |

Constrained (Type III) sums of squares.

One-way ANOVA for **REM Percentage**, x1: juvenile sex, using anovan MATLAB function

```
  Source   Sum Sq.   d.f.   Mean Sq.    F     Prob>F
----------------------------------------------------
  X1        372.78     1     372.78    4.42   0.0529
  Error    1265.7     15      84.38
  Total    1638.48    16
```

One-way ANOVA for **SWS Percentage**, x1: juvenile sex, using anovan MATLAB function

```
Source   Sum Sq.   d.f.   Mean Sq.    F     Prob>F
----------------------------------------------------
  X1        342.23     1    342.227    3.91   0.0667
  Error    1312.77    15     87.518
  Total    1655       16
```

One-way ANOVA for **IS Percentage**, x1: juvenile sex, using anovan MATLAB function

```
Source   Sum Sq.   d.f.   Mean Sq.    F     Prob>F
----------------------------------------------------
  X1       1344.5      1    1344.5     9.21   0.0084
  Error    2189.49    15     145.97
  Total    3533.99    16
```

One-way ANOVA for **REM Duration**, x1: juvenile sex, using anovan MATLAB function

```
Source   Sum Sq.   d.f.   Mean Sq.    F     Prob>F
----------------------------------------------------
  X1       21.3391     1    21.3391    54.31   2.33001e-06
  Error     5.8933    15     0.3929
  Total    27.2324    16
```

One-way ANOVA for **SWS Duration**, x1: juvenile sex, using anovan MATLAB function

```
Source   Sum Sq.   d.f.   Mean Sq.     F        Prob>F
-----------------------------------------------------------
  X1       28.5115     1    28.5115    117.58   1.70414e-08
  Error     3.6371    15     0.2425
  Total    32.1486    16
```

One-way ANOVA for **IS Duration**, x1: juvenile sex, using anovan MATLAB function

```
Source   Sum Sq.   d.f.   Mean Sq.     F       Prob>F
----------------------------------------------------------
  X1       12.4023     1    12.4023    34.76   2.93802e-05
  Error     5.3517    15     0.3568
  Total    17.754     16
```

Two-way ANOVA for **local wave occurrence rate**, x1: age, x2: sex, using anovan MATLAB function

| Source | Sum Sq. | d.f. | Mean Sq. | F | Prob>F |
|---|---|---|---|---|---|
| X1 | 0.78796 | 1 | 0.78796 | 25.1373 | 6.7767e-07 |
| X2 | 0.19424 | 1 | 0.19424 | 6.1967 | 0.013031 |
| Error | 21.8798 | 698 | 0.031346 | | |
| Total | 23.6767 | 700 | | | |

Constrained (Type III) sums of squares.

Two-way ANOVA for **connectivity across sleep stages in adults**, x1: [SWS, IS, REM stages], x2: [LL, RR, LR connectivity], using anova2 MATLAB function

| Source | SS | df | MS | F | Prob>F |
|---|---|---|---|---|---|
| Columns | 7.0207 | 2 | 3.5103 | 239.7073 | 1.4414e-52 |
| Rows | 0.075048 | 2 | 0.037524 | 2.5624 | 0.079799 |
| Interaction | 0.054864 | 4 | 0.013716 | 0.93661 | 0.44387 |
| Error | 2.7678 | 189 | 0.014644 | | |
| Total | 9.9184 | 197 | | | |

Two-way ANOVA for **connectivity across sleep stages in juveniles**, x1: [SWS, IS, REM stages], x2: [LL, RR, LR connectivity], using anova2 MATLAB function

| Source | SS | df | MS | F | Prob>F |
|---|---|---|---|---|---|
| Columns | 0.021983 | 2 | 0.010991 | 0.53371 | 0.5874 |
| Rows | 2.8498 | 2 | 1.4249 | 69.1902 | 9.6389e-23 |
| Interaction | 0.0043447 | 4 | 0.0010862 | 0.052742 | 0.99476 |
| Error | 3.5216 | 171 | 0.020594 | | |
| Total | 6.3978 | 179 | | | |

Two-way ANOVA for **REM-to-IS** transitions, x1: age, x2: sex, using anovan MATLAB function

| Source | Sum Sq. | d.f. | Mean Sq. | F | Prob>F |
|---|---|---|---|---|---|
| X1 | 2326266.7508 | 1 | 2326266.7508 | 27.0961 | 1.3043e-05 |
| X2 | 1315662.4251 | 1 | 1315662.4251 | 15.3247 | 0.00048249 |
| Error | 2575573.0455 | 30 | 85852.4348 | | |
| Total | 5157324.2424 | 32 | | | |

Two-way ANOVA for **REM-to-SWS** transitions, x1: age, x2: sex, using anovan MATLAB function

| Source | Sum Sq. | d.f. | Mean Sq. | F | Prob>F |
|---|---|---|---|---|---|
| X1 | 390367.1928 | 1 | 390367.1928 | 4.8759 | 0.03502 |
| X2 | 454779.787 | 1 | 454779.787 | 5.6804 | 0.023687 |
| Error | 2401833.4924 | 30 | 80061.1164 | | |
| Total | 2983183.5152 | 32 | | | |

Two-way ANOVA for **SWS-to-IS** transitions, x1: age, x2: sex, using anovan MATLAB function

| Source | Sum Sq. | d.f. | Mean Sq. | F | Prob>F |
|---|---|---|---|---|---|
| X1 | 1556397.3064 | 1 | 1556397.3064 | 46.906 | 1.3373e-07 |
| X2 | 623673.0918 | 1 | 623673.0918 | 18.796 | 0.0001508 |
| Error | 995435.3788 | 30 | 33181.1793 | | |
| Total | 2612580.2424 | 32 | | | |

Two-way ANOVA for **SWS-to-REM** transitions, x1: age, x2: sex, using anovan MATLAB function

| Source | Sum Sq. | d.f. | Mean Sq. | F | Prob>F |
|---|---|---|---|---|---|
| X1 | 341905.4848 | 1 | 341905.4848 | 4.8873 | 0.034822 |
| X2 | 347332.5143 | 1 | 347332.5143 | 4.9649 | 0.033512 |
| Error | 2098746.0152 | 30 | 69958.2005 | | |
| Total | 2571704.2424 | 32 | | | |

One-way ANOVA for **SWS-to-REM** transitions, x1: juvenile sex, using anovan MATLAB function

| Source | Sum Sq. | d.f. | Mean Sq. | F | Prob>F |
|---|---|---|---|---|---|
| X1 | 2412.03 | 1 | 2412.03 | 8.41 | 0.011 |
| Error | 4299.78 | 15 | 286.65 | | |
| Total | 6711.82 | 16 | | | |

One-way ANOVA for **REM-to-SWS** transitions, x1: juvenile sex, using anovan MATLAB function

| Source | Sum Sq. | d.f. | Mean Sq. | F | Prob>F |
|---|---|---|---|---|---|
| X1 | 3158.19 | 1 | 3158.19 | 7.42 | 0.0157 |
| Error | 6380.4 | 15 | 425.36 | | |
| Total | 9538.59 | 16 | | | |

One-way ANOVA for **REM-to-IS** transitions, x1: juvenile sex, using anovan MATLAB function

| Source | Sum Sq. | d.f. | Mean Sq. | F | Prob>F |
|---|---|---|---|---|---|
| X1 | 9136.5 | 1 | 9136.54 | 9.82 | 0.0068 |
| Error | 13956.2 | 15 | 930.41 | | |
| Total | 23092.7 | 16 | | | |

One-way ANOVA for **SWS-to-IS** transitions, x1: juvenile sex, using anovan MATLAB function

| Source | Sum Sq. | d.f. | Mean Sq. | F | Prob>F |
|---|---|---|---|---|---|
| X1 | 4331.06 | 1 | 4331.06 | 20.14 | 0.0004 |
| Error | 3226.43 | 15 | 215.1 | | |
| Total | 7557.49 | 16 | | | |

Two-way ANOVA for **CC** in **LL, RR,** and **LR** pair of channels, in **adults**, x1: SWS, IS, REM, x2: LL, RR, and LR, using anova2 MATLAB function

| Source | SS | df | MS | F | Prob>F |
|---|---|---|---|---|---|

| | | | | | |
|---|---|---|---|---|---|
| Columns | 7.0207 | 2 | 3.5103 | 239.7073 | 1.4414e-52 |
| Rows | 0.075048 | 2 | 0.037524 | 2.5624 | 0.079799 |
| Interaction | 0.054864 | 4 | 0.013716 | 0.93661 | 0.44387 |
| Error | 2.7678 | 189 | 0.014644 | | |
| Total | 9.9184 | 197 | | | |

Accompanying pairwise comparisons from Tukey multiple comparison test (multcompare function):

| Group1 | Group2 | p-value |
|---|---|---|
| LL | RR | 0.0396 |
| LL | LR | 9.56e-10 |
| RR | LR | 9.56e-10 |

Two-way ANOVA for **CC** in **LL, RR,** and **LR** pair of channels, in **juveniles**, x1: SWS, IS, REM, x2: LL, RR, and LR, using anova2 MATLAB function

| Source | SS | df | MS | F | Prob>F |
|---|---|---|---|---|---|
| Columns | 2.8498 | 2 | 1.4249 | 69.1902 | 9.6389e-23 |
| Rows | 0.021983 | 2 | 0.010991 | 0.53371 | 0.5874 |
| Interaction | 0.0043447 | 4 | 0.0010862 | 0.052742 | 0.99476 |
| Error | 3.5216 | 171 | 0.020594 | | |
| Total | 6.3978 | 179 | | | |

Accompanying pairwise comparisons from Tukey multiple comparison test (multcompare function):

| Group1 | Group2 | p-value |
|---|---|---|
| LL | RR | 0.5489 |
| LL | LR | 9.56e-10 |
| RR | LR | 9.56e-10 |

# Supplementary data two: supplementary figures

## Multi-channel recordings reveal age-related differences in the sleep of juvenile and adult zebra finches

**Hamed Yeganegi[1,2] and Janie M. Ondracek[1]***

[1]Chair of Zoology, Technical University of Munich, Liesel-Beckmann-Str. 4, 85354 Freising-Weihenstephan, Germany

[2]Graduate School of Systemic Neurosciences, Ludwig-Maximilians-University Munich, Großhaderner Str. 2, 82152 Planegg, Germany

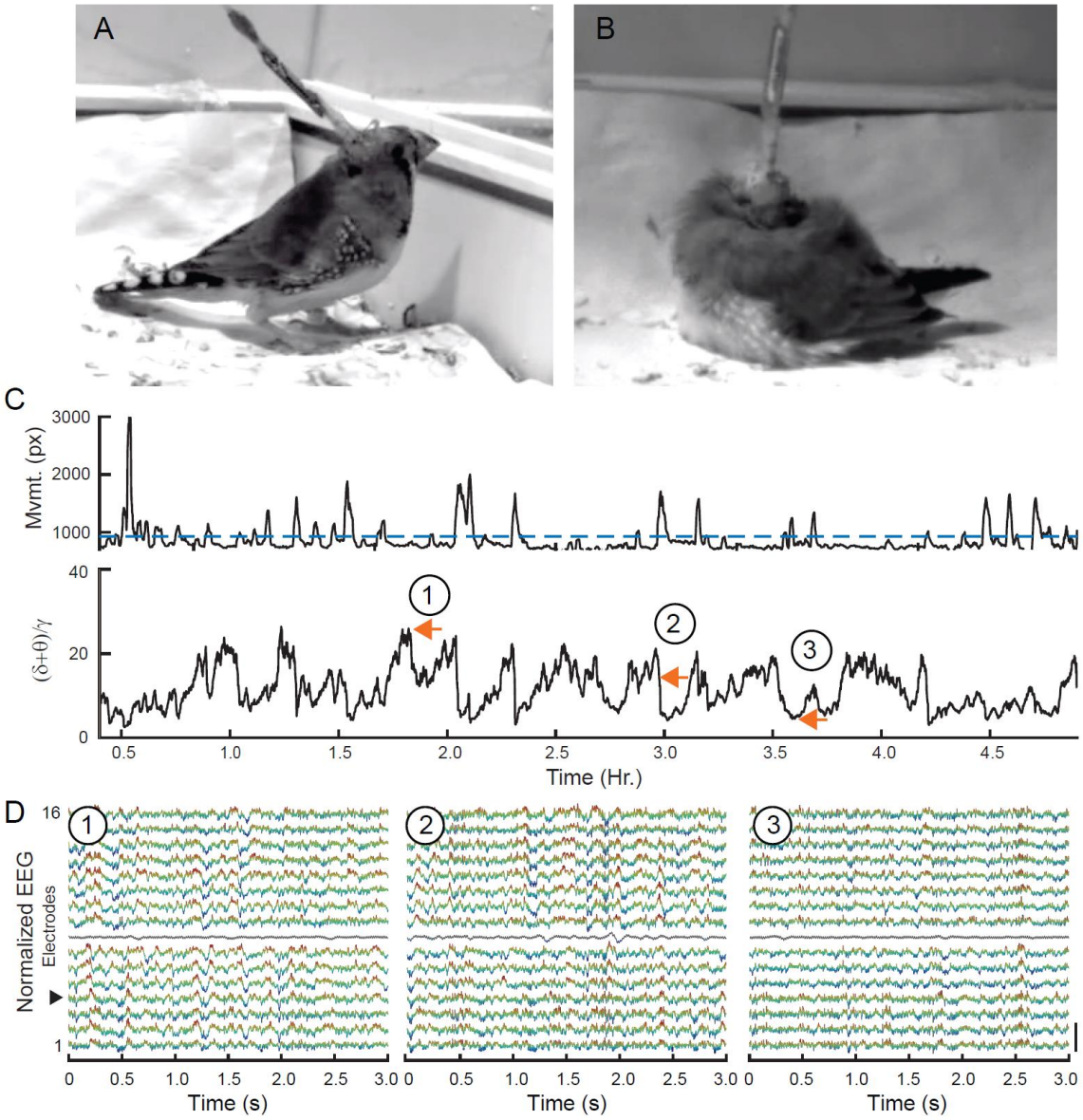


**Figure S1. Multichannel EEG recordings during sleep in a juvenile.** (A) Image of an awake tethered juvenile bird. (B) Image of a sleeping tethered juvenile. Same bird as in (A). Note how bird is able to assume a sleep-specific posture despite the tether cable. (C) Top: Bird movement extracted from the infrared video recording (px, pixels). Blue dashed line indicates the threshold delineating wake and sleep. Bottom: Corresponding $(\delta+\theta)/\gamma$ trace shows the oscillatory components of EEG, representing different sleep stages. Orange arrows 1, 2, and 3, correspond to EEG data in (D). Movement and $(\delta+\theta)/\gamma$ traces are smoothed with a 30s window for visualization purposes. (D) 3s examples of simultaneous EEG recorded from the 16 different electrodes (bottom trace, electrode 1; top trace, electrode 16). Circled numbers correspond to orange arrows in (B) and indicate examples of SWS (1), IS (2), and REM sleep (3). Color scheme is for visualization purposes only. Black arrow indicates electrode 4. Electrode 8 (grey line) was noisy and discarded in further analysis.

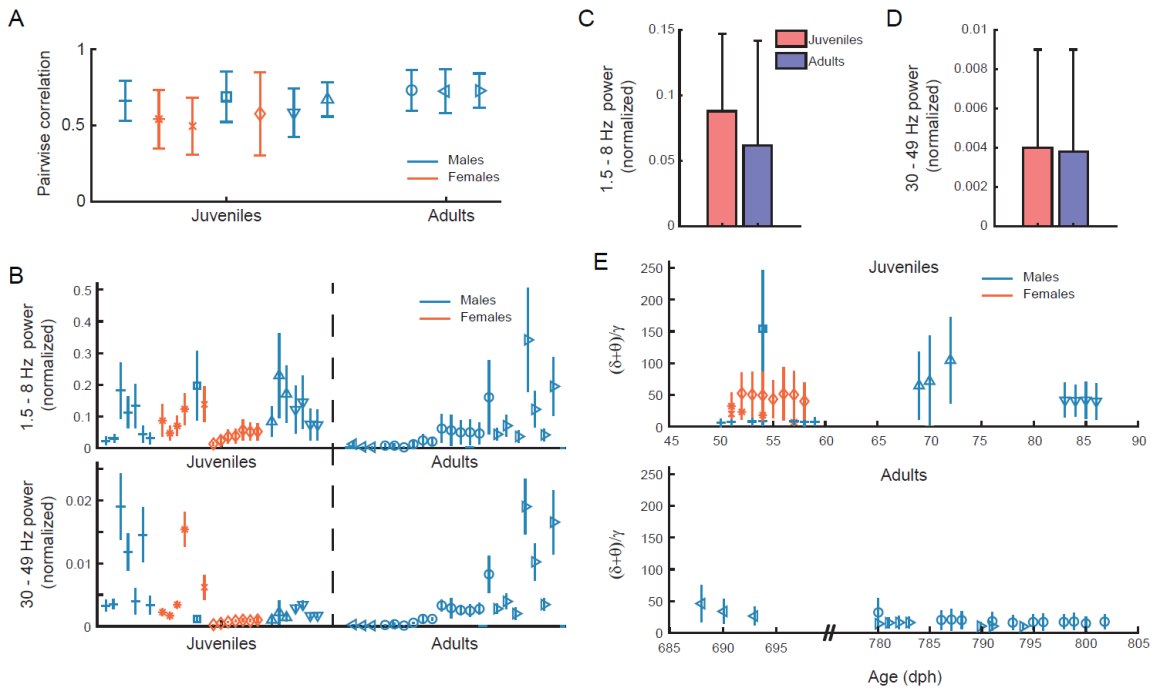


**Figure S2. Low and high frequency components of the (δ+θ)/γ trace in adults and juveniles.** (A) Mean correlation calculated for (δ+θ)/γ traces across all electrode pairs for the first recording night. Each symbol represents a different bird; blue symbols indicate males; orange symbols indicate females. Error bars indicate SD. (B) (δ+θ)/γ values were significantly larger in juveniles compared to adults. We examined the power in each of these bands separately for juveniles and adults. Top: (δ+θ) values calculated across 12 hours of sleep in 3 s bins, for all nights of each bird (median ± interquartile). Each symbol represents a different bird, and different nights of sleep are presented sequentially. Blue symbols indicate males; orange symbols indicate females. Bottom: γ values calculated across 12 hours of sleep in 3s bins, for all nights of each bird. (C) Mean relative power for the (δ+θ) band was larger in juveniles compared to adults, but this difference was not significant (p=0.07; two-way unbalanced ANOVA). (D). Mean relative power for the γ band was not significantly different between juveniles and adults (p=0.47; two-way unbalanced ANOVA). (E) (δ+θ)/γ values are plotted as function of age for juvenile birds (upper plot) and adults (lower plot). Data are the same as plotted in Fig.1E. Figure conventions same as in (B).

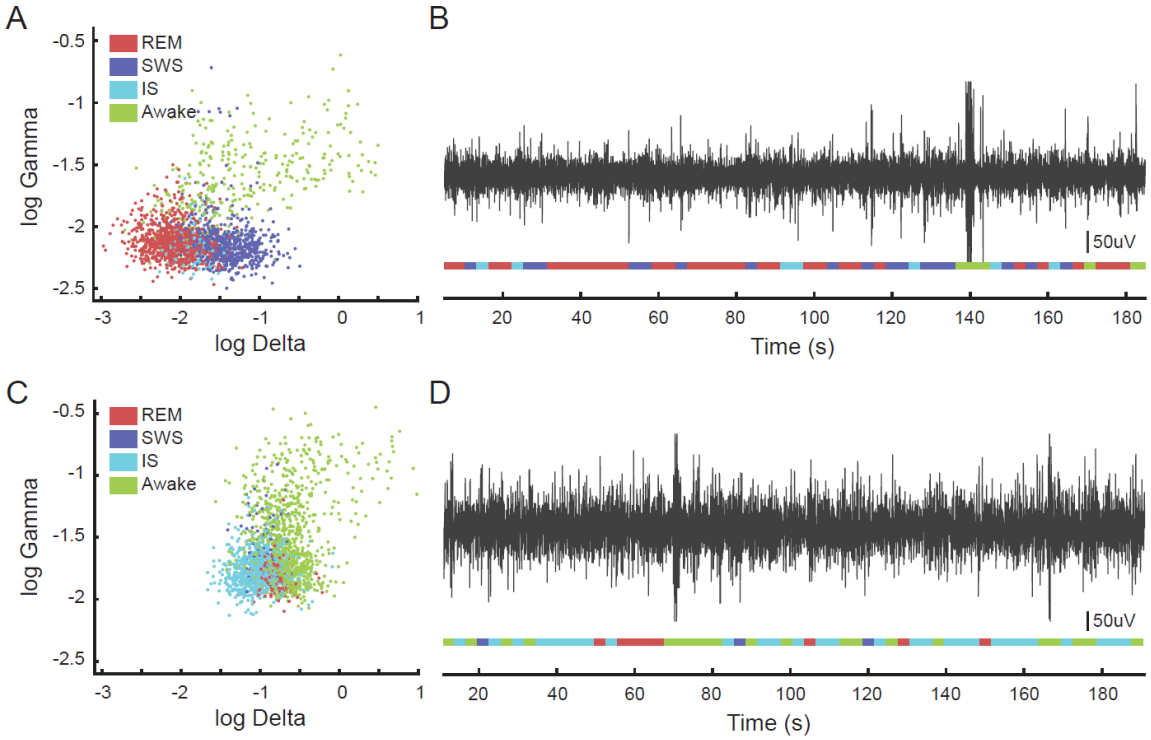


**Figure S3. Examples of successful and unsuccessful automatic segmentation of sleep stages.** (A) Clustering output for a successful segmentation (from adult 72-00). Note how clusters are separated in the log gamma and log delta space. (B) 3-minute example trace of EEG that is labeled according to clustering in (A). (C) Clustering output for an unsuccessful segmentation (from juvenile w018; none of the nights could be clustered for this bird). Note how clusters overlap heavily in the log gamma and log delta space. (D). 3-minute example trace of EEG that is labeled according to clustering in (C). Note how numerous segments are labeled as Awake or IS.

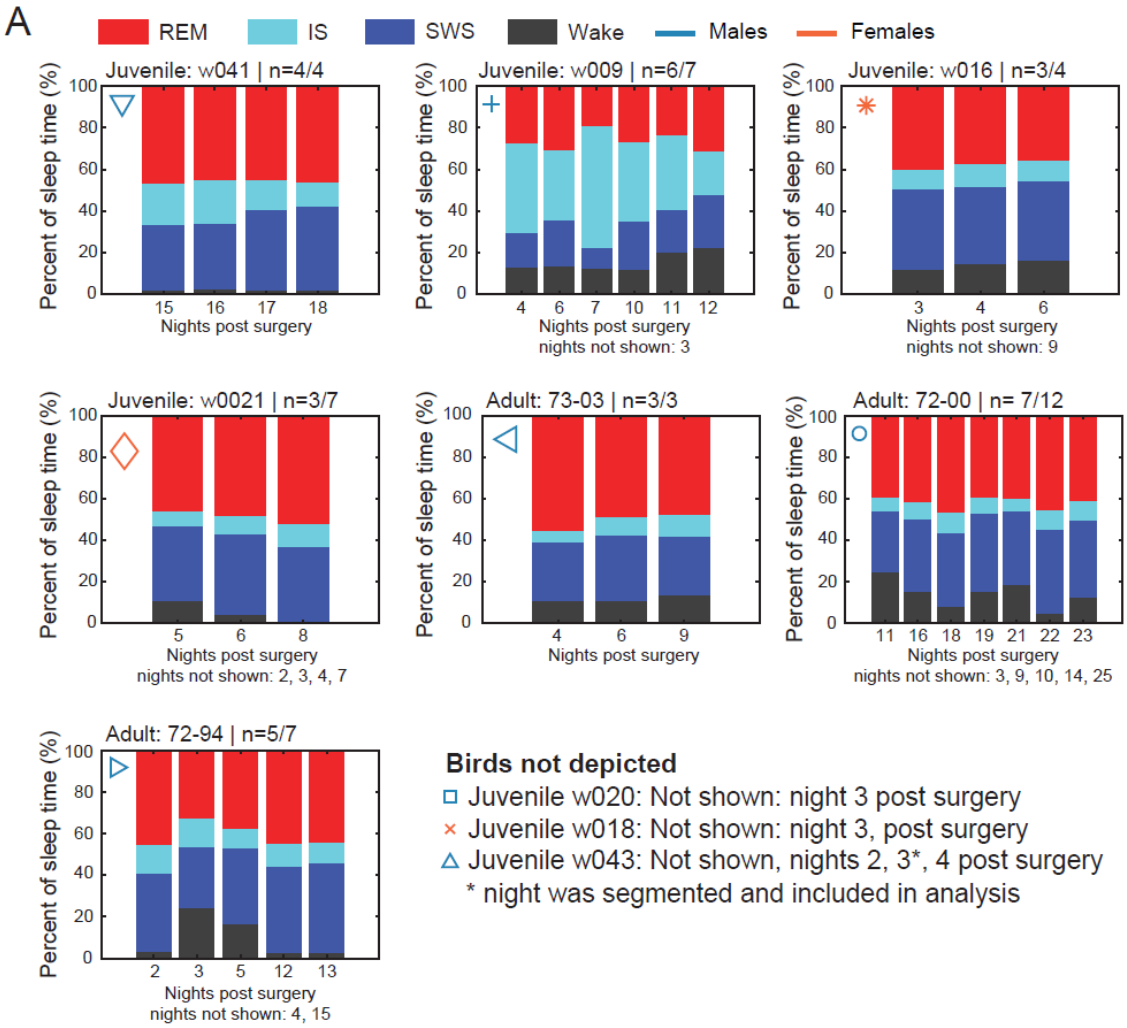


**Figure S4. Percentage of sleep stages across nights for each bird.** (A) Stacked plots represent the percentage of each sleep stage across recording nights. Each panel contains the data from an individual bird; the symbol in the upper left corner matches the identification of the bird in Fig. 1E. The sleep scoring used in this plot is the result of an automatic clustering algorithm.[1,2] Only one night of sleep was segmented for juvenile bird w043 (Δ) and therefore it is not included here. The number of successfully clustered nights out of the total number of nights are indicated in the title for each panel (e.g., n=4/4), and the specific nights that were not successfully clustered are indicated as "nights not shown". Note how the percentage of sleep across nights for individual birds is largely consistent across nights.

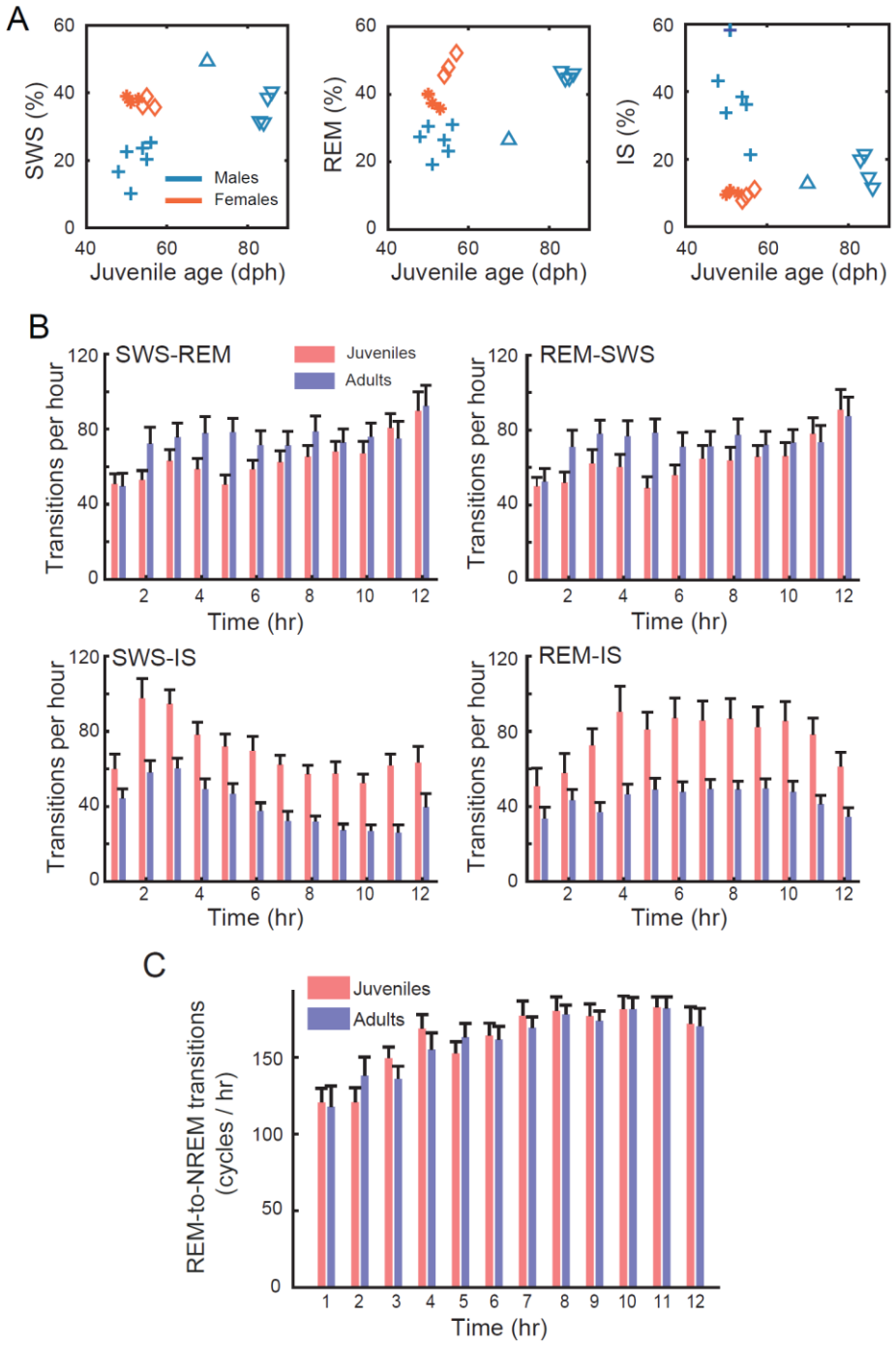


**Figure S5 Analysis of REM versus NREM sleep in adults and juveniles** (A)Scatter plots depict the percentage of SWS, REM sleep, or IS per night as a function of juvenile age. Same animals as in Fig. 2E. A clear linear relationship between sleep stage percentage and age is not present. (B) Bar plots indicate the average number of transitions per hour from SWS to REM, REM to SWS, SWS to IS, and REM to IS over 12 hours of sleep for juveniles (red) and adults (blue). Error bars indicated the s.e.m. (C) REM to NREM (IS+SWS) for juveniles (red) and adults (blue) over 12 hours of sleep. Error bars indicated the s.e.m.

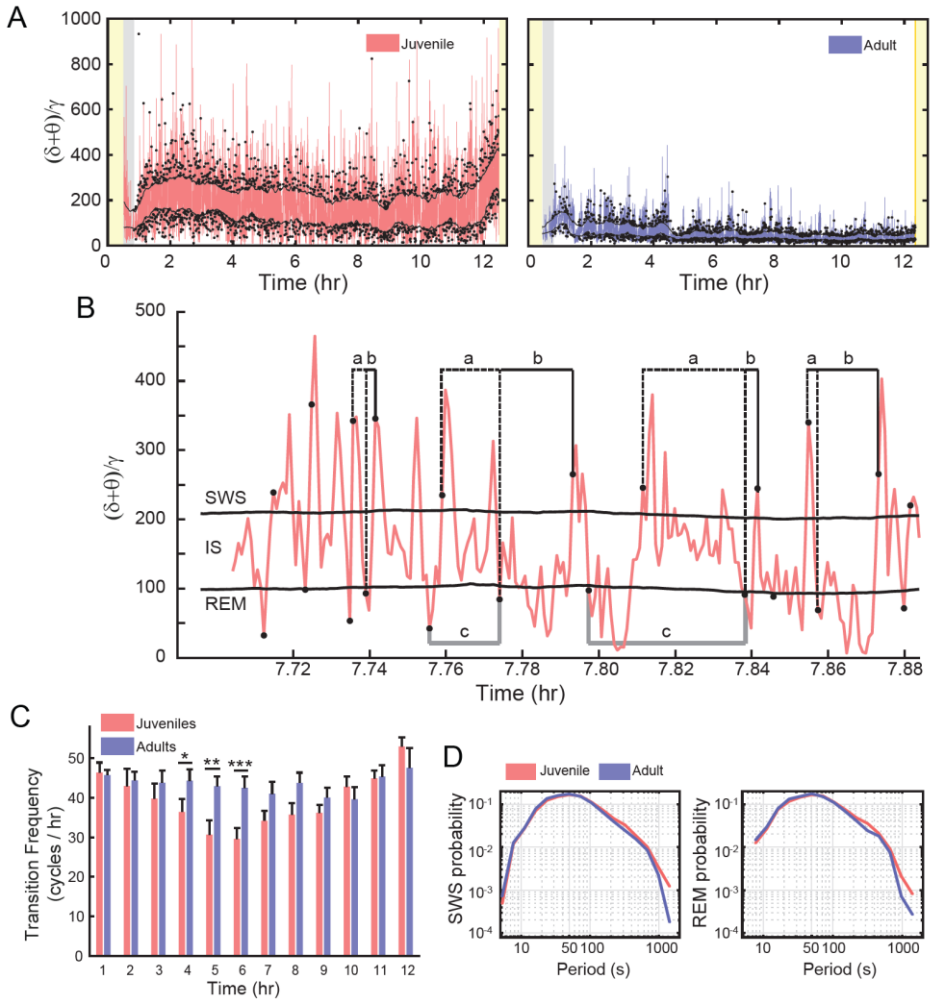


**Figure S6 State transitions during continuous sleep (**A) Unsmoothed $(\delta+\theta)/\gamma$ traces for a juvenile bird (left) and an adult bird (right) for 12 hours of sleep (same birds as depicted in Fig. 1D and indicated as black arrows in Fig. 1E). In each $(\delta+\theta)/\gamma$ trace, the upper and lower black lines indicate the SWS and REM detection threshold, respectively. Gray dots indicate the first detection after a threshold crossing (top dots, SWS; bottom dots, REM). The yellow bars indicated periods when the light was on. Gray shading indicates time periods after the lights were off that the birds were still awake based on movement detection. (B) Enlargement of a short window of the unsmoothed $(\delta+\theta)/\gamma$ trace from the juvenile in (A). Dotted black lines labeled 'a' indicate examples of detected SWS to REM transitions. Note how the duration of 'a' varies as a function of how much time is spent in SWS and IS. Solid black lines labeled 'b' indicate examples of REM to SWS transitions; the combined duration of 'a' plus 'b' completes one full cycle of SWS (SWS-REM-SWS). Solid gray lines labeled 'c' indicate examples of one full cycle of REM (REM-SWS-REM). (C) Bar plot indicates the average number of SWS-to-REM transitions (i.e., the number of transitions labeled as 'a' in (B) per hour during night in juveniles and adults. For adults, the transitions were relatively constant, whereas for juveniles, the transition frequency varied throughout the night (see text for details). The transition frequency was significantly lower for juveniles compared to adults for the 5$^{th}$, 6$^{th}$, and 7$^{th}$ hours. (D) The probability distribution functions for SWS cycles (left plot; SWS cycle indicated as 'a' plus 'b' in (B)) and REM cycles (right plot; REM cycle indicated as 'c' in (B)). The probability of observing long SWS and REM cycles is significantly higher in the juvenile group. SWS cycle was 92.86 ± 121.41 s in juveniles and 82.84 ± 102.80 s in adults (unpaired t-test, $p=5.7\times10^{-12}$). Similarly, REM cycles were also significantly longer in the juveniles (92.88 ± 115.07 s in juveniles, and 82.74 ± 99.15 s in adults; unpaired t-test, $p=5.5\times10^{-13}$).

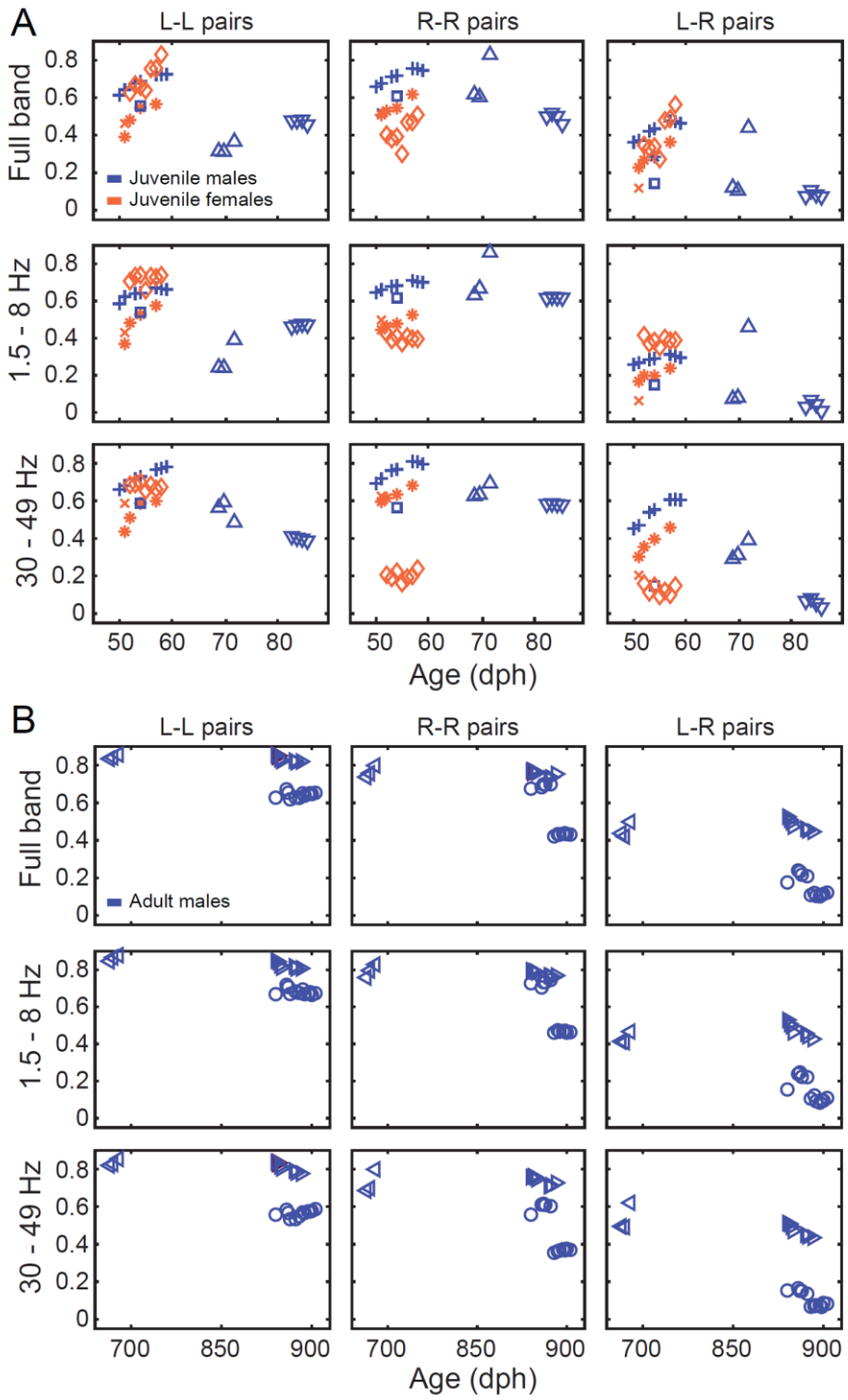


**Figure S7**. **Left intra-hemispheric functional connectivity increases linearly during early maturation in juveniles, but stabilizes or declines by approaching maturity.** (A) The increasing linear relationship between connectivity and age was only observed in younger juveniles (the 5 birds presented in Fig. 4B). Panels display the data from all 7 juveniles. Same figure convention as for Fig. 4 Note how an increasing linear trend does not exist for older juveniles. (B). This data supports the view that the connectivity elevates at a high pace in early juvenile stage and then stabilizes or declines before the age of maturation to the adulthood level.

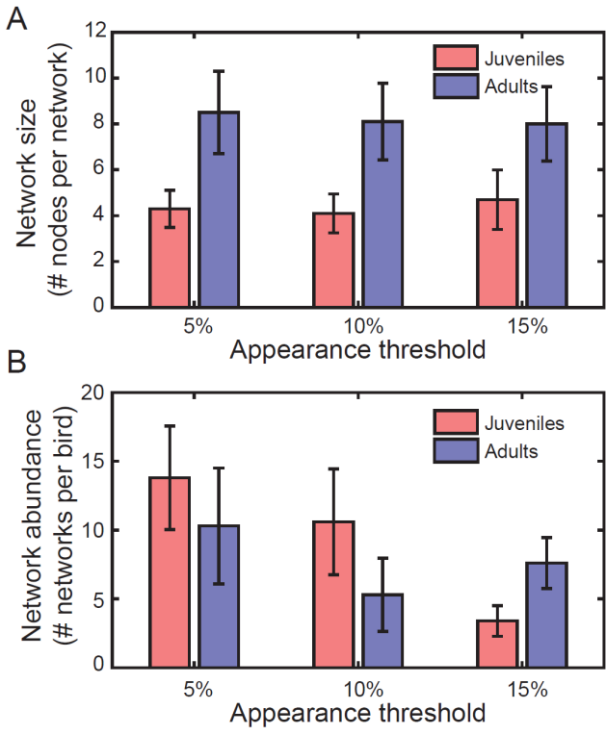


**Figure S8 Effects of setting different appearance thresholds on the network analysis results.** (A) The appearance threshold (x axis) is a parameter that we used to constrain the network analysis, such that a dominant network had to appear for at least 10% of the bins throughout the night, for three separate nights.

## References


1. Low, P., Shank, S. S., Sejnowski, T. J. & Margoliash, D. Mammalian-like features of sleep structure in zebra finches. *Proc Natl Acad Sci U A* **105**, 9081–9086 (2008).
2. Canavan, S. V. & Margoliash, D. Budgerigars have complex sleep structure similar to that of mammals. *PLOS Biol.* **18**, e3000929 (2020).

# Chapter 3

# Local sleep in songbirds: Different simultaneous sleep states across the avian pallium

**Summary**

Wakefulness and sleep have often been treated as distinct and global brain states. However, an emerging body of evidence on the local regulation of sleep stages challenges this conventional view. Apart from unihemispheric sleep, the current data that support local variations of neural oscillations during sleep are focused on the homeostatic regulation of local sleep, i.e., the role preceding awake activity. Here, to examine local differences in brain activity during natural sleep, we recorded the electroencephalogram (EEG) and the local field potential (LFP) across multiple sites within the avian pallium of zebra finches without perturbing the previous awake state. We scored the sleep stages independently in each pallial site and found that the sleep stages are not pallium-wide phenomena but rather deviate widely across electrode sites. Importantly, deeper electrode sites had a dominant role in defining the temporal aspects of sleep state congruence. Altogether, these findings show that local regulation of sleep oscillations also occurs in the avian brain without prior awake recruitment of specific pallial circuits and in the absence of mammalian cortical neural architecture.

**The manuscript published online as**

Yeganegi, Hamed, and Janie M. Ondracek. "Local sleep in songbirds: Different simultaneous sleep states across the avian pallium." *bioRxiv* (2023): 2023-10.

(Accepted for publication in the Journal of Sleep Research)

# Local sleep in songbirds: Different simultaneous sleep states across the avian pallium

Hamed Yeganegi[1,2], Janie M. Ondracek[1*]

1 Technical University of Munich, TUM School of Life Sciences, Chair of Zoology, Liesel-Beckmann-Str. 4, 85354 Freising-Weihenstephan, Germany.
2 Graduate School of Systemic Neurosciences, Ludwig-Maximilians-University Munich, Großhaderner Str. 2, 82152 Planegg, Germany.
* Correspondence: Janie M. Ondracek, Technical University of Munich, TUM School of Life Sciences, Chair of Zoology, Liesel-Beckmann-Str. 4, 85354 Freising-Weihenstephan, Germany Email: janie.ondracek@tum.de

## Summary

Wakefulness and sleep have often been treated as distinct and global brain states. However, an emerging body of evidence on the local regulation of sleep stages challenges this conventional view. Apart from unihemispheric sleep, the current data that support local variations of neural oscillations during sleep are focused on the homeostatic regulation of local sleep, i.e., the role preceding awake activity. Here, to examine local differences in brain activity during natural sleep, we recorded the electroencephalogram (EEG) and the local field potential (LFP) across multiple sites within the avian pallium of zebra finches without perturbing the previous awake state. We scored the sleep stages independently in each pallial site and found that the sleep stages are not pallium-wide phenomena but rather deviate widely across electrode sites. Importantly, deeper electrode sites had a dominant role in defining the temporal aspects of sleep state congruence. Altogether, these findings show that local regulation of sleep oscillations also occurs in the avian brain without prior awake recruitment of specific pallial circuits and in the absence of mammalian cortical neural architecture.

### Keywords

Local sleep, NREM, REM, avian brain, avian sleep, EEG

## Introduction

Sleep is a phenomenon that has been documented across animal species (Cirelli & Tononi, 2008; Siegel, 2008) and can be defined on at least two

levels: i) the behavior of the whole organism and ii) the patterns of neural activity in the brain (Vyazovskiy & Harris, 2013). Behavioral sleep is often simply defined as a state of quiescence and reduced responsiveness to the environment. In contrast, electrophysiological sleep is characterized by the complex spatiotemporal patterns of neural activity that occur during behavioral sleep.

In mammals, the sleeping brain generally oscillates between two principle states: rapid eye movement (REM) sleep and non-REM (NREM) sleep. These two states of sleep have also been documented in numerous non-mammalian animals, including birds (Canavan & Margoliash, 2020; Libourel et al., 2023; Low et al., 2008; Yeganegi & Ondracek, 2023), reptiles (Albeck et al., 2022; Libourel et al., 2018; Shein-Idelson et al., 2016), zebra fish (Leung et al., 2019), and cephalopods (Pophale et al., 2023). Similar to mammals, REM sleep-like states in these animals are characterized by low amplitude and aperiodic electrical activity, whereas NREM-like sleep is characterized by the emergence of periodic “slow” wave activity (1-4 Hz oscillations) during slow wave sleep (SWS).

REM sleep and NREM sleep states are conventionally described as unitary “global” phenomena, affecting the whole brain uniformly and simultaneously. However, recent work on “local” sleep in both humans (Bernardi et al., 2015; Huber et al., 2004; Nir et al., 2011) and rodents (Funk et al., 2016; Rector et al., 2005; Vyazovskiy et al., 2011) has challenged this understanding, suggesting that brain activity is much more complex and compartmentalized.

In the field of sleep research, the phrase “local sleep” has been used to describe a variety of different phenomena. In mammals, the term “local sleep” most commonly refers to two distinct concepts.

(1) Local sleep may refer to the use-dependent, or homeostatically influenced, differences in slow wave activity (SWA) observed during NREM sleep (Hanlon et al., 2009; Huber et al., 2004; Kattler et al., 1994; Lesku et al., 2011; Vyazovskiy & Tobler, 2008). Here “local” refers to the observation that after awake unilateral experience (e.g. motor learning, sensory stimulation), a “local” SWA asymmetry results across the hemispheres during subsequent sleep phases, with the hemisphere or brain area contralateral to the stimulation displaying larger SWA values. This phenomenon is thought to result from the unilateral and activity-dependent

upregulation of genes involved in long-term potentiation resulting in a “local” increase in sleep requirement (Hanlon et al., 2009).

(2) Local sleep may describe other disparities of sleep states, ranging from i) the intrusion of sleep-like activity in the cortex of awake and behaving animals (Vyazovskiy et al., 2011), where “local” sleep-like activity appears in one cortical area during awake periods, but not another; ii) the presence of “local” slow waves during REM sleep in mice (Funk et al., 2016); iii) “local” slow waves that are out of phase across brain regions in humans (Nir et al., 2011) and rats (Rector et al., 2005) or iv) the simultaneous co-existence of REM sleep and NREM sleep in different brain structures, such as the hippocampus and neocortex of rats (Durán et al., 2018; Emrick et al., 2016).

It is this second understanding of local sleep that we deal with in this article, and specifically, the exploration of disparate sleep states in smaller, “local” neural assemblies (Krueger et al., 2008), where sleep phenotypes may emerge from the integration and synchronization of local network states (Krueger et al., 2013).

The avian brain provides an important test ground for investigating these local differences during natural sleep. Although most of the theoretical models that examine the generation of neural oscillations depend on cytoarchitecturally regular structures, such as the layered structure of the mammalian cortex (Buzsáki et al., 2012; da Silva, 2010), the avian brain is capable of generating sleep oscillations comparable to that of mammalian slow waves (Canavan & Margoliash, 2020; Low et al., 2008), despite the absence of a layered cortex. By investigating local sleep in the avian brain, we extend the existing knowledge about local sleep across animal species and neural architectures.

In this study, we examined differences in sleep states across two parts of the avian pallium (telencephalon). We recorded 1) superficial EEG signals from the avian hyperpallium, which is homologous to the dorsal pallium (neocortex) of mammals and 2) deeper LFP signals from the avian dorsal ventricular ridge (DVR), which is a pallial structure unique to birds and reptiles. In birds, the DVR is further subdivided into the mesopallium, nidopallium, and arcopallium (Briscoe & Ragsdale, 2018). Importantly, sites in the hyperpallium have been shown to exhibit cortical-like, use-dependent regulation during sleep (Lesku et al., 2011), whereas hippocampal-like

sharp-wave ripple activity has been recorded in the DVR of both birds (Yeganegi et al., 2019) and reptiles (Norimoto et al., 2020; Shein-Idelson et al., 2016).

## Methods

### Experimental animals

All experimental procedures were conducted in accordance with the principles of laboratory animal care and were carried out in compliance with the current versions of the German and European laws on Animal Experimentation (Approval # ROB-55.2-2532.Vet_02-18-108: J.M.O.). Additionally, the experiments followed the guidelines set forth by ARRIVE (Animal Research: Reporting of In Vivo Experiments). Ethical approval for the study was obtained from the ethics committee of the Government of Upper Bavaria (Regierung von Oberbayern), which operates in accordance with § 14.1 TierSchG (German animal welfare law). Furthermore, the housing and breeding arrangements for the animals received the approval of the Veterinary Office of Freising, Germany (Approval # 32-568).

Electrophysiological recordings were made in three male zebra finches (*Taeniopygia guttata*), aged 83-91 days post-hatch (dph), all of which exhibited physical signs of maturity as indicated by feather and beak coloring. Details concerning the age and corresponding symbol used for each individual are presented in Table 1. The data analyzed here represent 36 hours of data recorded in 3, 12-hour long sleep recordings sessions from 3 animals.

| Bird ID | Age (dph) | Symbol used in this text | # Good EEG electrodes | Medial LFP location |
|---|---|---|---|---|
| w027 | 83 | ○ | 4/4 | 1.86 mm (RH) |
| w042 | 90 | + | 3/4 * | 1.74 mm (RH) |
| w044 | 91 | ◊ | 4/4 | 1.25 mm (RH) |

**Table. 1 Description of experimental birds used in experiments.** Bird ID, age, the corresponding symbol used in the figures, and the number of recording electrodes available are displayed. dph: days post-hatch, RH: right hemisphere. *: data from the left posterior EEG was not used in this bird.

Prior to the experiments, the birds were housed in aviaries with a 12:12-hour light:dark cycle. They were provided with access to a seed mix, millet, sepia bone, and water *ad libitum*. Additionally, fresh vegetables and cooked eggs

were given to the birds once a week. The recording chambers were equipped with LED lights, UV bird lights (Bird Systems, Germany), infrared LED panels (850 nm waves), and ventilation to ensure constant air circulation.

**Electrode preparation and positioning**

For each animal, an electrode implant was constructed that consisted of 4 EEG electrodes, 4-8 LFP electrodes, a ground and a reference electrode. The preparation and positioning of the EEG electrodes is described elsewhere (Yeganegi & Ondracek, 2023); briefly, EEG electrodes were constructed from silver wire (254 µm bare wire diameter, Science Products GmbH) by melting the tip into a smooth ball of approximately 0.50 mm in diameter. The LFP electrodes were made from 5 mm lengths of coated steel wire with a bare diameter of 127 µm (A-M Systems, Sequim, WA) and pinned to an omnetics connector with small gold EIB pins (Neuralynx Inc, Bozeman, MT, USA). Because the number of LFP electrodes was variable across animals, we chose one LFP electrode to use as the designated LFP electrode in the congruence analysis. This LFP electrode was the most medial LFP electrode, and across animals, it was positioned on average at 1.62 ± 0.32 mm (mean ± std; Supplementary Fig. S1).

**Anesthesia and Surgery**

The birds were anesthetized using oxygenated isoflurane gas (EverFlo OPI, Phillips, Netherlands) with a 3-4% concentration during induction and 0.8-1.5% during maintenance. A small tube was used to deliver the anesthetic gas through the bird's beak via a vaporizer (Isotec 4, Groppler, Germany). To prevent the accumulation of excess anesthetic gas, a scavenger (Scavenger LAS, Groppler, Germany) removed waste anesthetic gas. The bird was positioned on a heating pad with a closed-loop temperature monitoring device (Harvard Apparatus, MA, USA). Throughout anesthesia, body temperature was continuously monitored using an infrared thermometer and remained above 39.5°C.

The anesthetized bird was positioned in a stereotaxic frame (Kopf Instruments, CA, USA) and the head was immobilized. Anesthetic depth assessment was carried out by applying slight pressures on a toe using tweezers. When the toe reflex ceased, a local anesthetic was applied to the

scalp (Aspen, xylocaine pump spray), and the feathers on the head were removed with forceps. An incision was made in the scalp along the sagittal midline, and a dental drill (Volvere i7, NSK Europe GmbH, Germany) was used to make small holes in the skull for the (supradural) EEG electrodes (see the schematic in Fig. 1a) and a small craniotomy (1×1.5 mm) for the LFP electrodes. The dura matter was resected, the LFP electrodes were lowered altogether 1.8-2.2 mm deep into the pallium, targeting the mesopallium of the DVR (see the histology sample in Fig. 1B) and secured in place with dental cement (Paladur, Henry Schein Dental, Germany). The EEG electrodes were then positioned over the hyperpallium and secured with dental cement.

The LFP electrodes were positioned in a row orthogonal to the midline, where the LFP electrode closest to the midline was positioned 1.5 mm lateral from the midline, and the LFP electrode most lateral was positioned 2.5 mm lateral from the midline. LFP electrodes were 2-3 mm frontal to the junction between the frontal and parietal cranial bones. The two frontal EEG electrodes were positioned 2 mm lateral from the midline on each side and 5 mm anterior to the junction of frontal and parietal cranial bones. Posterior EEG electrodes were placed 2.5 mm lateral to the midline and 1 mm posterior to the frontal and parietal bones junction. Reference and ground electrodes (silver ball electrodes) were positioned over the cerebellum (Fig. 1A).

After the surgery, animals were released from the stereotaxic frame and administered an analgesic (Metamizole (100-150 mg/kg, i.m.). Animals were kept on the heating pad until signs of recovery from the anesthesia were observed. Following the surgery, an antibiotic (Baytril, 1025 mg/kg, i.m.) and an analgesic (Metamizole (100-150 mg/kg, i.m.) were administered for up to 3 days.

**Electrophysiology**

After surgery, the birds were habituated to the implant within the recording chambers. During a recording session, the preamplifier (Intan Technologies, RHD2132) and its associated tether cable were connected to the electrode implant one hour before the lights were turned off (light-off period: 10:00 PM - 10:00 AM) to allow the birds to adopt a natural sleeping position. The weight of the tether cable was counterbalanced using an elastic rubber band. Electrode signals were acquired at a sampling rate of 30 kHz using

an Open Ephys data acquisition board (OEPS, Portugal), filtered within the range of 0.1-9987 Hz, and saved in the Open Ephys GUI “continuous” format. A near-infrared sensitive camera (acA1300-60gm, Basler Ag, Germany) was used to acquire video recordings of the animals using custom-written software (ZR View, Robert Zollner). Camera frames were triggered using a pulse generator (Pulse Pal, Sanworks, NY, USA (35)) at a frame rate of 20 Hz. The tether cable was disconnected from the headstage half an hour after the lights were turned on the following morning.

### Histology

After the final recording session, the birds were deeply anesthetized using a lethal dose of sodium pentobarbital (250 mg/kg, i.m.). Once the corneal reflex and heartbeat had ceased, the bird was decapitated and the brain was extracted from the skull. The brain was subsequently immersed in a 4% paraformaldehyde solution in phosphate-buffered saline for a minimum duration of one day. 80 µm coronal sections were stained with cresyl violet to aid in electrode site verification.

### Data Analysis

Data were recorded from the birds for a period of approximately two weeks. The nighttime recordings analyzed in this study occurred after at least one week of habituation to the recording environment. For data analysis, one whole night of sleep (i.e., 12 hours) was analyzed for each bird. The nighttime recording was selected on the basis of behavior (i.e., sleeping behavior occurred in one long session and was not broken up during the night), the quality of electrophysiology data, and the quality of the video recording (the bird was visible within the recording frame throughout the night).

## Automatic sleep staging

All data analysis was conducted offline in Matlab (Matworks, Inc., Natick, MA). Electrophysiological data were down-sampled to 468.75 samples/s (equivalent to a down-sampling factor of 64). Similar to previous work (Yeganegi & Ondracek, 2023), a semi-automatic sleep staging procedure was employed to classify each 3-second data window into one of the following categories: awake, SWS, REM sleep, or Intermediate Sleep (IS). IS can be considered a transitional stage of NREM sleep, and it typically lacks the large slow oscillations that characterize SWS (Low et al., 2008).

In a first pass, the distinction between wake and sleep was determined by examining each 3-s bin for–the strong presence of gamma activity (30-50 Hz), since the wake-associated body movements were reflected in artifacts within this band. For this detection, the moving median and the moving interquartile interval (IQR) were computed in 10-minute windows for the data from the left anterior EEG channel. The 3-sec bins where 30-50 Hz power exceeded the threshold of (moving median + 3×moving IQR) were considered "wake". Wake detection was confirmed by inspecting the corresponding video frames; movement artifacts typically involved body twitches, eye-opening, or changes in posture.

Next, we segmented the rest of the bins, i.e., sleep bins, into three clusters of SWS, REM sleep, and IS by comparing the δ/γ power ratio in each bin. Similar to the detection of wake bins, the δ/γ in each 3-sec bin was compared to the moving median (δ/γ) + *A*×moving IQR(δ/γ) for SWS and moving median(δ/γ) - *A*×moving IQR(δ/γ) for REM sleep. The remaining bins were labeled as IS. Here *A* is a parameter that we iteratively increment from 0.1 to 2 to find the best clustering output. For each value of *A* we checked the output via two visualizations. 1) Visualization of the clustering results in a 3D space (Supplementary Fig. S2) composed of log(δ), log(γ), and max amplitude in each bin, similar to (Low et al., 2008) and (Canavan & Margoliash, 2020). 2) Visualization of the labels alongside the raw EEG trace (Supplementary Fig. S2). Based on these two visualizations, we selected the value of *A* with which the clustering output was maximally crisp and accepted the corresponding clustering results.

**Sleep state congruence**

To quantify differences in neural activity across different brain regions, we first scored the sleep states separately in each of the five electrode sites: right and left anterior EEG, right and left posterior EEG, and the medial-most LFP electrode in DVR. Then, we used the definition of congruence as stated in (Durán et al., 2018); that is, "congruence" was defined as the percentage with which a given electrode shows the same sleep stage as a baseline electrode. We chose the left anterior EEG electrode as the baseline electrode, similar to (Durán et al., 2018). Congruence was then computed for each pairwise electrode comparison for each stage of sleep.

For example, to determine the congruence between the right posterior electrode and the baseline electrode (left anterior EEG) during SWS, we identified all of the 3-s bins that were labeled as SWS in the baseline

electrode, and then calculated the percentage of those bins that were also labeled as SWS in the right posterior electrode. If all SWS bins in the baseline electrode corresponded to matching SWS bins in the comparison electrode, then the congruence was 100%. If some of those bins did not match, i.e., a SWS bin in the baseline electrode was labeled as a IS bin in the comparison electrode, then the congruence measurement equaled less than 100%.

### Spectral analysis

Power spectral analysis was computed using the Welch method on 3-s windows of data for each electrode. The number of discrete Fourier transform (DFT) points to use in the PSD estimate was set to 512. A 95% confidence interval was then estimated by computing the standard error as described in (Altman & Bland, 2005). To estimate the spectrograms visualized in Fig. 1D, the continuous wavelet transform ('cwt' function in Matlab) was used with a Gabor kernel

### Comparison of δ/γ power ratio

As an alternative approach to the congruence analysis, we compared the δ/γ power ratio between the most medial LFP channel and the left anterior EEG channels, i.e., the same channels used in the congruence analysis. δ and γ were defined as spectral band power in 1-4 Hz and 30-48 Hz respectively. First, the δ/γ power ratio was calculated in each channel in 3-sec bins and then smoothed in 30-sec windows to factor out transient fluctuations in the power. In each bird, this resulted in two vectors of δ/γ values, one for the EEG and one for the LFP signals. Then, each δ/γ vector of values in each channel, EEG and LFP, were normalized by their range, so that both δ/γ vector of values in the EEG and LFP channel had the same range, that is, zero to one. Finally, we found the difference between the two δ/γ vectors by subtracting them in each bin and calculating the absolute value of the difference.

### Temporal characteristics of congruence

In order to track the temporal characteristics of congruence and specifically how it evolved over a night of sleep, we also computed the congruence in sliding windows throughout the night. The window length was set to five minutes so that we had enough bins of each stage of sleep for the congruence calculation while maintaining a high temporal resolution.

### Sleep stage transition analysis

To investigate possible temporal precedence between the left and right hemispheres during the transitions between REM sleep and SWS stages, we compared the spectrograms of the EEGs between the left and right hemispheres. These comparisons were performed separately for the anterior and posterior channels between the hemispheres. First, based on the sleep scoring labels in the left anterior EEG (used as reference in the congruence analysis), we found all periods of SWS longer than one bin which were followed immediately by a period of REM sleep longer than one bin (and vice versa for REM sleep to SWS). Then, we calculated the spectrograms around these transition times in the left and right hemisphere EEGs separately, using continuous wavelet transform with Gabor kernels. Finally, we calculated the sum of power in the 5-25 Hz band in the spectrograms to obtain the transition-locked spectral power traces.

### Statistical analysis

To compare the duration and the percentage of each stage of sleep across the recording sits, we used the Wilcoxon rank-sum test (also known as the Mann-Whitney U-test). The U-test is a non-parametric test which does not require the assumption of a normal-distribution. Since we aimed to make the comparisons between five different sites, that is, the four EEGs and the most medial LFP, we considered 10 pair-wise comparisons and used a post-hoc Bonferroni correction to determine significance (e.g., $\alpha = 0.05 == 0.005$ after correction; $\alpha = 0.01 == 0.0001$ after correction). Mean and standard errors are also reported (See Supplementary Information for statistical tests).

## Results

### Local variations in sleep state are present across the avian pallium

We recorded surface EEGs from the left and right hemisphere over the hyperpallium and LFPs from the DVR (nidopallium and mesopallium) in three zebra finches. Two silver ball electrodes recorded surface EEG activity in anterior and posterior sites in each hemisphere (four EEG electrodes in total) (Fig. 1A). In addition, 4-8 steel electrodes recorded the LFP in the DVR (Fig. 1A and 1B). Of the 4-8 LFP electrodes, only the LFP signal from the

most medial electrode was used in the analysis (Fig 1B, electrode e4); the other LFP signals were not analyzed. During sleep, both EEG and LFP electrodes showed brain oscillations typical of sleep, i.e., alternative periods of high amplitude slow wave activity, periods of low amplitude gamma oscillations, and periods of mixed frequency EEG activity. A 25-sec trace of EEG and LFP activity during sleep is depicted in Fig. 1C.

As a whole, the EEG and LFP activity was highly heterogeneous across sites (Fig. 1C, dashed box): high-amplitude peaks, deflections, and bursts of activity appeared on only one EEG electrode or only in the LFP recordings. In addition to these fast variations, we also observed sustained periods of time when different oscillations appeared simultaneously across different sites (Fig. 1D, red shading). To better characterize these local differences in neural activity, we segmented the EEG and LFP into discrete sleep states for each electrode separately using a sleep segmentation algorithm that clustered and scored the sleep data on the basis of spectral features typical of avian sleep (Canavan & Margoliash, 2020; Low et al., 2008). We labeled each 3-sec bin of neural activity as either of awake, SWS, IS (intermediate sleep), or REM sleep (Fig. 1D). The differences in sleep states, as scored individually across different electrode sites, correspond with the local variations in the spectral composition of the neural activity at these sites (gray shading, Fig. 1D).

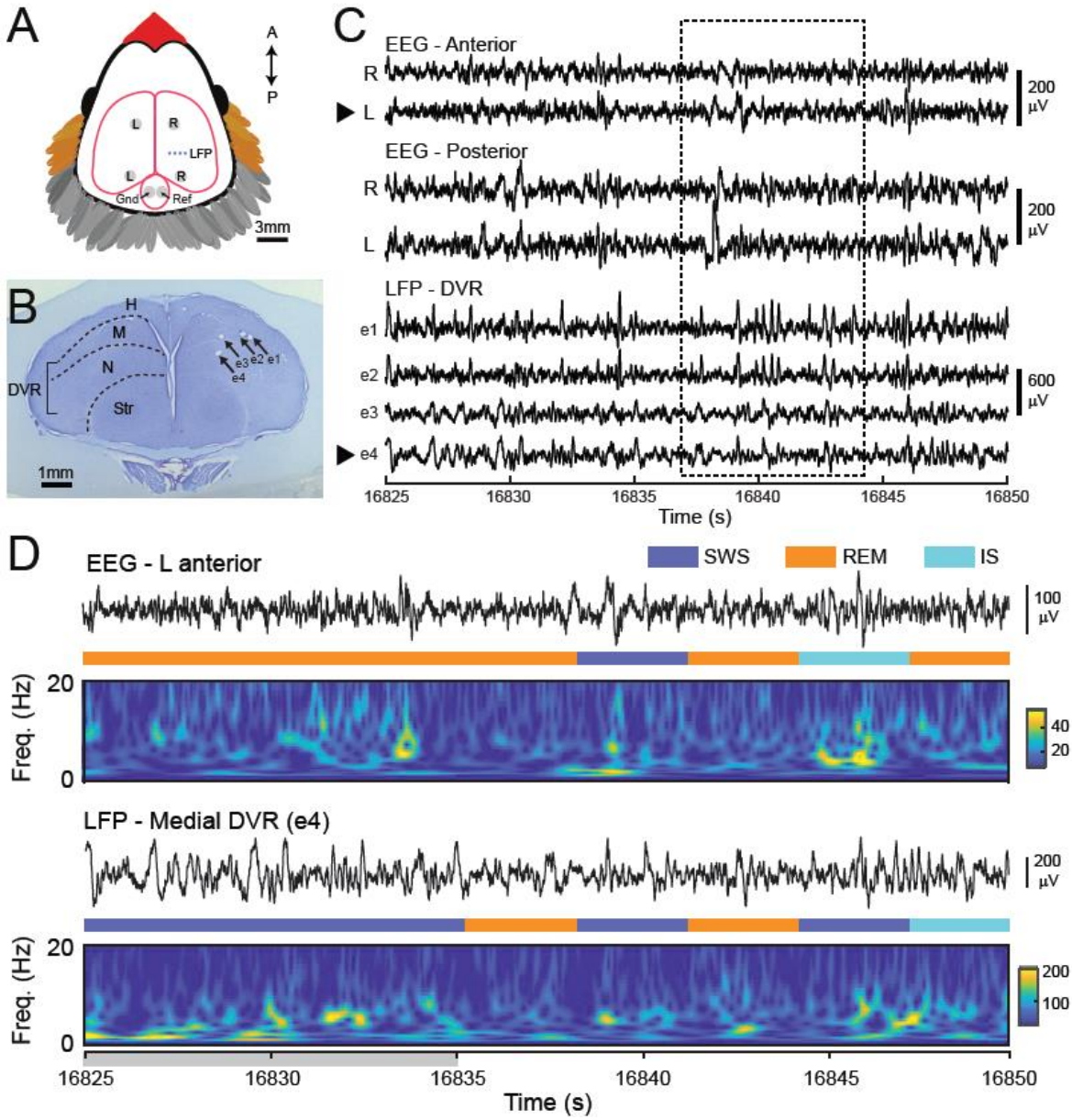


**Fig. 1 Local variations in sleep oscillations across pallial areas. (A)** Schematic depicts the locations of the EEG and LFP electrodes. 2 silver-ball EEG electrodes were implanted above the hyperpalium in both the right (R) and left (L) hemisphere in an anterior (A) and posterior (P) position. 4-8 steel wire LFP electrodes were implanted in the right hemisphere in 3 birds. Of the 4 to 8 LFP electrodes, only the most medial LFP electrode (e.g., e4) was used in the analysis. Two silver-ball EEG electrodes were placed over the cerebellum and used as the ground electrode (Gnd) and reference electrode (Ref). **(B)** Histological section from bird w042 depicts LFP electrode tracts (black arrows; e1-e4). Electrode tips were 1.8-2.2 mm deep in the mesopallium and nidopallium of the dorsal ventricular ridge (DVR). H, hyperpallium; M, mesopallium; N, nidopallium; Str, striatum. **(C)** Simultaneous recordings across different sites and depths reveal variations in sleep oscillations across pallial areas, with notable differences between EEG and LFP electrodes (dashed box). LFP traces from top to bottom correspond to sites from most lateral (e1) to most medial (e4). Black arrowheads indicate the data traces enlarged in (D). **(D)** Simultaneously recorded left anterior EEG

trace (top) and the most medial LFP trace (e4; bottom) with corresponding sleep state labels (colored bars) and spectrograms. Gray shaded area (16825-16835 s) indicates a region of contrasting sleep state labels; note the differences in EEG and LFP amplitude (black traces) as well as the spectral content (spectrograms). Data traces are the same as those in (C).

## Sleep stage segmentation are in line with previously published results

We first quantified the statistics of the sleep staging as a function of the recording sites. We compared the overall percentage of time spent in each sleep state for each electrode site (Fig. 2A). Percentages of time spent in SWS, REM sleep, and IS sleep states were not significantly different as a function of electrode site (Mann-Whitney U-test, Bonferroni correction for multiple comparisons, $p > 0.005$ for all comparisons).

We also analyzed the duration of time spent in SWS, IS, and REM sleep across the different recording sites. Bouts of SWS were significantly longer for the LFP electrode by around 1 sec compared to the EEG sites (Fig. 2B; see Supplementary Information for statistical tests), but overall the differences between electrodes were minimal. These results are in line with previously published results (Yeganegi & Ondracek, 2023).

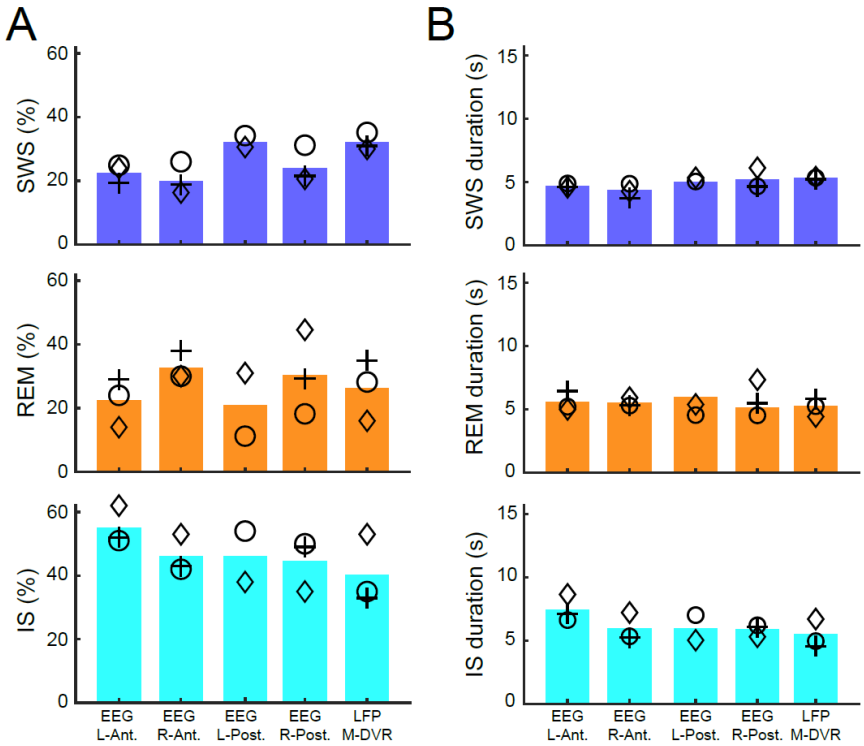


**Fig. 2 Sleep stage durations vary as a function of electrode location. (A)** Bar plots indicate the mean percentages of SWS (top), REM sleep (middle), and IS (bottom) pooled over all nights (n=3) for the 5 different recording sites. Symbols indicate individual animals (see Table 1 for details). **(B)**

Mean durations for SWS, REM sleep, and IS sleep states. Figure conventions same as in (A). Notably, sleep state durations were significantly different as a function of recording location, particularly for SWS and IS stages. Although the differences in the duration across nights are small, in most of the cases, they were statistically significant (see the Supplementary Information for the statistical tests).

## Congruence analysis reveals local sleep states

Next we asked how frequently two distant electrode sites share the same sleep stage at the same time. Our data suggested that this was a relatively rare event: we observed that sleep scores were infrequently identical for distinct recording sites (Fig. 3A, B). In order to quantify this, we calculated the “congruence” between each electrode and a designated baseline electrode (Durán et al., 2018)). Matching (Durán et al., 2018), we chose to use the left anterior EEG electrode as the baseline electrode (Fig. 3A, B). Congruence is an estimate of the probability that two electrode sites display the same sleep state at the same time (see Methods for details). Congruence values less than 100% indicate a state difference between the two electrodes sites and thus identify local differences in sleep states. The congruence values for each electrode and for each sleep state are presented in Fig. 3C. We observed that for all sleep states and across all electrodes, the congruence did not surpass 54%. This suggests that the neural oscillations during sleep, to a large extent, occur within a small anatomical network. In other words, a given sleep state is not a brain-wide phenomenon, but is a local event.

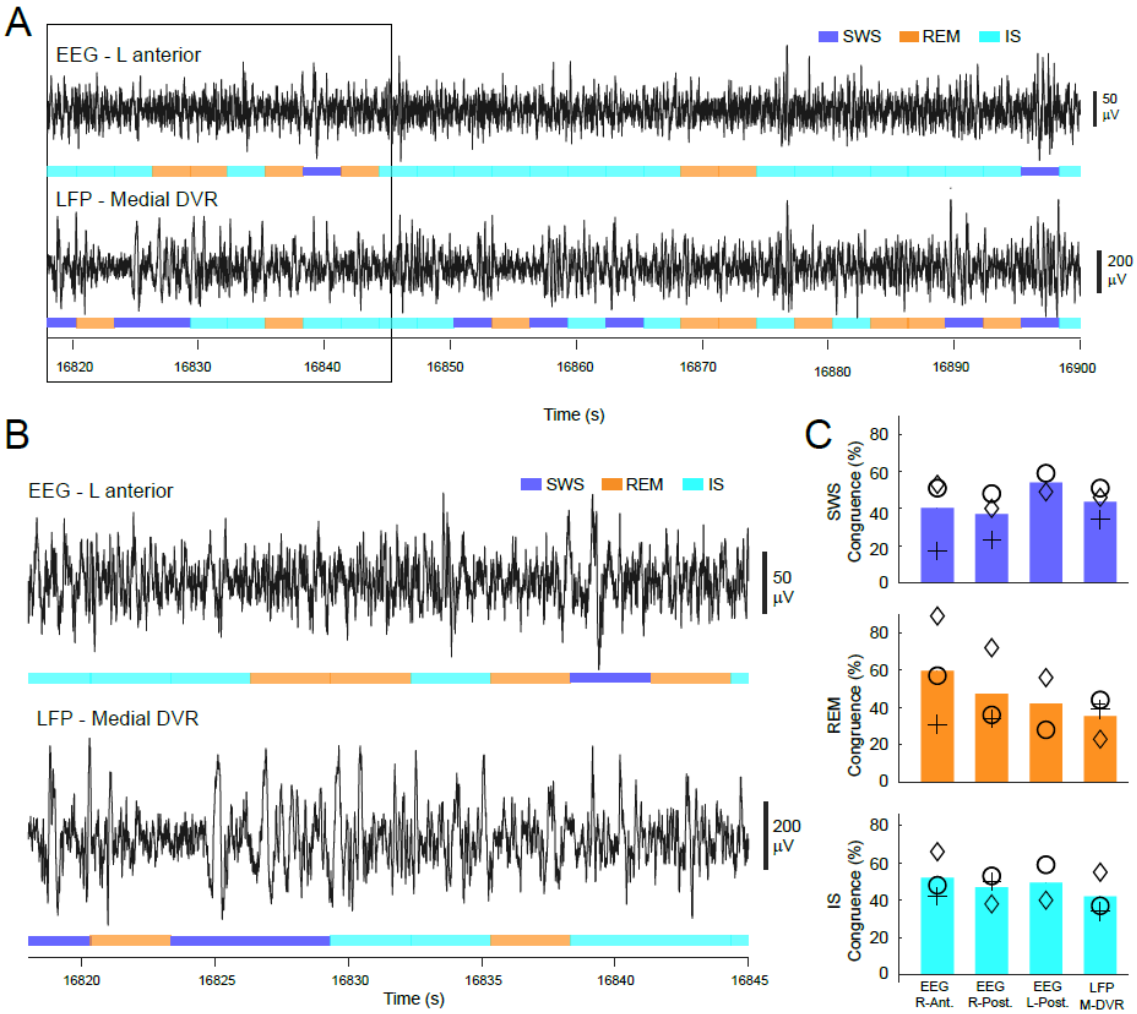


**Fig. 3 Quantification of simultaneous local differences in sleep state across the recording sites.** (A) Traces depict the simultaneous left anterior EEG and medial DVR LFP with the corresponding sleep states scores (colored bars). Black box indicates a section that is enlarged in (B). Sleep state differences between the recording sites are evident through the color-coded representations of sleep stages for the same time windows. (C) Bar plots indicate the mean percentages of congruence for SWS (top), REM sleep (middle), and IS (bottom) pooled over all nights (n=3) for the 4 different recording sites compared to the baseline electrode (the left anterior EEG).

## δ/γ power of neural activity differs in DVR and hyperpallium

Critically, the congruence analysis outlined in the preceding section may be influenced by the distinct outputs of the clustering algorithm when applied to EEG and LFP signals. To address this potential confound and provide an alternative assessment of inter-site differences, we compared the δ/γ power ratio between the most medial LFP and the left anterior EEG (the baseline electrode in congruence analysis). Although the δ/γ power ratio of the EEG

and LFP fluctuate generally in conjunction, we frequently observed periods in which the two δ/γ power ratios diverge from each other (Fig. 4A). For a considerable portion of bins (26.0±1.7%, averaged across birds), the difference between the two δ/γ ratios was above 10% (see the example in Fig. 4B, and the histograms in Fig. 4D). Importantly, these periods of divergence of δ/γ ratios overlaps with the time bins where sleep scoring labels in EEG and LFP are different (in Fig. 4, juxtapose B and C). This analysis further supplements our argument of dissimilar sleep stages that appear simultaneously across the pallial sites.

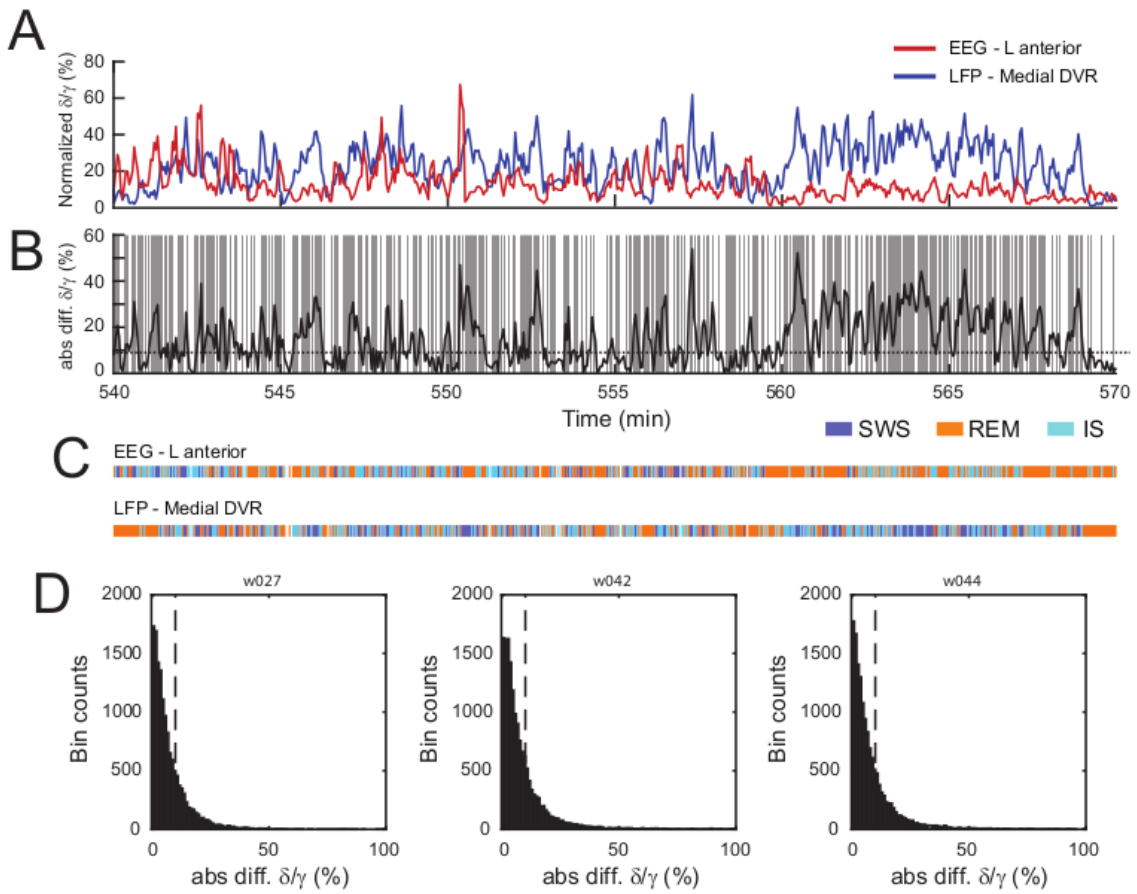


**Fig. 4 δ/γ power ratios show divergence between EEG and LFP signals. (A)** Traces show the normalized δ/γ power ratio for the left anterior EEG baseline electrode (red line) and the most medial LFP electrode (blue line). Note the divergence between the traces during the last ten minutes. δ/γ normalization for visualization purposes only. **(B)** The absolute value of the difference between the EEG and LFP δ/γ ratios. Dashed line indicates the 10% difference threshold. Gray shading indicates divergence values that exceeded 10%. **(C)** Corresponding sleep scoring labels for the EEG and LFP for the same period as in (A) and (B). Note that periods with dissimilar sleep stage labels in the EEG and LFP (gray shading in B) coincide with periods of high divergence of

δ/γ ratios in (B). **(D)** Histograms illustrate the distribution of δ/γ ratio differences between the EEG and LFP. For a large portion of bins, the divergence was above 10% (10% threshold indicated with dashed line; exact percentage of bins above 10%: 24%, 27%, and 27% from left to right).

## Congruence of sleep states changes throughout the night

To explore the temporal dynamics of local sleep as it evolved during sleep, we also tracked the changes in the "instantaneous" congruence between the recording sites by computing the congruence in 5-minute long sliding windows (Fig. 5, A and B). We focused this analysis on the DVR electrode and the left anterior EEG. We observed that the instantaneous congruence between the right DVR and the left hyperpallium did indeed change throughout the sleep time and was largely dependent on the sleep state.

During the first half of night, the congruence between the DVR and baseline electrode decreased for SWS and increased for REM sleep (Fig. 5, C and D). This temporal dynamic was closely coupled to the temporal dynamics of SWS and REM sleep in DVR, and not in the baseline channel. To prove this, we calculated the correlation coefficient between the instantaneous congruence and the likelihood of the corresponding stage of sleep, for both SWS and REM sleep stages (the instantaneous likelihood of SWS and REM sleep are denoted by p(SWS) and p(REM) in Fig. 5). The instantaneous congruence of SWS in the DVR was highly correlated with the likelihood of SWS in the DVR: 0.86 ± 0.12 (correlation coefficient, mean and std among birds). Similar results were true for the REM sleep state (0.93 ± 0.04). In contrast, the correlation coefficient between the congruence and the likelihood of SWS and REM sleep in the baseline electrode (anterior left EEG) was comparably low: 0.47 ± 0.18 for SWS (mean and sd among birds) and 0.52 ± 0.31 for the REM sleep state.

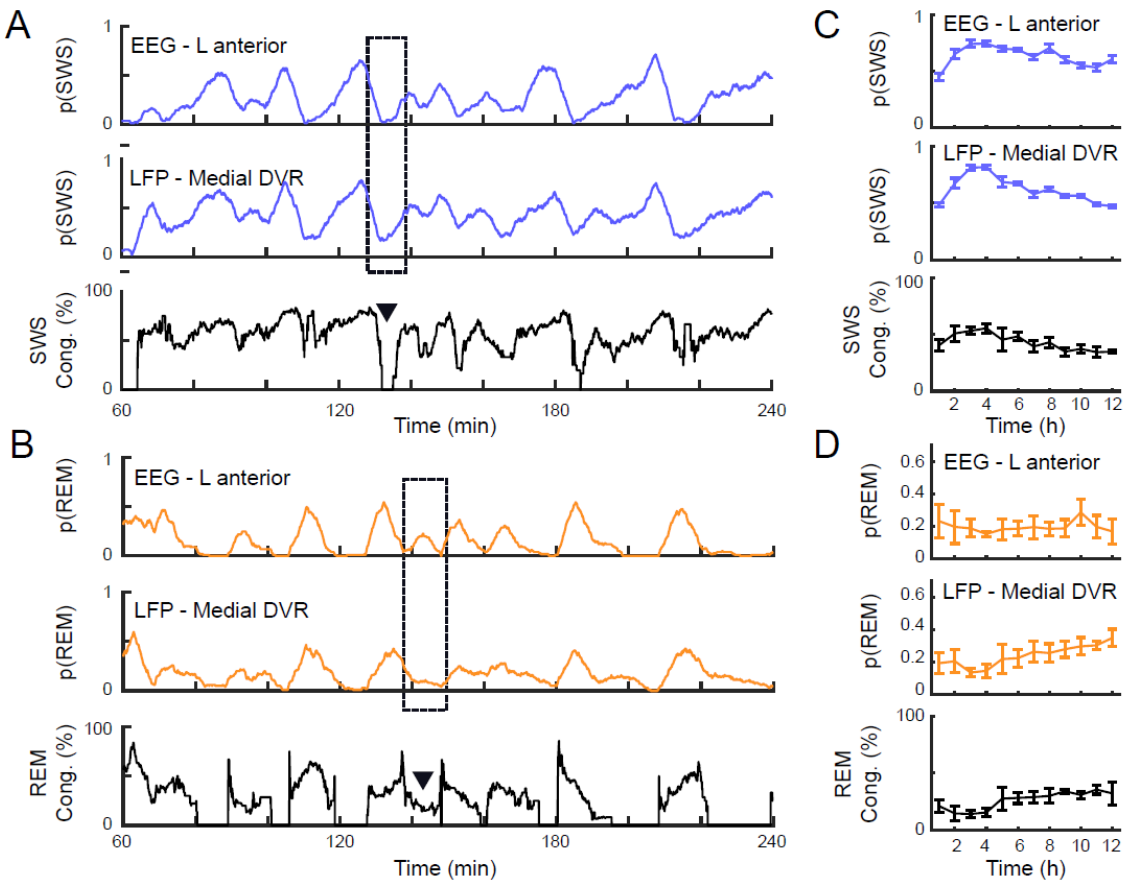


**Fig. 5 Instantaneous congruence changes throughout the night. (A)** Instantaneous likelihood of SWS, p(SWS), in the baseline electrode (top), in the DVR (middle), and the congruence of SWS between these two sites (bottom) are shown. Congruence dynamics were closely tied to the likelihood of SWS in both channels, especially the DVR channel. The dotted box and arrowhead in the lower subplot highlights a period of low congruence between the two electrodes. This period coincides with a differential likelihood of SWS in the DVR and the left anterior EEG. **(B)** Similar to (A), but for the dynamics of the REM sleep. Note again that the marked period with low REM sleep congruence coincides with different likelihood of REM sleep in the two recording sites. **(C)** SWS shows a characteristic decrease for the first half of sleep time, both in the left anterior EEG and in the DVR. The congruence between the DVR and the left anterior EEG changes during sleep time in concert with the likelihood of SWS in the DVR. **(D)** In contrast to SWS, REM sleep likelihood increases both in the left anterior EEG and in the DVR for the first half of sleep time. Similar to SWS, the congruence of REM sleep episodes between the DVR and the left anterior EEG changes during sleep time in concert with the likelihood of REM sleep in the DVR.

## Transient hemispheric asymmetries during state transitions

Lastly, we analyzed whether consistent hemispheric differences exist in the timing of sleep state transitions (that is, transitions from SWS to REM sleep and vice versa). To that end, we compared the transition-locked spectrograms of the left and right EEG channels (Fig. 6, top two rows). Our

analysis revealed that across both hemispheres, power in the 5-25 Hz frequency band increased during transitions to SWS and decreased during transitions to REM sleep. Aggregated power within this frequency band was computed and analyzed (Fig. 6, bottom row). The spectral profiles from left and right hemispheres showed a high degree of similarity, with no clear temporal precedence observed at the temporal scale we examined. However, within these similar patterns, transient divergences in power profiles were detected. Particularly, ~300 ms before REM-to-SWS transitions, a slight differential increase in power was observed in the left hemisphere compared to the right (indicated by arrows in Fig. 6B and 6D). However, this difference did not reach statistical significance (rank-sum test; $p > 0.05$). In summary, our data suggests the presence of asymmetric activity between the hemispheres during sleep state transitions, but these differences were not statistically robust.

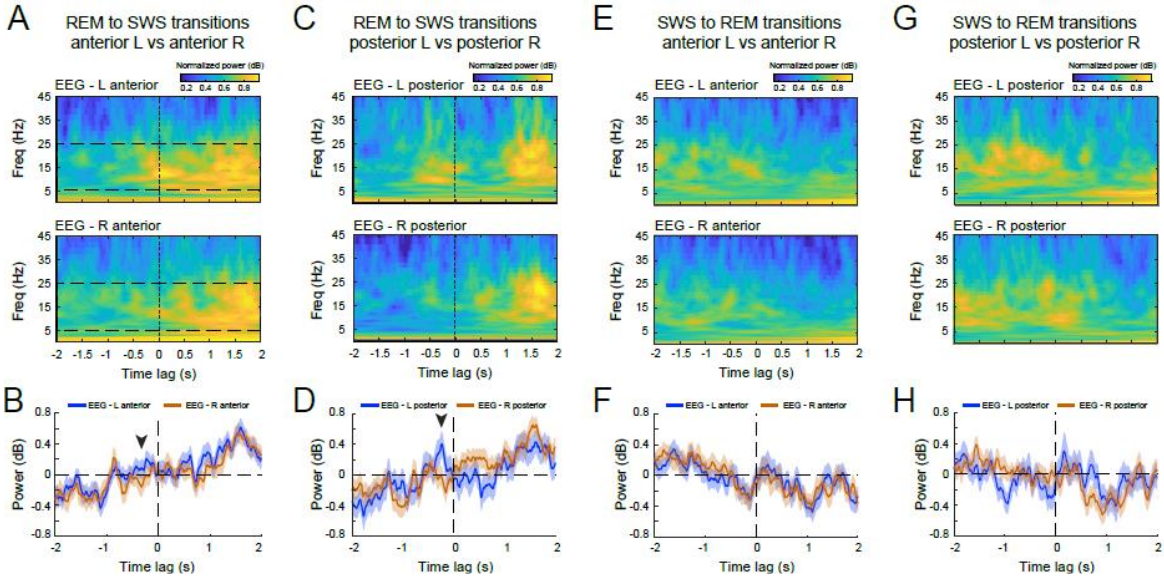


**Fig 6. Spectral analysis of sleep state transitions across hemispheres**. **(A)** Spectrograms indicate the peri-transitions time window for REM-to-SWS transitions for the anterior left (top) and anterior right (bottom) EEG channels. **(B)** The aggregated spectral power in the 5-25 Hz band for EEG data locked to REM-to-SWS transitions are displayed for the anterior left EEG channel (blue line) and anterior right EEG channel (red line). Black arrowhead indicates a transient divergence between the two electrodes at approximately 300 ms before the REM-to-SWS; however, this hemispheric difference was not statistically significant. **(C, D)** Figure conventions same as in (A, B); data displayed for posterior left and posterior right EEG electrodes during REM-to-SWS transitions. In (D), note similar divergence between electrode sites as in (B; black arrowhead). **(E)**. Data displayed for the anterior left (top) and anterior right (bottom) EEG channels for SWS-REM transitions. **(F)** The aggregated spectral power for EEG data locked to SWS-to-REM transitions are displayed for the anterior left EEG channel (blue line) and anterior right EEG channel (red line). Note the tight correspondence between traces, in contrast to the REM-SWS transitions (e.g., B, D).

**(G, H)** Figure conventions same as in (E, F); data displayed for posterior left and posterior right EEG electrodes during SWS-to-REM transitions.

## Discussion

Our findings highlight the presence of local neural oscillations linked to discrete sleep stages across diverse sites within the avian pallium, which is in line with emerging evidence that suggests that sleep may be locally regulated across the brain (Krueger et al., 2008).

Local regulation of sleep under homeostatic control has already been demonstrated in birds. In (Lesku et al., 2011), one eye in the pigeons was covered, while the other eye was presented with a visual stimulus. On the following night, after the asymmetric visual exposure, EEG was recorded during sleep from the left and right hemispheres. The slow wave activity increased only in the hemisphere contralateral to the visually stimulated eye, demonstrating the local regulation of sleep as a homeostatic mechanism. In contrast to these results, our findings show that local differences in sleep also exist after unperturbed awake activity and is not necessarily the result of homeostatic control.

The idea that sleep could be regulated locally challenges conventional theories that favor the concept of brain-wide sleep that is driven by sleep regulatory *centers* (Saper et al., 2010; Scammell et al., 2017). Indeed, recent studies have suggested that sleep may be a default characteristic of neuronal networks, as demonstrated by the observation of sleep-like oscillations in isolated neural tissues (Bandarabadi et al., 2020; Hinard et al., 2012) and relies on preceding (asymmetrical) activity during wakefulness (Huber et al., 2004; Kattler et al., 1994; Vyazovskiy et al., 2000). Other studies have suggested that metabolically driven changes in sleep-regulatory substances could also regulate local sleep patterns (Hinard et al., 2012). Finally, mathematical modeling has highlighted that the synchronization of sleep-like states across individual cortical columns could ultimately culminate in brain-wide sleep as an emergent property of local-network interactions, without a need for a central switch (Roy et al., 2008). These recent findings collectively propose that the regulation of sleep might not exclusively hinge on a designated neural circuit that switches whole cortical areas between discrete states. Our observation of distinct sleep

stages existing simultaneously across sites within the avian pallium adds evidence to this growing body of emerging data.

The original work that quantified the homogeneity of sleep stages across the cortical sites using congruence was conducted in rats (Durán et al., 2018). In that study, the activity in cortical sites (medial prefrontal, and superficial parietal) and a hippocampal site was compared to a baseline cortical site (superficial frontal). The authors reported average congruence during SWS and REM sleep above 87%. But during IS sleep, the value dropped to 36%. In comparison, in the zebra finch pallium, we observed that the average congruence over all three stages was not higher than 54%, without a significant distinction between the IS and the SWS and REM sleep states (see Fig. 3C). These findings were further supported by our comparison of the δ/γ power ratio for the LFP and left anterior EEG channel (Fig. 4). Here we saw that for as much as 27 % of the sleep time, the δ/γ power ratios calculated individually for these electrodes deviated by more than 10%. As such, we have found a much higher level of heterogeneity in the sleep stages across avian pallium as compared to the mammalian brain.

This observation could be explained considering the differences in the pallial designs between the mammalian and avian brains, most prominently the laminar organization of cortical areas and the presence of the corpus callosum in the placental mammal's brain. However, there are caveats to this explanation. First, the technical differences in sleep scoring methods could account for differences in the estimated congruence. Second, in rats, the IS sleep occupied only 2.2% percentage of the time, including the wake period. In this work (Fig. 2A), we observed that the IS sleep occupies a much larger percentage of sleep (more than 40%) in all channels. Third, the differences in the recording sites might account for marked differences. For instance, it has been reported that under isoflurane anesthesia, slow waves are present in the nidopallium (a subdivision of avian pallium ventral to mesopallium) but not the avian hippocampus (van der Meij et al., 2020).

Finally, our data has implications regarding the origin of slow waves in the avian pallium. In the mammalian brain, slow oscillations seem to emerge from various neocortical regions, subsequently propagating horizontally across the neocortex akin to a traveling wave (Murphy et al., 2009; Nir et al., 2011). Although the neocortex possesses the inherent capacity to generate slow oscillations after recovery from thalamotomy, thalamic input plays a

critical role in the generation of slow waves under normal physiological circumstances (Crunelli & Hughes, 2010; Lemieux et al., 2014). Notably, the inception of slow waves tends to manifest predominantly within layer 5, a layer that receives inputs from the thalamus (Constantinople & Bruno, 2013), and subsequently propagates vertically within cortical columns (Capone et al., 2019).

In the avian brain, two subregions of the visual hyperpallium are known to receive extensive thalamic input, namely the Interstitial part of the apical hyperpallium and the intercalated part of the hyperpallium (Reiner et al., 2004; Wild, 1987). A multichannel LFP recording that allowed simultaneous recordings from these two regions as well as a subregion with far less thalamic input, i.e., hyperpallium densocellulare, showed that the amplitude of slow waves was higher in the thalamic recipient subdivisions (van der Meij et al., 2019). In addition, it was reported that the slow waves tend to appear first in these subdivisions and then propagate through, and outward, from these areas. Slow wave amplitude during sleep has not been directly investigated in the songbird pallium, which also receives extensive thalamic input to brain areas involved in vocal learning (Akutagawa & Konishi, 2005; Boettiger & Doupe, 1998; Coleman et al., 2007; Ondracek & Hahnloser, 2013).

Could local EEG patterns be regulated by thalamic input, or is it instead locally regulated by the pallium itself? Given the distinctions between the mammalian cortex and the avian pallium, further investigations are necessary to elucidate the underlying mechanisms responsible for the genesis of slow waves and their local modulations in the avian brain.

**Author Contributions**

Conceptualization, H.Y. and J.M.O.; Methodology, H.Y. and J.M.O.; Software: H.Y. and J.M.O.; Validation, J.M.O.; Formal Analysis, H.Y.; Investigation, H.Y.; Writing – Original Draft, H.Y.; Writing – Review & Editing, J.M.O.; Funding Acquisition, J.M.O.; Resources, J.M.O.; Visualization, H.Y. and J.M.O.; Supervision, J.M.O.; Project Administration, J.M.O.

**Acknowledgements**

The authors are thankful to B. Seibel and Y. Schwarz for technical assistance; C. Fink and E. Jochen for help with mechanical design, fabrication, and electronics; A. Schuhbauer for administrative assistance, and H. Luksch, for feedback and support of this research.

**Funding Information**

This study was funded by grants from the German Research Foundation (Deutsche Forschungsgemeinschaft; ON 151/1-1) and the Daimler and Benz Foundation (Postdoctoral scholarship) awarded to Janie M. Ondracek.

**Conflict of Interest Statement**

The authors declare no conflicts of interest related to this work.

**Data Availability Statement**

The data that support the findings will be available in upon request from the corresponding author.

**ORCID**

Hamed Yeganegi https://orcid.org/0000-0002-1737-0038

Janie M. Ondracek https://orcid.org/0000-0002-4570-447X

## References

Akutagawa, E., & Konishi, M. (2005). Connections of thalamic modulatory centers to the vocal control system of the zebra finch. *Proceedings of the National Academy of Sciences of the United States of America*, *102*(39), 14086–14091. https://doi.org/10.1073/pnas.0506774102

Albeck, N., Udi, D. I., Eyal, R., Shvartsman, A., & Shein-Idelson, M. (2022). Temperature-robust rapid eye movement and slow wave sleep in the lizard

Laudakia vulgaris. *Communications Biology*, *5*(1), Article 1. https://doi.org/10.1038/s42003-022-04261-4

Altman, D. G., & Bland, J. M. (2005). Standard deviations and standard errors. *BMJ (Clinical Research Ed.)*, *331*(7521), 903. https://doi.org/10.1136/bmj.331.7521.903

Bandarabadi, M., Vassalli, A., & Tafti, M. (2020). Sleep as a default state of cortical and subcortical networks. *Current Opinion in Physiology*, *15*, 60–67. https://doi.org/10.1016/j.cophys.2019.12.004

Bernardi, G., Siclari, F., Yu, I., Zennig, C., Bellesi, M., Ricciardi, E., Cirelli, C., Ghilardi, M. F., Pietrini, P., & Tononi, G. (2015). Neural and behavioral correlates of extended training during sleep deprivation in humans: Evidence for local, task-specific effects. *Journal of Neuroscience*, *35*(11), 4487–4500. Scopus. https://doi.org/10.1523/JNEUROSCI.4567-14.2015

Boettiger, C. A., & Doupe, A. J. (1998). Intrinsic and Thalamic Excitatory Inputs Onto Songbird LMAN Neurons Differ in Their Pharmacological and Temporal Properties. *Journal of Neurophysiology*, *79*(5), 2615–2628. https://doi.org/10.1152/jn.1998.79.5.2615

Briscoe, S. D., & Ragsdale, C. W. (2018). Homology, neocortex, and the evolution of developmental mechanisms. *Science*, *362*(6411), 190–193. https://doi.org/10.1126/science.aau3711

Buzsáki, G., Anastassiou, C. A., & Koch, C. (2012). The origin of extracellular fields and currents—EEG, ECoG, LFP and spikes. *Nature Reviews. Neuroscience*, *13*(6), 407–420. https://doi.org/10.1038/nrn3241

Canavan, S. V., & Margoliash, D. (2020). Budgerigars have complex sleep structure similar to that of mammals. *PLOS Biology*, *18*(11), e3000929. https://doi.org/10.1371/journal.pbio.3000929

Capone, C., Rebollo, B., Muñoz, A., Illa, X., Del Giudice, P., Sanchez-Vives, M. V., & Mattia, M. (2019). Slow Waves in Cortical Slices: How Spontaneous Activity is Shaped by Laminar Structure. *Cerebral Cortex (New York, N.Y.: 1991)*, *29*(1), 319–335. https://doi.org/10.1093/cercor/bhx326

Cirelli, C., & Tononi, G. (2008). Is sleep essential? *PLoS Biology*, *6*(8), e216. https://doi.org/10.1371/journal.pbio.0060216

Coleman, M. J., Roy, A., Wild, J. M., & Mooney, R. (2007). Thalamic gating of auditory responses in telencephalic song control nuclei. *The Journal of Neuroscience : The Official Journal of the Society for Neuroscience*, *27*(37), 10024–10036. https://doi.org/10.1523/JNEUROSCI.2215-07.2007

Constantinople, C. M., & Bruno, R. M. (2013). Deep cortical layers are activated directly by thalamus. *Science (New York, N.Y.)*, *340*(6140), 1591–1594. https://doi.org/10.1126/science.1236425

Crunelli, V., & Hughes, S. W. (2010). The slow (<1 Hz) rhythm of non-REM sleep: A dialogue between three cardinal oscillators. *Nature Neuroscience*, *13*(1), 9–17. https://doi.org/10.1038/nn.2445

da Silva, F. L. (2010). EEG: Origin and Measurement. In C. Mulert & L. Lemieux (Eds.), *EEG - fMRI: Physiological Basis, Technique, and Applications* (pp. 19–38). Springer. https://doi.org/10.1007/978-3-540-87919-0_2

Durán, E., Oyanedel, C. N., Niethard, N., Inostroza, M., & Born, J. (2018). Sleep stage dynamics in neocortex and hippocampus. *Sleep*, *41*(6). https://doi.org/10.1093/sleep/zsy060

Emrick, J. J., Gross, B. A., Riley, B. T., & Poe, G. R. (2016). Different Simultaneous Sleep States in the Hippocampus and Neocortex. *Sleep*, *39*(12), 2201–2209. https://doi.org/10.5665/sleep.6326

Funk, C. M., Honjoh, S., Rodriguez, A. V., Cirelli, C., & Tononi, G. (2016). Local Slow Waves in Superficial Layers of Primary Cortical Areas during REM Sleep. *Current Biology : CB*, *26*(3), 396–403. https://doi.org/10.1016/j.cub.2015.11.062

Hanlon, E. C., Faraguna, U., Vyazovskiy, V. V., Tononi, G., & Cirelli, C. (2009). Effects of skilled training on sleep slow wave activity and cortical gene expression in the rat. *Sleep*, *32*(6), 719–729. https://doi.org/10.1093/sleep/32.6.719

Hinard, V., Mikhail, C., Pradervand, S., Curie, T., Houtkooper, R. H., Auwerx, J., Franken, P., & Tafti, M. (2012). Key electrophysiological, molecular, and metabolic signatures of sleep and wakefulness revealed in primary cortical cultures. *The Journal of Neuroscience: The Official Journal of the Society for Neuroscience*, *32*(36), 12506–12517. https://doi.org/10.1523/JNEUROSCI.2306-12.2012

Huber, R., Ghilardi, M. F., Massimini, M., & Tononi, G. (2004). Local sleep and learning. *Nature*, *430*(6995), 78–81. https://doi.org/10.1038/nature02663

Kattler, H., Dijk, D. J., & Borbély, A. A. (1994). Effect of unilateral somatosensory stimulation prior to sleep on the sleep EEG in humans. *Journal of Sleep Research*, *3*(3), 159–164. https://doi.org/10.1111/j.1365-2869.1994.tb00123.x

Krueger, J. M., Huang, Y. H., Rector, D. M., & Buysse, D. J. (2013). Sleep: A synchrony of cell activity-driven small network states. *European Journal of Neuroscience*, *38*(2), 2199–2209. https://doi.org/10.1111/ejn.12238

Krueger, J. M., Rector, D. M., Roy, S., Van Dongen, H. P. A., Belenky, G., & Panksepp, J. (2008). Sleep as a fundamental property of neuronal assemblies. *Nature Reviews Neuroscience*, *9*(12), Article 12. https://doi.org/10.1038/nrn2521

Lemieux, M., Chen, J.-Y., Lonjers, P., Bazhenov, M., & Timofeev, I. (2014). The impact of cortical deafferentation on the neocortical slow oscillation. *The Journal of Neuroscience: The Official Journal of the Society for Neuroscience*, *34*(16), 5689–5703. https://doi.org/10.1523/JNEUROSCI.1156-13.2014

Lesku, J. A., Vyssotski, A. L., Martinez-Gonzalez, D., Wilzeck, C., & Rattenborg, N. C. (2011). Local sleep homeostasis in the avian brain: Convergence of sleep function in mammals and birds? *Proceedings. Biological Sciences / The Royal Society*, *278*(1717), 2419–2428. https://doi.org/10.1098/rspb.2010.2316

Leung, L. C., Wang, G. X., Madelaine, R., Skariah, G., Kawakami, K., Deisseroth, K., Urban, A. E., & Mourrain, P. (2019). Neural signatures of sleep in zebrafish. *Nature*, *571*(7764), 198–204. https://doi.org/10.1038/s41586-019-1336-7

Libourel, P.-A., Barrillot, B., Arthaud, S., Massot, B., Morel, A. L., Beuf, O., Herrel, A., & Luppi, P. H. (2018). Partial homologies between sleep states in lizards, mammals, and birds suggest a complex evolution of sleep states in amniotes. *PLoS Biology*, *16*(10), e2005982. https://doi.org/10.1371/journal.pbio.2005982

Libourel, P.-A., Lee, W. Y., Achin, I., Chung, H., Kim, J., Massot, B., & Rattenborg, N. C. (2023). Nesting chinstrap penguins accrue large quantities of sleep through seconds-long microsleeps. *Science*, *382*(6674), 1026–1031. https://doi.org/10.1126/science.adh0771

Low, P., Shank, S. S., Sejnowski, T. J., & Margoliash, D. (2008). Mammalian-like features of sleep structure in zebra finches. *Proc Natl Acad Sci U S A*, *105*(26), 9081–9086. https://doi.org/0703452105 [pii]10.1073/pnas.0703452105

Murphy, M., Riedner, B. A., Huber, R., Massimini, M., Ferrarelli, F., & Tononi, G. (2009). Source modeling sleep slow waves. *Proceedings of the National Academy of Sciences of the United States of America*, *106*(5), 1608–1613. https://doi.org/10.1073/pnas.0807933106

Nir, Y., Staba, R. J., Andrillon, T., Vyazovskiy, V. V., Cirelli, C., Fried, I., & Tononi, G. (2011). Regional Slow Waves and Spindles in Human Sleep. *Neuron*, *70*(1), 153–169. https://doi.org/10.1016/j.neuron.2011.02.043

Norimoto, H., Fenk, L. A., Li, H. H., Tosches, M. A., Gallego-Flores, T., Hain, D., Reiter, S., Kobayashi, R., Macias, A., Arends, A., Klinkmann, M., & Laurent, G. (2020). A claustrum in reptiles and its role in slow-wave sleep. *Nature*, *578*(7795), 413–418. https://doi.org/10.1038/s41586-020-1993-6

Ondracek, J. M., & Hahnloser, R. H. R. (2013). Advances in Understanding the Auditory Brain of Songbirds. In C. Köppl, G. A. Manley, A. N. Popper, & R. R. Fay (Eds.), *Insights from Comparative Hearing Research* (pp. 347–388). Springer New York. https://doi.org/10.1007/2506_2013_31

Pophale, A., Shimizu, K., Mano, T., Iglesias, T. L., Martin, K., Hiroi, M., Asada, K., Andaluz, P. G., Van Dinh, T. T., Meshulam, L., & Reiter, S. (2023). Wake-like skin patterning and neural activity during octopus sleep. *Nature*, *619*(7968), Article 7968. https://doi.org/10.1038/s41586-023-06203-4

Rector, D. M., Topchiy, I. A., Carter, K. M., & Rojas, M. J. (2005). Local functional state differences between rat cortical columns. *Brain Research*, *1047*(1), 45–55. https://doi.org/10.1016/j.brainres.2005.04.002

Reiner, A. J., Perkel, D. J., Bruce, L. L., Butler, A. B., Csillag, A., Kuenzel, W., Medina, L., Paxinos, G., Shimizu, T., Striedter, G. F., Wild, J. M., Ball, G. F., Durand, S. E., Güntürkün, O., Lee, D. W., Mello, C. V., Powers, A. S., White, S. A., Hough, G. E., … Gütürkün, O. (2004). Revised nomenclature for avian telencephalon and some related brainstem nuclei. *The Journal of Comparative Neurology*, *473*(3), 377–414. https://doi.org/10.1002/cne.20118

Roy, S., Krueger, J. M., Rector, D. M., & Wan, Y. (2008). A Network Model for Activity-Dependent Sleep Regulation. *Journal of Theoretical Biology*, *253*(3), 462–468. https://doi.org/10.1016/j.jtbi.2008.03.033

Saper, C. B., Fuller, P. M., Pedersen, N. P., Lu, J., & Scammell, T. E. (2010). Sleep State Switching. *Neuron*, *68*(6), 1023–1042. https://doi.org/10.1016/j.neuron.2010.11.032

Scammell, T. E., Arrigoni, E., & Lipton, J. (2017). Neural Circuitry of Wakefulness and Sleep. *Neuron*, *93*(4), 747–765. https://doi.org/10.1016/j.neuron.2017.01.014

Shein-Idelson, M., Ondracek, J. M., Liaw, H., Reiter, S., & Laurent, G. (2016). Slow waves, sharp waves, ripples, and REM in sleeping dragons. *Science (New York, N.Y.)*, *352*(6285), 590–595. https://doi.org/10.1126/science.aaf3621

Siegel, J. M. (2008). Do all animals sleep? *Trends in Neurosciences*, *31*(4), 208–213. https://doi.org/10.1016/j.tins.2008.02.001

van der Meij, J., Martinez-Gonzalez, D., Beckers, G. J. L., & Rattenborg, N. C. (2019). Intra-"cortical" activity during avian non-REM and REM sleep: Variant and invariant traits between birds and mammals. *Sleep*, *42*(2), 1–13. https://doi.org/10.1093/sleep/zsy230

van der Meij, J., Rattenborg, N. C., & Beckers, G. J. L. (2020). Divergent neuronal activity patterns in the avian hippocampus and nidopallium. *European Journal of Neuroscience*, *7*, 0–2. https://doi.org/10.1111/ejn.14675

Vyazovskiy, V. V., Borbély, A. A., & Tobler, I. (2000). Unilateral vibrissae stimulation during waking induces interhemispheric EEG asymmetry during subsequent sleep in the rat. *Journal of Sleep Research*, *9*(4), 367–371. https://doi.org/10.1046/j.1365-2869.2000.00230.x

Vyazovskiy, V. V., & Harris, K. D. (2013). Sleep and the single neuron: The role of global slow oscillations in individual cell rest. *Nature Reviews Neuroscience*, *14*(6), 443–451. https://doi.org/10.1038/nrn3494

Vyazovskiy, V. V., Olcese, U., Hanlon, E. C., Nir, Y., Cirelli, C., & Tononi, G. (2011). Local sleep in awake rats. *Nature*, *472*(7344), 443–447. https://doi.org/10.1038/nature10009

Vyazovskiy, V. V., & Tobler, I. (2008). Handedness leads to interhemispheric EEG asymmetry during sleep in the rat. *Journal of Neurophysiology*, *99*(2), 969–975. https://doi.org/10.1152/jn.01154.2007

Wild, J. M. (1987). Thalamic projections to the paleostriatum and neostriatum in the pigeon (Columba livia). *Neuroscience*, *20*(1), 305–327. https://doi.org/10.1016/0306-4522(87)90022-4

Yeganegi, H., Luksch, H., & Ondracek, J. M. (2019). Hippocampal-like network dynamics underlie avian sharp wave-ripples. *bioRxiv*, 825075. https://doi.org/10.1101/825075

Yeganegi, H., & Ondracek, J. M. (2023). Multi-channel recordings reveal age-related differences in the sleep of juvenile and adult zebra finches. *Scientific Reports*, *13*(1), Article 1. https://doi.org/10.1038/s41598-023-35160-1

# Supplementary data

## Local sleep in songbirds: Different simultaneous sleep states across the avian pallium

Hamed Yeganegi[1,2], Janie M. Ondracek[1*]

1 Technical University of Munich, TUM School of Life Sciences, Chair of Zoology, Liesel-Beckmann-Str. 4, 85354 Freising-Weihenstephan, Germany.
2 Graduate School of Systemic Neurosciences, Ludwig-Maximilians-University Munich, Großhaderner Str. 2, 82152 Planegg, Germany.
* Correspondence: Janie M. Ondracek, Technical University of Munich, TUM School of Life Sciences, Chair of Zoology, Liesel-Beckmann-Str. 4, 85354 Freising-Weihenstephan, Germany Email: janie.ondracek@tum.de

### Supplementary figures

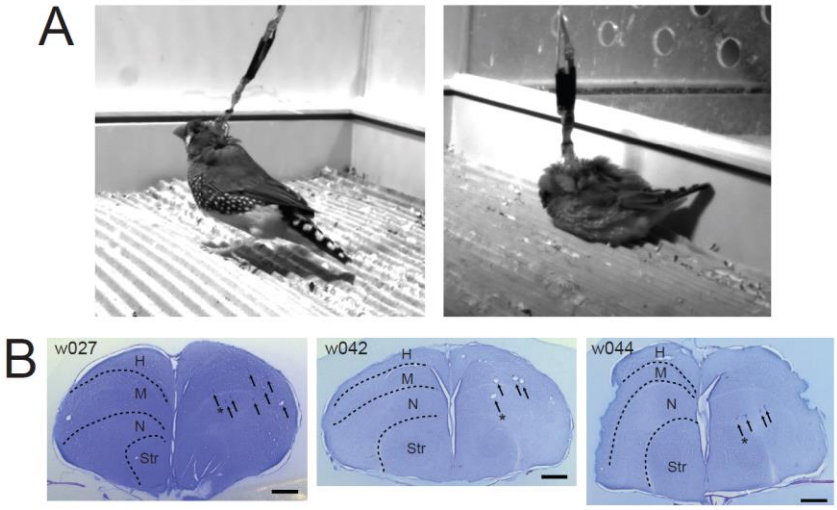


**Fig. S1 Animal posture and histology.** (A) Left, image of an awake tethered juvenile bird (w042). Right, image of the same bird sleeping. Note how bird is able to assume a sleep-specific posture despite the tether cable. (B) Histological sections stained with cresyl violet indicate the LFP electrode tracts (black arrows, n=8 LFP tracts in w027, n=4 LFP tracts in w042 and w044). Asterisk indicates the most medial LFP electrode that was used in the LFP analysis. Error bar indicates 1 mm. H, hyperpallium; M, mesopallium; N, nidopallium; Str, striatum.

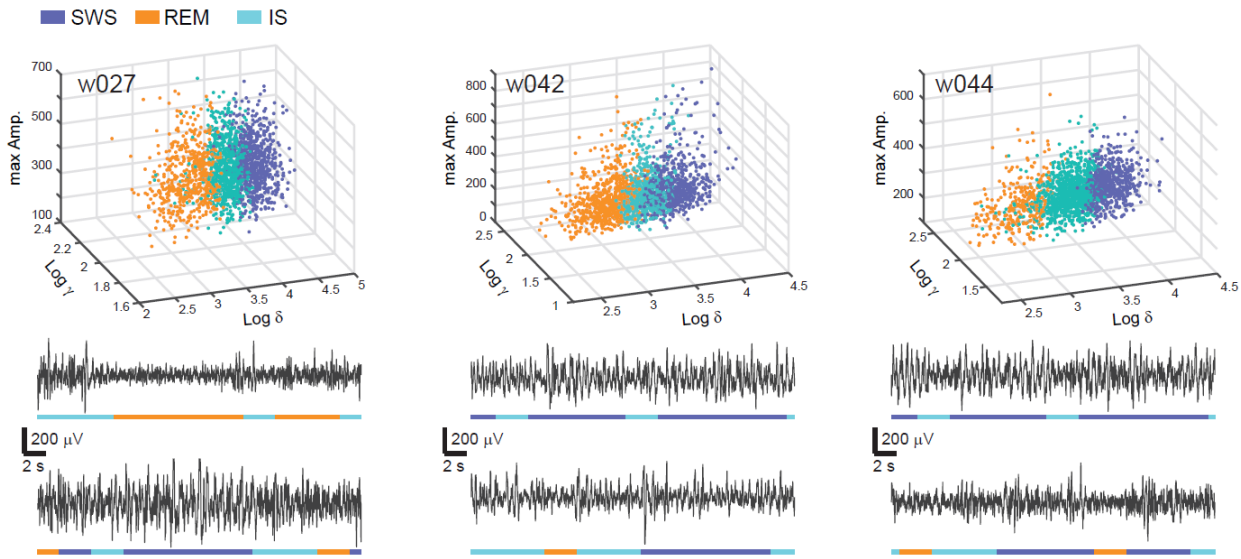


**Fig. S2 Examples of sleep staging for LFP signals.** Each panel (w027, left; w042, middle; and w044, right) is a 3-D plot of the 3-s bins of sleep time that were clustered as either SWS (blue), IS (cyan), or REM sleep (orange) for each bird. Each dot represents a different 3-s bin of sleep time, color coded according to its sleep state label. Note how sleep state clusters are segregated in 3-D spaces as a function of the spectral power of gamma (γ), delta (δ) and the maximum amplitude of the LFP signal. Below each panel are two 30-s long examples of the color-coded sleep state classification for the LFP channel for each bird. Note how orange REM states correspond to low amplitude LFP signals, blue SWS sleep states correspond to large-amplitude LFP signals, and cyan IS corresponds to an intermediate state.

## Supplementary Information

**Statistical Test Results**
**Differences in the Duration and Percentage of Sleep Stages Across Sites**

5 sites, so we will have 5*4/2=10 pair-wise tests.

The Wilcoxon rank sum test is used (a.k.a. Mann-Whitney U-test), because U-test is a non-parametric one, and dos not require normal-distribution assumption. For the multiple comparisons, i.e. 10 pair-wise tests, a Bonferroni correction factor (of 10) is applied. The mean and the standard error (SE=SD/sqrt(n)) is also reported.

α = 0.05 == 0.005
α = 0.01 == 0.001
α = 0.001 == 0.001

**1. Duration**

**Test results for SWS:**
5 recording sites, which leads to 5*4/2=10 pair-wise tests.

The Wilcoxon ranksum test is used (a.k.a. Mann-Whitney U-test). The U-test is a non-parametric test, and does not require normal-distribution assumption. To account for the multiple comparison, i.e. 10 pair-wise comparisons, a Bonferroni correction factor of 10 is applied.
Mean and the standard error (SE=SD/sqrt(n)) are also reported.

**Test results for SWS:**
Between EEG-L-Ant. and EEG-R-Ant., p= 0.15906
N_EEG-L-Ant. = 6361, N_EEG-R-Ant. = 5276
mean: EEG-L-Ant. = 4.4455, SE: EEG-L-Ant. = 0.040837
mean: EEG-R-Ant. = 4.3505, SE: EEG-R-Ant. = 0.04225
---
Between EEG-L-Ant. and EEG-R-Post., p= 9.1636e-05
N_EEG-L-Ant. = 6361, N_EEG-R-Post. = 5562
mean: EEG-L-Ant. = 4.4455, SE: EEG-L-Ant. = 0.040837
mean: EEG-R-Post. = 4.938, SE: EEG-R-Post. = 0.10873
---
Between EEG-L-Ant. and EEG-L-Post., p= 4.6472e-15
N_EEG-L-Ant. = 6361, N_EEG-L-Post. = 6843
mean: EEG-L-Ant. = 4.4455, SE: EEG-L-Ant. = 0.040837
mean: EEG-L-Post. = 4.9448, SE: EEG-L-Post. = 0.054698
---
Between EEG-L-Ant. and LFP, p= 3.2229e-51
N_EEG-L-Ant. = 6361, N_LFP = 8057
mean: EEG-L-Ant. = 4.4455, SE: EEG-L-Ant. = 0.040837
mean: LFP = 5.4921, SE: LFP = 0.057616
---
Between EEG-R-Ant. and EEG-R-Post., p= 3.3184e-07
N_EEG-R-Ant. = 5276, N_EEG-R-Post. = 5562
mean: EEG-R-Ant. = 4.3505, SE: EEG-R-Ant. = 0.04225
mean: EEG-R-Post. = 4.938, SE: EEG-R-Post. = 0.10873
---
Between EEG-R-Ant. and EEG-L-Post., p= 7.0596e-19
N_EEG-R-Ant. = 5276, N_EEG-L-Post. = 6843
mean: EEG-R-Ant. = 4.3505, SE: EEG-R-Ant. = 0.04225

mean: EEG-L-Post. = 4.9448,  SE: EEG-L-Post. = 0.054698
---
Between EEG-R-Ant. and LFP, p= 3.249e-55
N_EEG-R-Ant. = 5276, N_LFP = 8057
mean: EEG-R-Ant. = 4.3505,  SE: EEG-R-Ant. = 0.04225
mean: LFP = 5.4921,  SE: LFP = 0.057616
---
Between EEG-R-Post. and EEG-L-Post., p= 0.00034267
N_EEG-R-Post. = 5562, N_EEG-L-Post. = 6843
mean: EEG-R-Post. = 4.938,  SE: EEG-R-Post. = 0.10873
mean: EEG-L-Post. = 4.9448,  SE: EEG-L-Post. = 0.054698
---
Between EEG-R-Post. and LFP, p= 1.4066e-25
N_EEG-R-Post. = 5562, N_LFP = 8057
mean: EEG-R-Post. = 4.938,  SE: EEG-R-Post. = 0.10873
mean: LFP = 5.4921,  SE: LFP = 0.057616
---
Between EEG-L-Post. and LFP, p= 2.6066e-13
N_EEG-L-Post. = 6843, N_LFP = 8057
mean: EEG-L-Post. = 4.9448,  SE: EEG-L-Post. = 0.054698
mean: LFP = 5.4921,  SE: LFP = 0.057616

**Test results for REM:**
Between EEG-L-Ant. and EEG-R-Ant., p= 2.1039e-37
N_EEG-L-Ant. = 5519, N_EEG-R-Ant. = 8103
mean: EEG-L-Ant. = 4.8579,  SE: EEG-L-Ant. = 0.054642
mean: EEG-R-Ant. = 5.8686,  SE: EEG-R-Ant. = 0.06276
---
Between EEG-L-Ant. and EEG-R-Post., p= 2.2611e-46
N_EEG-L-Ant. = 5519, N_EEG-R-Post. = 7264
mean: EEG-L-Ant. = 4.8579,  SE: EEG-L-Ant. = 0.054642
mean: EEG-R-Post. = 6.235,  SE: EEG-R-Post. = 0.075723
---
Between EEG-L-Ant. and EEG-L-Post., p= 2.5338e-35
N_EEG-L-Ant. = 5519, N_EEG-L-Post. = 6822
mean: EEG-L-Ant. = 4.8579,  SE: EEG-L-Ant. = 0.054642
mean: EEG-L-Post. = 5.8817,  SE: EEG-L-Post. = 0.066523
---
Between EEG-L-Ant. and LFP, p= 2.4203e-14
N_EEG-L-Ant. = 5519, N_LFP = 6563
mean: EEG-L-Ant. = 4.8579,  SE: EEG-L-Ant. = 0.054642
mean: LFP = 5.473,  SE: LFP = 0.061067
---
Between EEG-R-Ant. and EEG-R-Post., p= 0.030357
N_EEG-R-Ant. = 8103, N_EEG-R-Post. = 7264
mean: EEG-R-Ant. = 5.8686,  SE: EEG-R-Ant. = 0.06276
mean: EEG-R-Post. = 6.235,  SE: EEG-R-Post. = 0.075723
---
Between EEG-R-Ant. and EEG-L-Post., p= 0.92656
N_EEG-R-Ant. = 8103, N_EEG-L-Post. = 6822
mean: EEG-R-Ant. = 5.8686,  SE: EEG-R-Ant. = 0.06276
mean: EEG-L-Post. = 5.8817,  SE: EEG-L-Post. = 0.066523
---
Between EEG-R-Ant. and LFP, p= 3.8446e-07
N_EEG-R-Ant. = 8103, N_LFP = 6563
mean: EEG-R-Ant. = 5.8686,  SE: EEG-R-Ant. = 0.06276

mean: LFP = 5.473,  SE: LFP = 0.061067
---
Between EEG-R-Post. and EEG-L-Post., p= 0.04757
N_EEG-R-Post. = 7264, N_EEG-L-Post. = 6822
mean: EEG-R-Post. = 6.235,  SE: EEG-R-Post. = 0.075723
mean: EEG-L-Post. = 5.8817,  SE: EEG-L-Post. = 0.066523
---
Between EEG-R-Post. and LFP, p= 3.7584e-12
N_EEG-R-Post. = 7264, N_LFP = 6563
mean: EEG-R-Post. = 6.235,  SE: EEG-R-Post. = 0.075723
mean: LFP = 5.473,  SE: LFP = 0.061067
---
Between EEG-L-Post. and LFP, p= 7.1787e-07
N_EEG-L-Post. = 6822, N_LFP = 6563
mean: EEG-L-Post. = 5.8817,  SE: EEG-L-Post. = 0.066523
mean: LFP = 5.473,  SE: LFP = 0.061067

**Test results for IS:**
Between EEG-L-Ant. and EEG-R-Ant., p= 1.3063e-66
N_EEG-L-Ant. = 10141, N_EEG-R-Ant. = 10294
mean: EEG-L-Ant. = 7.8359,  SE: EEG-L-Ant. = 0.078792
mean: EEG-R-Ant. = 6.2221,  SE: EEG-R-Ant. = 0.055506
---
Between EEG-L-Ant. and EEG-R-Post., p= 5.7832e-70
N_EEG-L-Ant. = 10141, N_EEG-R-Post. = 9921
mean: EEG-L-Ant. = 7.8359,  SE: EEG-L-Ant. = 0.078792
mean: EEG-R-Post. = 6.2289,  SE: EEG-R-Post. = 0.057793
---
Between EEG-L-Ant. and EEG-L-Post., p= 1.5251e-100
N_EEG-L-Ant. = 10141, N_EEG-L-Post. = 10243
mean: EEG-L-Ant. = 7.8359,  SE: EEG-L-Ant. = 0.078792
mean: EEG-L-Post. = 5.9007,  SE: EEG-L-Post. = 0.051058
---
Between EEG-L-Ant. and LFP, p= 3.1836e-151
N_EEG-L-Ant. = 10141, N_LFP = 9807
mean: EEG-L-Ant. = 7.8359,  SE: EEG-L-Ant. = 0.078792
mean: LFP = 5.5457,  SE: LFP = 0.04734
---
Between EEG-R-Ant. and EEG-R-Post., p= 0.48394
N_EEG-R-Ant. = 10294, N_EEG-R-Post. = 9921
mean: EEG-R-Ant. = 6.2221,  SE: EEG-R-Ant. = 0.055506
mean: EEG-R-Post. = 6.2289,  SE: EEG-R-Post. = 0.057793
---
Between EEG-R-Ant. and EEG-L-Post., p= 3.1147e-05
N_EEG-R-Ant. = 10294, N_EEG-L-Post. = 10243
mean: EEG-R-Ant. = 6.2221,  SE: EEG-R-Ant. = 0.055506
mean: EEG-L-Post. = 5.9007,  SE: EEG-L-Post. = 0.051058
---
Between EEG-R-Ant. and LFP, p= 1.621e-21
N_EEG-R-Ant. = 10294, N_LFP = 9807
mean: EEG-R-Ant. = 6.2221,  SE: EEG-R-Ant. = 0.055506
mean: LFP = 5.5457,  SE: LFP = 0.04734
---
Between EEG-R-Post. and EEG-L-Post., p= 0.00065375
N_EEG-R-Post. = 9921, N_EEG-L-Post. = 10243
mean: EEG-R-Post. = 6.2289,  SE: EEG-R-Post. = 0.057793

mean: EEG-L-Post. = 5.9007,  SE: EEG-L-Post. = 0.051058
---
Between EEG-R-Post. and LFP, p= 2.9154e-18
N_EEG-R-Post. = 9921, N_LFP = 9807
mean: EEG-R-Post. = 6.2289,  SE: EEG-R-Post. = 0.057793
mean: LFP = 5.5457,  SE: LFP = 0.04734
---
Between EEG-L-Post. and LFP, p= 5.4635e-08
N_EEG-L-Post. = 10243, N_LFP = 9807
mean: EEG-L-Post. = 5.9007,  SE: EEG-L-Post. = 0.051058
mean: LFP = 5.5457,  SE: LFP = 0.04734

**2. Percentage**

**Test results for SWS:**
Between EEG-L-Ant. and EEG-R-Ant., p= 0.7
N_EEG-L-Ant. = 3, N_EEG-R-Ant. = 3
mean: EEG-L-Ant. = 22.7333,  SE: EEG-L-Ant. = 1.7362
mean: EEG-R-Ant. = 20.3667,  SE: EEG-R-Ant. = 2.9077
---
Between EEG-L-Ant. and EEG-R-Post., p= 1
N_EEG-L-Ant. = 3, N_EEG-R-Post. = 3
mean: EEG-L-Ant. = 22.7333,  SE: EEG-L-Ant. = 1.7362
mean: EEG-R-Post. = 24.4333,  SE: EEG-R-Post. = 3.3933
---
Between EEG-L-Ant. and EEG-L-Post., p= 0.2
N_EEG-L-Ant. = 3, N_EEG-L-Post. = 2
mean: EEG-L-Ant. = 22.7333,  SE: EEG-L-Ant. = 1.7362
mean: EEG-L-Post. = 32.4,  SE: EEG-L-Post. = 1.8
---
Between EEG-L-Ant. and LFP, p= 0.1
N_EEG-L-Ant. = 3, N_LFP = 3
mean: EEG-L-Ant. = 22.7333,  SE: EEG-L-Ant. = 1.7362
mean: LFP = 32.0667,  SE: LFP = 1.593
---
Between EEG-R-Ant. and EEG-R-Post., p= 0.4
N_EEG-R-Ant. = 3, N_EEG-R-Post. = 3
mean: EEG-R-Ant. = 20.3667,  SE: EEG-R-Ant. = 2.9077
mean: EEG-R-Post. = 24.4333,  SE: EEG-R-Post. = 3.3933
---
Between EEG-R-Ant. and EEG-L-Post., p= 0.2
N_EEG-R-Ant. = 3, N_EEG-L-Post. = 2
mean: EEG-R-Ant. = 20.3667,  SE: EEG-R-Ant. = 2.9077
mean: EEG-L-Post. = 32.4,  SE: EEG-L-Post. = 1.8
---
Between EEG-R-Ant. and LFP, p= 0.1
N_EEG-R-Ant. = 3, N_LFP = 3
mean: EEG-R-Ant. = 20.3667,  SE: EEG-R-Ant. = 2.9077
mean: LFP = 32.0667,  SE: LFP = 1.593
---
Between EEG-R-Post. and EEG-L-Post., p= 0.4
N_EEG-R-Post. = 3, N_EEG-L-Post. = 2
mean: EEG-R-Post. = 24.4333,  SE: EEG-R-Post. = 3.3933
mean: EEG-L-Post. = 32.4,  SE: EEG-L-Post. = 1.8
---
Between EEG-R-Post. and LFP, p= 0.4

N_EEG-R-Post. = 3, N_LFP = 3
mean: EEG-R-Post. = 24.4333,  SE: EEG-R-Post. = 3.3933
mean: LFP = 32.0667,  SE: LFP = 1.593
---
Between EEG-L-Post. and LFP, p= 1
N_EEG-L-Post. = 2, N_LFP = 3
mean: EEG-L-Post. = 32.4,  SE: EEG-L-Post. = 1.8
mean: LFP = 32.0667,  SE: LFP = 1.593

**Test results for REM:**
Between EEG-L-Ant. and EEG-R-Ant., p= 0.4
N_EEG-L-Ant. = 3, N_EEG-R-Ant. = 3
mean: EEG-L-Ant. = 55,  SE: EEG-L-Ant. = 3.5119
mean: EEG-R-Ant. = 46,  SE: EEG-R-Ant. = 3.5119
---
Between EEG-L-Ant. and EEG-R-Post., p= 0.1
N_EEG-L-Ant. = 3, N_EEG-R-Post. = 3
mean: EEG-L-Ant. = 55,  SE: EEG-L-Ant. = 3.5119
mean: EEG-R-Post. = 44.6667,  SE: EEG-R-Post. = 4.8419
---
Between EEG-L-Ant. and EEG-L-Post., p= 0.8
N_EEG-L-Ant. = 3, N_EEG-L-Post. = 2
mean: EEG-L-Ant. = 55,  SE: EEG-L-Ant. = 3.5119
mean: EEG-L-Post. = 46,  SE: EEG-L-Post. = 8
---
Between EEG-L-Ant. and LFP, p= 0.4
N_EEG-L-Ant. = 3, N_LFP = 3
mean: EEG-L-Ant. = 55,  SE: EEG-L-Ant. = 3.5119
mean: LFP = 40.3333,  SE: LFP = 6.3596
---
Between EEG-R-Ant. and EEG-R-Post., p= 1
N_EEG-R-Ant. = 3, N_EEG-R-Post. = 3
mean: EEG-R-Ant. = 46,  SE: EEG-R-Ant. = 3.5119
mean: EEG-R-Post. = 44.6667,  SE: EEG-R-Post. = 4.8419
---
Between EEG-R-Ant. and EEG-L-Post., p= 1
N_EEG-R-Ant. = 3, N_EEG-L-Post. = 2
mean: EEG-R-Ant. = 46,  SE: EEG-R-Ant. = 3.5119
mean: EEG-L-Post. = 46,  SE: EEG-L-Post. = 8
---
Between EEG-R-Ant. and LFP, p= 0.5
N_EEG-R-Ant. = 3, N_LFP = 3
mean: EEG-R-Ant. = 46,  SE: EEG-R-Ant. = 3.5119
mean: LFP = 40.3333,  SE: LFP = 6.3596
---
Between EEG-R-Post. and EEG-L-Post., p= 0.8
N_EEG-R-Post. = 3, N_EEG-L-Post. = 2
mean: EEG-R-Post. = 44.6667,  SE: EEG-R-Post. = 4.8419
mean: EEG-L-Post. = 46,  SE: EEG-L-Post. = 8
---
Between EEG-R-Post. and LFP, p= 0.8
N_EEG-R-Post. = 3, N_LFP = 3
mean: EEG-R-Post. = 44.6667,  SE: EEG-R-Post. = 4.8419
mean: LFP = 40.3333,  SE: LFP = 6.3596
---
Between EEG-L-Post. and LFP, p= 0.4

N_EEG-L-Post. = 2, N_LFP = 3
mean: EEG-L-Post. = 46,  SE: EEG-L-Post. = 8
mean: LFP = 40.3333,  SE: LFP = 6.3596

**Test results for IS:**
Between EEG-L-Ant. and EEG-R-Ant., p= 0.1
N_EEG-L-Ant. = 3, N_EEG-R-Ant. = 3
mean: EEG-L-Ant. = 22.3333,  SE: EEG-L-Ant. = 4.4096
mean: EEG-R-Ant. = 32.6667,  SE: EEG-R-Ant. = 2.6667
---
Between EEG-L-Ant. and EEG-R-Post., p= 0.4
N_EEG-L-Ant. = 3, N_EEG-R-Post. = 3
mean: EEG-L-Ant. = 22.3333,  SE: EEG-L-Ant. = 4.4096
mean: EEG-R-Post. = 30.7,  SE: EEG-R-Post. = 7.6531
---
Between EEG-L-Ant. and EEG-L-Post., p= 1
N_EEG-L-Ant. = 3, N_EEG-L-Post. = 2
mean: EEG-L-Ant. = 22.3333,  SE: EEG-L-Ant. = 4.4096
mean: EEG-L-Post. = 21.1,  SE: EEG-L-Post. = 9.9
---
Between EEG-L-Ant. and LFP, p= 0.7
N_EEG-L-Ant. = 3, N_LFP = 3
mean: EEG-L-Ant. = 22.3333,  SE: EEG-L-Ant. = 4.4096
mean: LFP = 26.4,  SE: LFP = 5.5582
---
Between EEG-R-Ant. and EEG-R-Post., p= 0.6
N_EEG-R-Ant. = 3, N_EEG-R-Post. = 3
mean: EEG-R-Ant. = 32.6667,  SE: EEG-R-Ant. = 2.6667
mean: EEG-R-Post. = 30.7,  SE: EEG-R-Post. = 7.6531
---
Between EEG-R-Ant. and EEG-L-Post., p= 0.8
N_EEG-R-Ant. = 3, N_EEG-L-Post. = 2
mean: EEG-R-Ant. = 32.6667,  SE: EEG-R-Ant. = 2.6667
mean: EEG-L-Post. = 21.1,  SE: EEG-L-Post. = 9.9
---
Between EEG-R-Ant. and LFP, p= 0.4
N_EEG-R-Ant. = 3, N_LFP = 3
mean: EEG-R-Ant. = 32.6667,  SE: EEG-R-Ant. = 2.6667
mean: LFP = 26.4,  SE: LFP = 5.5582
---
Between EEG-R-Post. and EEG-L-Post., p= 0.8
N_EEG-R-Post. = 3, N_EEG-L-Post. = 2
mean: EEG-R-Post. = 30.7,  SE: EEG-R-Post. = 7.6531
mean: EEG-L-Post. = 21.1,  SE: EEG-L-Post. = 9.9
---
Between EEG-R-Post. and LFP, p= 0.7
N_EEG-R-Post. = 3, N_LFP = 3
mean: EEG-R-Post. = 30.7,  SE: EEG-R-Post. = 7.6531
mean: LFP = 26.4,  SE: LFP = 5.5582
---
Between EEG-L-Post. and LFP, p= 0.8
N_EEG-L-Post. = 2, N_LFP = 3
mean: EEG-L-Post. = 21.1,  SE: EEG-L-Post. = 9.9
mean: LFP = 26.4,  SE: LFP = 5.5582

**Congruence in each stage of sleep, averages over sites**

Congruence SWS: mean = 44.1667,  SD = 10.7266
---
Congruence REM: mean = 54.5,  SD = 19.7967
---
Congruence IS: mean = 47.8333,  SD = 9.3306

# Chapter 4

# General Discussion

## Local aspects of sleep: interpretations and outlooks

We studied local aspects of sleep in zebra finches from three points of view. In manuscript one, we examined 1) local waves and 2) local networks of highly correlated activity. In manuscript two, we examined 3) the occurrence of simultaneous different sleep stages. Each analysis provided a distinct view of the spatiotemporal dynamics of the sleeping avian brain.

In the EEG recordings, we observed local waves, defined as simultaneous peaks or troughs that only spanned a part of the brain surface (Fig 1C of manuscript one). Since these waves were brief with durations less than half a second, they suggest short-lived neural activities exist in the underlying local circuits.

An interesting question is whether the local activities, whether short or long in time, are related to the global dynamics of the brain, which probably is controlled centrally. Two of the analysis that we did in manuscript one suggest that these local activities are indeed related to the global activity. First, we showed that ($\sigma+\theta/\gamma$) power, i.e. the power of low-frequency EEG oscillations relative to EEG Gamma oscillations, is a global measure of brain dynamics (Fig. 1D). Secondly, we also showed that the ($\sigma+\theta/\gamma$) power is correlated with the rate with which local waves appear (Fig 3A and B). This data thus implies a strong link between the local and global activity during sleep. However, whether the global activity drives the local activities or local activities shape the global activity cannot be concluded from this data. A recent study has shown that the traveling waves observed in field potentials, either LFP or EEG, are associated with an underlying sequential activation of discrete specially-adjacent groups of neurons (129). Therefore, a mechanistic link exists between the local activities (in the discrete groups of neurons) and the global activity (in the form of far-reaching travelling waves).

In the context of sleep, further investigations are required to mechanistically uncover the link between the sleep centers (e.g., sleep associated areas of hypothalamus) and the local activity across the pallium. This could be achieved via simultaneous LFP

recordings from the sleep centers, and multi-channel surface EEG recordings across a large part of pallium. By examining the temporal order of events in the central sleep centers and the pallial local activities, one could test whether the activity in the sleep centers precedes the formation of sleep-associated waves (e.g., delta waves) in the local circuits. Alternatively, delta waves could appear first independently in the local circuits and then lead to (behavioral) sleep and the consequent emergence of activity in the sleep-associated areas of the hypothalamus and basal forebrain (i.e., sleep centers). For example, by optogenetically manipulating the sleep centers, one could test the hypothesis as to whether the sleep centers drive the local pallial activity, or the local pallial activity is generated independently in local circuits.

Beside local waves, network analysis of highly correlated electrodes provided a complementary insight into the local neural activity during sleep (here, local means a subset of recording sites, see figure 5B and 5C of manuscript one). We demonstrated the presence of locally synchronized activity in the form of synchronized waves (three seconds or longer) that appear in constrained areas over the surface of the brain. Next, we asked whether the synchronized activities appeared in a random subset of EEG sites, or if there was a consistent pattern in their spatial appearance.

We examined this question by analyzing networks of highly correlated EEG electrodes for three consecutive nights. We showed that there were subsets of highly-correlated EEG electrodes that persisted over consecutive nights (Fig 5B and 5C of manuscript one). This consistency in the local activity points to distinct circuits that underlie the persistent local activity across days, and thus offers a mechanism to explain the origin of local activity observed during sleep. These circuits might have their origin in either the neural connectivity of the songbird brain or might arise independently in each individual, as a consequence of learning processes. The observation of two times larger networks in adults compared to juveniles (spanning on average 8.2 electrode sites in adults versus 4.2 electrode sites in juveniles) supports the argument that the formation of these networks is highly influenced by the plastic processes that occur in the learning brains. This observation is consistent with the increase of functional connectivity over distant sites across the brain, during the first year of life or as a result of learning experience in humans (130-132). For example, a functional magnetic resonance imaging (fMRI) in sleeping infants of 4 to 9 months of age demonstrated that at 9 months the connectivity strength decreases within small networks and increases between more distant networks (130).

Furthermore, we observed high variability in the number and the size of networks across individuals (network size varied from those with three electrodes to the ones covering a whole hemisphere). As such, the learning processes, rather than the fixed

anatomical connectivity of the brain, offer a mechanistic substrate that contributes to the local aspects of neural activity during sleep. Indeed, learning a new task leads to heightened activity in the newly used brain circuit during the following sleep, as it shown in the mammalian brains (5). Therefore, local sleep in both mammalian and avian brains could be explained through a shared mechanism: reactivation of the local circuits that have been used during the previous wake. This wake-dependent neural activity during sleep could be related to the replay of neural populations during sleep, which is recently observed in birds (99).

To further examine this statement, it would be interesting to track the highly correlated networks over longer time frames, for example, months or years. When paired with regular assessment of cognitive skills (such as verbal or memory tests), such a study could correlate the architecture of the emerging networks with the learning performance and cognitive development. Such experiments are specifically suitable to be performed in humans, given the standard positioning system of EEG electrode placement that guarantees the consistency of electrode sites across the recording intervals (133).

To further substantiate the local aspects of sleep in zebra finches, we showed that the oscillations associated with different stages of sleep appear simultaneously across the pallium (manuscript two). Specifically, we found that LFP categorized as REM sleep occasionally occurred in one part of the brain at the same time that EEG categorized as SWS occurred in a different part of the brain. This work contributes to the growing body of evidence examining the local aspects of sleep (as reviewed in the Introduction). This growing literature demonstrates that many sleep-specific waves that are implicated in cognitive functions, such as sleep spindles (134) and slow waves (135) have a local distribution. In fact, the majority of sleep slow waves and the underlying activity in the neural populations differ across sites.(41) Since such major brain waves are thought of as carriers of information across the cerebral areas (136, 137), the discovery of their local action profoundly impacts our understanding of neural communication in the brain. That is, during sleep, communication within the brain is spatially constrained, because slow waves and sleep spindle frequently occur out of phase across various brain regions. (41). This asynchronous activity, and the resulting impediment of information transfer across brain areas it incurs, might underlie the loss of 'consciousness' that occurs during sleep. Indeed, perturbation experiments using transcranial magnetic stimulation have demonstrated the breakdown of brain connectivity during the 'unconscious' states of NREM sleep (138) as well as during anesthesia (139).

## Development of neural lateralization

One of the interesting observations that we made was that in adult zebra finches, the functional connectivity, a measure of synchrony across EEG electrodes, was significantly higher within the left hemisphere than within the right hemisphere (Fig 4 A of manuscript one). Furthermore, we showed that the functional connectivity increases once finches are 50 to 60 days post-hatch in the left hemisphere but not in the right hemisphere (Fig 4B, 4C, and 4D). This asymmetric development of functional connectivity in the left and right hemispheres suggests an underlying brain lateralization. With this observation arise a few important questions. First, why should there be asymmetrical brain activity in the first place? And second, is this asymmetry or lateralization a consequence of learning or is it an innate phenotype? Here we discuss the adaptive advantages or disadvantages of the lateralized behavior and lateralized neural processing in a broader context, beyond the avian brain.

Brain lateralization, as mentioned in the Introduction chapter, is common across the animal kingdom. The commonality of brain lateralization thus suggests that it confers advantages to the survival of the organism. On the other hand, not every behavior nor its underlying neural circuitry in the brain is lateralized. As such, there should be a cost-benefit tradeoff involved in the development of brain laterality.

Several benefits have been suggested for a lateralized brain. First, the specialization of each hemisphere in controlling different functions might reduce the neural processing, and lead to faster responses (140). Secondly, lateralization allows for sparing neural tissue by avoiding duplication of functions in the two hemispheres and thus could increase neural capacity (141). Thirdly, lateralization could facilitate parallelization of information processing, and thus help the organism in situations involving divided attention (142). For instance, the last hypothesis, i.e., parallelization of neural processing, has been tested in chicks (143) and also has been reexamined in fish (144). Interestingly, several species of fish offer emerging model organisms to study lateralization in the vertebrate brain, thanks to their small size that allows for studying group behavior, and relatively short maturation time that facilitates selective breeding of (visually) lateralized, and non-lateralized individuals (118).

Despite the aforementioned benefits, lateralization can come with disadvantages. In the natural environment, a predator or a prey could approach an individual from every side, and thus its direction is unpredictable. A lateralized organism is therefore more vulnerable to the risk of predation, or might miss a feeding opportunity, if the target is not approaching from the 'preferred' side (145). Therefore, laterality does not necessarily offer a survival benefit and, thus should be examined with regard to the

organism's ecosystem. Although it is still not clear why singing in songbirds and language in humans is lateralized, there is evidence that supports laterality (and corresponding lateralized brain circuitry) in other social behaviors.

Is there a correlation between laterality and the individual's position in a large group of conspecifics? A study in rainbow fish, showed that the individuals place themselves in the fish school based on the eye preferences (146). Fish with a right-eye preference were located on the left side of the school, while fish with a left-eye bias preferred a position on the right side of the school. This data suggest that lateralization increases the chance of survival in collective behaviors, and thus facilitating the formation of larger groups by allowing individuals to specialize differentially. Collective behaviors such as swimming in a school of fish or flying in a flock of birds could provide the evolutionary pressure that drives both lateralization and non-lateralization across individuals. For instance, in a school of fish, lateralization offers a benefit to be on the periphery, while the center which is safer than the periphery, could be best occupied by individuals without any laterality. This argument is also in line with the evolution of the laterality as a means to cope with parallel processing of multiple tasks. The individuals in the center of the group mainly need to only avoid collision with conspecifics, whereas the ones on the periphery need to avoid collision on one side while monitoring the periphery for predation risks. As such, the coexistence of symmetric and asymmetric behavioral preferences could evolve as a consequence of social behavior. Although coordination in a school of fish is a different behavior than vocal communication in songbirds, it demonstrates how laterality supports group behavior.

One aspect of vocal communication is perception of signals in a noisy environment; In such an environment, laterality appears to be beneficial. Several lines of evidence support this argument. For example, individual pigeons with laterality in visual object recognition are more successful in finding grains that are scattered among pebbles (184).

Further evidence comes from the examination of language laterality in humans measured by the dichotic listening task. In the dichotic listening task, consonant-vowel pairs of syllables are presented to the right and left ear simultaneously, in a way that each ear receives a different syllable. In this test, a participant typically reports more syllables from one ear (usually the right ear), which is considered a marker of (left) hemispheric dominance (147, 148). A study found that the individuals who score highest in the dichotic listening task, are the ones who have a directional bias (that is, the higher the bias, regardless of side, the higher the number of correct answers) (149).

One possible interpretation of these findings is that in a highly-ambiguous environment, a lateralized (or rather biased) brain makes better decisions. (In such environment the input data does not help with the decision making). Decision-making when the options have similar prominence is inherently hard, and reducing options (through a lateral bias) could be a helpful strategy with regard to the time and energy expenditure. Considering that most of the time vocal communication is performed in a noisy environment (imagine talking to a friend in a bar or birds communicating in a large singing colony), lateralization proves advantageous in vocal communication. Collectively, the current data on brain lateralization studies supports the benefits of a lateralized brain in songbirds as they heavily rely on vocal communication. Our observation of the lateralized functional connectivity might thus be a reflection of such inherent lateralization organization of the brain in zebra finches.

## IS sleep and development

We observed that juveniles had less SWS and REM sleep, relative to the adults, but significantly more IS sleep (Fig 2C and 2E of manuscripts one). In addition, our observation of significantly higher percentage and longer duration of IS stage in male juveniles versus female juveniles supports the idea that IS sleep plays a role in learning and memory, considering that only male juveniles are undergoing the vocal learning process. In fact, level of IS sleep in female juveniles is similar to the level of IS sleep in adult zebra finches, both in percentage and duration (Fig 2C-F). Altogether, this data signifies the role of IS sleep in the memory function of sleep in zebra finches.

IS sleep is comparable to N1 and N2 stages of NREM in humans (78). In humans, N2 stage of sleep is marked by the appearance of sleep spindles (refer to the 'Common NREM characteristics in mammals' in the Introduction chapter). Sleep spindles are important for memory function in humans and rodents. Behavioral studies have found significant correlations between the recall performance in a variety of learning tasks, and the amount of sleep spindles in the intervening sleep (150). Moreover, optogenetic induction of thalamic spindles, when phase-locked to the slow oscillation ON-states, enhances hippocampus-dependent memory consolidation (151).

Sleep spindles have not been reported in the avian studies. However, in mammals, they are coupled to other waves such as ripples, delta waves, and slow oscillations, all of which are involved in memory function and are observable also in the avian brain during sleep (136, 152, 153). In fact, cortical spindles are synchronized with the hippocampal ripples in rats (154). That is, sleep spindles are the pallial representation of hippocampal ripples. Ripples are observed in the avian brain, in both hippocampal

(99), and other pallial sites (100). It might be that due to the cytoarchitectural differences between the mammalian and the avian pallium, a pallial representation of ripples is not as conspicuous in birds as it is in mammals. A simultaneous study of ripple-coupled EEG (or ripple-triggered EEG) could possibly unveil the pallial representation of ripples in the avian brain.

Whether ripples are present during SWS, IS sleep, or both, is not known in birds. If a future study could show that ripples occur during the IS sleep, it supports the argument that IS stage is potentially implicated in the memory function (whether the avian ripples are implicated in memory is not yet studied).

## Linking together sleep oscillations, memory function of sleep, and local aspects of sleep

Brain oscillations that appear during sleep are shown to be associated with the memory function of sleep. Importantly, this memory-supporting role does not depend on the frequency, as this function has been demonstrated for a range of frequencies, including Delta (155, 156), Theta (57, 155, 156), and slow waves (157-159). However, a unifying theory that mechanistically links these oscillations to memory consolidation has yet to be established. I argue that the synchronized neural oscillations occurring during sleep are an inherent property of the brain at rest. These synchronized oscillations, rather than being an adaptation specifically evolved for memory consolidation, may incidentally predispose the brain to facilitate the memory process. In other words, the electrophysiological aspect of, i.e., the neural oscillations of sleep, has not specifically evolved to support memory functions, but emergent sleep oscillations, which are the default dynamics of the brain at rest, provide a substrate for neural communication that can be exploited for memory consolidation. This framework is further supported by observations of local differences in sleep oscillations. Specifically, variations in wake-time neural activity lead to localized increases in oscillatory activity during sleep, which, in turn, enhance the brain's capacity for information processing in these regions during rest.

Although in the mammalian brain, the cortico-thalamic loop is emphasized in the generation of Delta and slow oscillations, recent observations in much simpler neural assemblies suggest that these waves do not require such a specific circuitry. Notably, several studies with *in vitro* preparation of cortical cultures across different labs have shown that synchronized oscillations, akin to those observed during sleep, could also emerge in such simpler neural assemblies. For instance, in (160), *ex vivo* cultures

extracted from embryonic mouse cortex, upon maturation (after about 10 days) exhibited a default state characterized by synchronized burst–pause firing activity, which closely resembles ON-OFF patterns of NREM. Moreover, this innate state can be transiently shifted to tonic firing, similar to that of wakefulness neural activity, upon pharmacological stimulation with a mixture of arousal-associated neurotransmitters, such as NMDA, kainate, AMPA, dopamine, and orexin A. The system spontaneously reverts to its sleep-like state thereafter. Complementing these electrophysiological observations, the transcriptomic profile of pharmacologically 'awakened' cultures resembled that of sleep-deprived mice.

Extending these findings, a similar study utilizing dissociated cortical cells extracted from rat embryos has also shown synchronized, low-frequency firing patterns that mirror *in vivo* slow-wave oscillations (161). These cultures inherently lacked the high-frequency waves characteristic of wakefulness. However, a desynchronized wake-like pattern emerged upon the administration of Carbachol, a receptor agonist of acetylcholine, a wake-promoting neurotransmitter. This observation mimics the change in the firing activity of the cortex during arousal from natural sleep under cholinergic stimulation by basal ganglia projections in intact animals (162).

Collectively, these experiments provide profound insight into the basic mechanisms underlying synchronized neural activity. First, these studies demonstrate that the emergence of synchronized neural activity associated with sleep, such as slow oscillations, does not require a specific architecture of the neural circuitry, e.g., the cortico-thalamic loop. Second, these findings suggest that the synchronized neural activity observed during sleep, not the desynchronized activity during wake, is the default dynamics of undisturbed neural assemblies, at least in the case of mammalian telencephalic neurons. That is, by transition into sleep and the reduction of external stimuli to the brain, the telencephalon exhibits its intrinsic (or default) mode of activity, i.e., synchronized oscillations.

It remains to clarify the mechanistic link between the long-range oscillations, especially during NREM sleep, and the consolidation of newly acquired memory. First, ample evidence demonstrates that brain areas that had been highly activated during wake show increased activity during the subsequent sleep (for example see this review article (163)). In a simplified abstract scenario, consider two brain areas, A and B, which have been highly stimulated during the wake time. During the following (NREM) sleep, the membrane potential of the neurons in A and B is simultaneously exposed to and modulated by the sleep-time neural oscillations. Therefore, neuronal activities in both A and B are increased due to the previous wake-time activity and are synchronized due to the sleep-time oscillations. Thus, according to the Hebbian theory, the axonal

connections between the neural populations in A and B are strengthened. Critically, it is important to notice that this axonal upscaling could not occur between other arbitrary pair of areas, since if those areas have not been intensely stimulated during the preceding wake period, they do not show increased activity during sleep. As such, sleep provides prime conditions for selectively strengthening the axonal connections by engendering long-range oscillations. This selective strengthening of axonal connections could be considered as a physiological materialization of memory consolidation. Furthermore, the intense activation of a given brain area during wake, which results in pronounced oscillations in that area during the proceeding sleep (5, 164, 165), is one of the major mechanisms of the local regulation of sleep. In short, the brain assumes its default dynamic mode during sleep, characterized by synchronized oscillations. These neural oscillations provide a substrate for the selective strengthening of axonal connection or consolidation of memory traces based on the preceding wake-time activity.

Here, we accepted the assumption that sleep is characterized by the associated neural oscillations. However, sleep-associated neural oscillations are not a universal feature of sleep across all animal phyla. In the following section, I explore the origins of sleep's neural signature, specifically the two-stage sleep, characterized by the two alternating stages of synchronized and desynchronized neural activity. In light of new data, I speculate on the origins of the two-stage sleep from multiple perspectives, ranging from recent comparative studies to insights derived from mathematical analysis of the brain as a complex system.

## Speculations on the origin of two-stage sleep

In this section, drawing on recent evidence, I discuss the origins of two-stage sleep. It is important to clarify that by "two-stage sleep," I am referring to the two distinct types of neural oscillations that occur during sleep, generally labeled as SWS and paradoxical sleep (PS). While rapid eye movements often accompany PS in most species studied to date, eye movements are not the primary focus here (see this article for further discussion on the relationship between eye movements and PS (166)). I argue that the two-stage neural dynamics observed in the brain during sleep in mammals and birds represent a specific case of a more general phenomenon present in a much broader assortment of neural networks. Importantly, although these dynamics depend on certain properties of the neural assembly, they do not require a specific neural circuitry or a 'sleep center' in the brain.

As noted in the previous section, neural oscillations resembling those observed during SWS spontaneously emerge in undisturbed primary cortical cultures, displaying sleep-like LFP and firing patterns, as well as comparable molecular, metabolic, and homeostatic signatures. This finding suggests that no specific brain region, neural architecture, or wiring pattern is required for these oscillations to occur. It is important to note that these experiments have been conducted exclusively with cortical cultures extracted from rats or mice. Replicating these experiments with pallial cells from other vertebrate taxa could help determine the generalizability of these findings (of note, sharp wave-ripples have been observed in brain slices of avian (100) and non-avian (167) reptiles).

Second, as mentioned in the Slow Oscillations section of the Introduction, although both the cortex and thalamus are involved in generating slow oscillations, these oscillations reemerge after several hours and persist for weeks following thalamic ablation, or in isolated cortical slabs (37). This indicates that the thalamocortical feedback loop is not necessary for the generation of slow oscillations.

Third, a complementary perspective on the inherent capacity of neural assemblies to form synchronized oscillations originates from mathematical studies of nonlinear dynamical systems (for an overview of such computational models, see (168)). In this framework, the brain is modeled as a network of multiple oscillators, each representing local assemblies of neurons such as cortical columns, coupled together through synaptic connections (169-171). In such simulation studies, each oscillator is initially out of phase with the others and has a gamma intrinsic frequency, reflecting the resonant frequency of isolated neural masses driven by local feedback inhibition (170, 172). Interestingly, the simulations show that these oscillators can partially or globally synchronize after a transient time, in a 'collective' lower frequency. Furthermore, the oscillators alternate between periods of synchronization, associated with a collective lower frequency, and desynchronization, associated with the individual gamma frequency. Notably, these slower global oscillations emerge without any synchronizing external input; they are an emergent property of a network of coupled oscillators.

Importantly, synchrony occurs only when the coupling strength—i.e., the inter-areal synaptic strength—is within a specific range. Simulation studies based on parameters extracted from electromagnetogram (EMG) data have demonstrated that, indeed, this condition for coupling strength is met (170). Under a realistic, data-driven set of parameters, modeling the human brain as a network of coupled oscillators with intrinsic gamma frequency for the oscillators, shows the spontaneous emergence of partial or global oscillations in the theta and delta frequency ranges, similar to those observed during sleep (170). These computational studies provide a strong theoretical basis for

the enigmatic neural oscillations that appear in the brain when the external input is inhibited, states such as anesthesia, and sleep.

The final line of evidence supporting the idea that sleep is an emergent property of neural assemblies, rather than being governed by specific circuitry, comes from recent neurobiological investigations in diverse model species. Although the two-stage structure of sleep was first studied in several mammalian and avian vertebrate species, recent investigations in several non-avian reptiles, such as bearded dragon (18), and Argentinian Tegu (173), as well as zebrafish (20), have expanded this concept beyond the originally studied taxa.

Fluorescent neural imaging in zebrafish, facilitated by their transparent bodies, suggests a highly conserved circuitry associated with the synchronized and desynchronized stages of sleep (20). Similar to the mammalian SWS, zebrafish exhibit slow, synchronous neuronal oscillations in the dorsal pallium of the telencephalon (which forms the cerebral cortex in mammals). This SWS-like activity increases following sleep deprivation and shares similarities in molecular pathways, such as being triggered by histamine H1 receptor antagonists. Furthermore, the REM-like sleep stage in zebrafish is characterized by brainstem activation and a neural wave that moves from the pons along the posterior-anterior axis, resembling the ponto-geniculo-occipital waves typical of REM sleep in mammals. These observations underscore conserved neural circuitry and neurotransmitters involved in the regulation of sleep stages across vertebrates. Consequently, it is likely that the two-stage structure of sleep appeared early in vertebrate evolution and is regulated by a shared neuronal circuitry across this taxon. While this suggests that the two-stage structure of sleep depends on an ancestral neural circuitry that evolved in vertebrates, recent reports of two-stage sleep in several invertebrate taxa challenge this view by showing that the two-stage sleep could arise from brain architectures beyond that of the vertebrate design.

Among studied invertebrate species, cuttlefish display two phases of sleep: quiet sleep, with little to no chromophore activity, and "active sleep," characterized by body surges, intense, non-camouflaging chromophore patterns, and eye movements (174). Within the Mollusca phylum, similar behavioral states have been observed in octopuses (175-177). Notably, recent neural recordings from the octopus's brain have revealed that active sleep is indeed characterized by wake-like neural activity (21). Beyond cephalopod molluscs, behavioral recording in a species of jumping spider shows regular bouts of body twitches and rapid retinal movements (178). The last common ancestor of vertebrates, molluscs, and arthropods was likely a worm-like bilaterian that lived around 600 million years ago (179) (see figure 4). Given the stark differences in brain structure among these three taxa, it is more plausible that the two-stage sleep does not

depend on specific circuitries in the ancestral vertebrate brain but is instead an emergent property of a much broader range of nervous systems at the resting state.

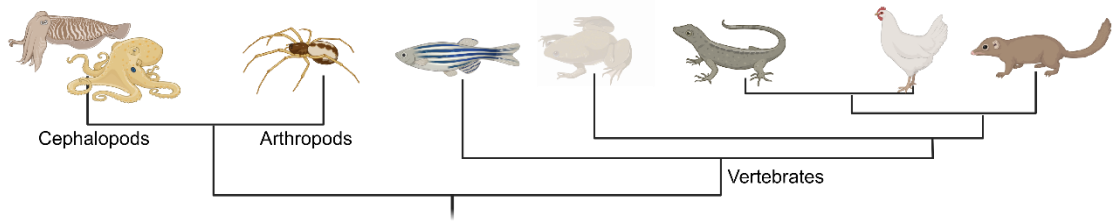


**Figure 4 Phylogenetic tree of species exhibiting two-stage sleep.** To date, apart from amphibians, two distinct stages of sleep with corresponding electrophysiological signatures have been identified across all major vertebrate taxa. Among invertebrates, behaviorally distinct sleep stages have been observed in jumping spiders, cuttlefish, and octopuses. In octopuses, electrophysiological recordings have further confirmed the distinction between the two stages. The widespread presence of two-stage sleep across such a diverse range of species with fundamentally different brain architectures supports the idea that this sleep dynamic is an intrinsic feature of the brain, occurring in the absence of external stimuli. The last common ancestor of these species evolved around 600 million years ago. The length of lines in the phylogenetic tree does not necessarily represent the evolutionary distance and is rather optimized for illustration.

Lastly, if we believe that specific circuitry in the brain was evolved to control the REM (or the desynchronized) sleep, we are facing another puzzling observation, i.e., the extremely short REM (or REM-like) stage observed in many vertebrate and non-vertebrate species. When considering animals with REM-like bouts lasting only seconds, such as mice, zebra finch, tegu, or octopus, one wonders how quickly a dedicated neural circuit could switch its characteristics because critical molecular and cellular processes, such as transcription and translation needed for the synaptic plasticity associated with REM sleep, require several minutes to unfold in cells, rather than a few seconds (180).

Previously, it was thought that the large brain size and more extensive cortical structures in humans were responsible for the prolonged bouts of consolidated sleep seen in humans, as humans have the largest brain and cortex relative to body size even among primates (181). However, across nature, sleep consolidation does not consistently correlate with brain size or complexity (182). While the fine temporal structure of sleep varies markedly across species, even within the same taxa, the general two-stage dynamic is a pervasive feature across studied vertebrates as well as a few invertebrates that have been carefully investigated. If we consider this two-stage dynamic to be an inherent property of neural assemblies, rather than entirely controlled by a specific circuitry, the mystery of extremely short REM-like episodes can be more easily resolved. Brains, regardless of vast inter-species differences, alternate between a synchronized and a desynchronized state, during the rest. Indeed, the inter-species

differences in the PS stage length could be linked with a combination of system parameters such as brain size, the relative pallial portion, axonal density, inhibitory/excitatory balance, etc. Further simulation studies could help to determine which factors of the brain's dynamical system affect the length of the desynchronized stage.

In summary, while there is substantial evidence supporting the role of specific brain nuclei in regulating REM and NREM sleep in intact mammalian brains, the emergence of these sleep states does not appear to rely exclusively on these specific regions. These dynamic states can arise even in brains with ablated areas, isolated cortical slabs, or invertebrate brains with fundamentally different brain architecture. Recent evidence suggests that the two-stage structure of sleep is an inherent and emergent property of the neural assemblies. Currently, our understanding of the specific brain structures that regulate sleep is based mainly on studies in a few mammalian species. To gain a more comprehensive understanding of how brains—across a broader range of species, not just mammals—regulate sleep, more mechanistic studies are needed across diverse animal taxa.

# References


1. W. Dement, N. Kleitman, Cyclic variations in EEG during sleep and their relation to eye movements, body motility, and dreaming. *Electroencephalography and Clinical Neurophysiology* **9**, 673-690 (1957).
2. C. B. Saper, P. M. Fuller, N. P. Pedersen, J. Lu, T. E. Scammell, Sleep State Switching. *Neuron* **68**, 1023-1042 (2010).
3. T. E. Scammell, E. Arrigoni, J. O. Lipton, Neural circuitry of wakefulness and sleep. *Neuron* **93**, 747-765 (2017).
4. C. M. Funk, S. Honjoh, A. V. Rodriguez, C. Cirelli, G. Tononi, Local slow waves in superficial layers of primary cortical areas during REM sleep. *Current Biology* **26**, 396-403 (2016).
5. R. Huber, M. Felice Ghilardi, M. Massimini, G. Tononi, Local sleep and learning. *Nature* **430**, 78-81 (2004).
6. V. V. Vyazovskiy *et al.*, Local sleep in awake rats. *Nature* **472**, 443-447 (2011).
7. I. Feinberg, Changes in sleep cycle patterns with age. *Journal of psychiatric research* **10**, 283-306 (1974).
8. I. G. Campbell, I. Feinberg, Longitudinal trajectories of non-rapid eye movement delta and theta EEG as indicators of adolescent brain maturation. *Proceedings of the National Academy of Sciences* **106**, 5177-5180 (2009).
9. A. Buchmann *et al.*, EEG sleep slow-wave activity as a mirror of cortical maturation. *Cerebral cortex* **21**, 607-615 (2011).
10. J.-P. Bourgeois, P. Rakic, Changes of synaptic density in the primary visual cortex of the macaque monkey from fetal to adult stage. *Journal of Neuroscience* **13**, 2801-2820 (1993).
11. A. P. Vorster, J. Born, Sleep and memory in mammals, birds and invertebrates. *Neuroscience & Biobehavioral Reviews* **50**, 103-119 (2015).

12. M. Jouvet, F. Michel, Electromyographic correlations of sleep in the chronic decorticate & mesencephalic cat. *Comptes rendus des seances de la Societe de biologie et de ses filiales* **153**, 422-425 (1959).
13. D. Jouvet-Mounier, L. Astic, D. Lacote, Ontogenesis of the states of sleep in rat, cat, and guinea pig during the first postnatal month. *Developmental Psychobiology: The Journal of the International Society for Developmental Psychobiology* **2**, 216-239 (1969).
14. L. M. Mukhametov, Unihemispheric slow-wave sleep in the Amazonian dolphin, Inia geoffrensis. *Neuroscience letters* **79**, 128-132 (1987).
15. T. Ookawa, J. Gotoh, Electroencephalographs Study of Chickens: Periodic Recurrence of Low Voltage and Fast Waves during Behavioral Sleep. *Poultry Science* **43**, 1603-1604 (1964).
16. C. J. Schlehuber, D. G. Flaming, G. D. Lange, C. E. Spooner, Paradoxical sleep in the chick (Gallus domesticus). *Behavioral Biology* **11**, 537-546 (1974).
17. G. Dewasmes, F. Cohen-Adad, H. Koubi, Y. Le Maho, Polygraphic and behavioral study of sleep in geese: existence of nuchal atonia during paradoxical sleep. *Physiology & behavior* **35**, 67-73 (1985).
18. M. Shein-Idelson, J. M. Ondracek, H.-P. Liaw, S. Reiter, G. Laurent, Slow waves, sharp waves, ripples, and REM in sleeping dragons. *Science* **352**, 590-595 (2016).
19. N. Albeck, D. I. Udi, R. Eyal, A. Shvartsman, M. Shein-Idelson, Temperature-robust rapid eye movement and slow wave sleep in the lizard Laudakia vulgaris. *Communications Biology* **5**, 1310 (2022).
20. L. C. Leung *et al.*, Neural signatures of sleep in zebrafish. *Nature* **571**, 198-204 (2019).
21. A. Pophale *et al.*, Wake-like skin patterning and neural activity during octopus sleep. *Nature* **619**, 129-134 (2023).
22. H. Kattler, D.-J. Dijk, A. A. Borbély, Effect of unilateral somatosensory stimulation prior to sleep on the sleep EEG in humans. *Journal of sleep research* **3**, 159-164 (1994).
23. M. M. Ohayon, M. A. Carskadon, C. Guilleminault, M. V. Vitiello, Meta-analysis of quantitative sleep parameters from childhood to old age in healthy individuals: developing normative sleep values across the human lifespan. *Sleep* **27**, 1255-1273 (2004).
24. H. Schulz, Rethinking sleep analysis: Comment on the AASM manual for the scoring of sleep and associated events. *Journal of Clinical Sleep Medicine* **4**, 99-103 (2008).
25. R. B. Berry *et al.* (2017) AASM scoring manual updates for 2017 (version 2.4). (American Academy of Sleep Medicine), pp 665-666.
26. L. M. Fernandez, A. Lüthi, Sleep spindles: mechanisms and functions. *Physiological reviews* **100**, 805-868 (2020).
27. A. R. Adamantidis, C. Gutierrez Herrera, T. C. Gent, Oscillating circuitries in the sleeping brain. *Nature Reviews Neuroscience* **20**, 746-762 (2019).
28. L. Glin *et al.*, The intermediate stage of sleep in mice. *Physiology & behavior* **50**, 951-953 (1991).
29. M. Steriade, A. Nunez, F. Amzica, A novel slow (< 1 Hz) oscillation of neocortical neurons in vivo: depolarizing and hyperpolarizing components. *Journal of neuroscience* **13**, 3252-3265 (1993).
30. V. V. Vyazovskiy, K. D. Harris, Sleep and the single neuron: the role of global slow oscillations in individual cell rest. *Nature Reviews Neuroscience* **14**, 443-451 (2013).
31. M. Steriade, A. Nunez, F. Amzica, Intracellular analysis of relations between the slow (< 1 Hz) neocortical oscillation and other sleep rhythms of the electroencephalogram. *Journal of Neuroscience* **13**, 3266-3283 (1993).
32. F. David *et al.*, Essential thalamic contribution to slow waves of natural sleep. *Journal of Neuroscience* **33**, 19599-19610 (2013).
33. I. Timofeev, F. Grenier, M. Bazhenov, T. Sejnowski, M. Steriade, Origin of slow cortical oscillations in deafferented cortical slabs. *Cerebral cortex* **10**, 1185-1199 (2000).
34. I. Timofeev, M. Steriade, Low-frequency rhythms in the thalamus of intact-cortex and decorticated cats. *Journal of neurophysiology* **76**, 4152-4168 (1996).

35. T. C. Gent, M. Bandarabadi, C. G. Herrera, A. R. Adamantidis, Thalamic dual control of sleep and wakefulness. *Nature neuroscience* **21**, 974-984 (2018).
36. R. Baker *et al.*, Altered activity in the central medial thalamus precedes changes in the neocortex during transitions into both sleep and propofol anesthesia. *Journal of Neuroscience* **34**, 13326-13335 (2014).
37. M. Lemieux, J.-Y. Chen, P. Lonjers, M. Bazhenov, I. Timofeev, The Impact of Cortical Deafferentation on the Neocortical Slow Oscillation. *The Journal of Neuroscience* **34**, 5689-5703 (2014).
38. C. Capone *et al.*, Slow Waves in Cortical Slices: How Spontaneous Activity is Shaped by Laminar Structure. *Cerebral Cortex* **29**, 319-335 (2017).
39. M. Massimini, R. Huber, F. Ferrarelli, S. Hill, G. Tononi, The sleep slow oscillation as a traveling wave. *Journal of Neuroscience* **24**, 6862-6870 (2004).
40. S. Chauvette, M. Volgushev, I. Timofeev, Origin of active states in local neocortical networks during slow sleep oscillation. *Cerebral cortex* **20**, 2660-2674 (2010).
41. Y. Nir *et al.*, Regional slow waves and spindles in human sleep. *Neuron* **70**, 153-169 (2011).
42. B. A. Riedner, B. K. Hulse, M. J. Murphy, F. Ferrarelli, G. Tononi, Temporal dynamics of cortical sources underlying spontaneous and peripherally evoked slow waves. *Progress in brain research* **193**, 201-218 (2011).
43. S. Sarasso *et al.*, Hippocampal sleep spindles preceding neocortical sleep onset in humans. *Neuroimage* **86**, 425-432 (2014).
44. M. Magnin *et al.*, Thalamic deactivation at sleep onset precedes that of the cerebral cortex in humans. *Proceedings of the National Academy of Sciences* **107**, 3829-3833 (2010).
45. Z. Zhang *et al.*, Neuronal ensembles sufficient for recovery sleep and the sedative actions of α2 adrenergic agonists. *Nature Neuroscience* **18**, 553-561 (2015).
46. C. Anaclet *et al.*, The GABAergic parafacial zone is a medullary slow wave sleep–promoting center. *Nature neuroscience* **17**, 1217-1224 (2014).
47. Y. Oishi *et al.*, Slow-wave sleep is controlled by a subset of nucleus accumbens core neurons in mice. *Nature communications* **8**, 734 (2017).
48. K. Liu *et al.*, Lhx6-positive GABA-releasing neurons of the zona incerta promote sleep. *Nature* **548**, 582-587 (2017).
49. Y. Hayashi *et al.*, Cells of a common developmental origin regulate REM/non-REM sleep and wakefulness in mice. *Science* **350**, 957-961 (2015).
50. R. J. Berger, I. Oswald, Eye movements during active and passive dreams. *Science* **137**, 601-601 (1962).
51. F. Siclari, G. Bernardi, J. Cataldi, G. Tononi, Dreaming in NREM Sleep: A High-Density EEG Study of Slow Waves and Spindles. *The Journal of Neuroscience* **38**, 9175-9185 (2018).
52. M. Solms, Dreaming and REM sleep are controlled by different brain mechanisms. *Behavioral and Brain Sciences* **23**, 843-850 (2000).
53. S. M. Montgomery, A. Sirota, G. Buzsáki, Theta and gamma coordination of hippocampal networks during waking and rapid eye movement sleep. *Journal of Neuroscience* **28**, 6731-6741 (2008).
54. J. L. Cantero *et al.*, Sleep-dependent θ oscillations in the human hippocampus and neocortex. *Journal of Neuroscience* **23**, 10897-10903 (2003).
55. Z. Clemens *et al.*, Phase coupling between rhythmic slow activity and gamma characterizes mesiotemporal rapid-eye-movement sleep in humans. *Neuroscience* **163**, 388-396 (2009).
56. J. Courtin *et al.*, Prefrontal parvalbumin interneurons shape neuronal activity to drive fear expression. *Nature* **505**, 92-96 (2014).
57. D. Popa, S. Duvarci, A. T. Popescu, C. Léna, D. Paré, Coherent amygdalocortical theta promotes fear memory consolidation during paradoxical sleep. *Proceedings of the National Academy of Sciences* **107**, 6516-6519 (2010).
58. T. Andrillon, Y. Nir, C. Cirelli, G. Tononi, I. Fried, Single-neuron activity and eye movements during human REM sleep and awake vision. *Nature communications* **6**, 7884 (2015).

59. L. L. Colgin, Rhythms of the hippocampal network. *Nature Reviews Neuroscience* **17**, 239-249 (2016).
60. M. Vandecasteele *et al.*, Optogenetic activation of septal cholinergic neurons suppresses sharp wave ripples and enhances theta oscillations in the hippocampus. *Proceedings of the National Academy of Sciences* **111**, 13535-13540 (2014).
61. J. Robinson *et al.*, Optogenetic activation of septal glutamatergic neurons drive hippocampal theta rhythms. *Journal of Neuroscience* **36**, 3016-3023 (2016).
62. S. Datta, Cellular basis of pontine ponto-geniculo-occipital wave generation and modulation. *Cellular and molecular neurobiology* **17**, 341-365 (1997).
63. S. Datta, D. F. Siwek, E. H. Patterson, P. B. Cipolloni, Localization of pontine PGO wave generation sites and their anatomical projections in the rat. *Synapse* **30**, 409-423 (1998).
64. G. Vanni-Mercier, G. Debilly, A key role for the caudoventral pontine tegmentum in the simultaneous generation of eye saccades in bursts and associated ponto-geniculo-occipital waves during paradoxical sleep in the cat. *Neuroscience* **86**, 571-585 (1998).
65. A. Karashima, N. Katayama, M. Nakao, Enhancement of synchronization between hippocampal and amygdala theta waves associated with pontine wave density. *Journal of neurophysiology* **103**, 2318-2325 (2010).
66. H. H. Jasper, H. L. Andrews, Brain potentials and voluntary muscle activity in man. *Journal of Neurophysiology* **1**, 87-100 (1938).
67. G. Buzsáki, X.-J. Wang, Mechanisms of gamma oscillations. *Annual review of neuroscience* **35**, 203-225 (2012).
68. P. L. Madsen, S. Vorstrup, Cerebral blood flow and metabolism during sleep. *Cerebrovascular and brain metabolism reviews* **3**, 281-296 (1991).
69. C. Kaufmann *et al.*, Brain activation and hypothalamic functional connectivity during human non-rapid eye movement sleep: an EEG/fMRI study. *Brain* **129**, 655-667 (2006).
70. N. N. Aalling, M. Nedergaard, M. DiNuzzo, Cerebral Metabolic Changes During Sleep. *Curr Neurol Neurosci Rep* **18**, 57 (2018).
71. L. Xie *et al.*, Sleep drives metabolite clearance from the adult brain. *Science* **342**, 373-377 (2013).
72. A. K. Bourdon *et al.*, Metabolomic analysis of mouse prefrontal cortex reveals upregulated analytes during wakefulness compared to sleep. *Scientific Reports* **8**, 11225 (2018).
73. B. Sancristóbal, B. Rebollo, P. Boada, M. V. Sanchez-Vives, J. Garcia-Ojalvo, Collective stochastic coherence in recurrent neuronal networks. *Nature Physics* **12**, 881-887 (2016).
74. F. Fröhlich, M. Bazhenov, I. Timofeev, M. Steriade, T. J. Sejnowski, Slow state transitions of sustained neural oscillations by activity-dependent modulation of intrinsic excitability. *Journal of Neuroscience* **26**, 6153-6162 (2006).
75. J. van der Meij, D. Martinez-Gonzalez, G. J. L. Beckers, N. C. Rattenborg, Intra-"cortical" activity during avian non-REM and REM sleep: variant and invariant traits between birds and mammals. *Sleep* **42**, zsy230 (2019).
76. J. A. Lesku, A. L. Vyssotski, D. Martinez-Gonzalez, C. Wilzeck, N. C. Rattenborg, Local sleep homeostasis in the avian brain: convergence of sleep function in mammals and birds? *Proceedings of the Royal Society B: Biological Sciences* **278**, 2419-2428 (2011).
77. P. S. Low, S. S. Shank, T. J. Sejnowski, D. Margoliash, Mammalian-like features of sleep structure in zebra finches. *Proceedings of the National Academy of Sciences* **105**, 9081-9086 (2008).
78. S. V. Canavan, D. Margoliash, Budgerigars have complex sleep structure similar to that of mammals. *PLoS biology* **18**, e3000929 (2020).
79. L. Medina, A. Reiner, Do birds possess homologues of mammalian primary visual, somatosensory and motor cortices? *Trends in neurosciences* **23**, 1-12 (2000).
80. E. D. Jarvis *et al.*, Avian brains and a new understanding of vertebrate brain evolution. *Nature Reviews Neuroscience* **6**, 151-159 (2005).
81. J. Rose, The avian brain. *Current Biology* **32**, R1076-R1079 (2022).
82. L. Puelles *et al.* (2017) Evolution of nervous systems. (Amsterdam: Elsevier).

83. R. G. Northcutt, J. H. Kaas, The emergence and evolution of mammalian neocortex. *Trends in neurosciences* **18**, 373-379 (1995).
84. A. Reiner *et al.*, Revised nomenclature for avian telencephalon and some related brainstem nuclei. *Journal of Comparative Neurology* **473**, 377-414 (2004).
85. C. Mulert, L. Lemieux, *EEG-fMRI: physiological basis, technique, and applications* (Springer Nature, 2023).
86. S. Olkowicz *et al.*, Birds have primate-like numbers of neurons in the forebrain. *Proceedings of the National Academy of Sciences* **113**, 7255-7260 (2016).
87. H. J. Karten, W. Hodos, *A stereotaxic atlas of the brain of the pigeon:(Columba Livia)* (Johns Hopkins Press Baltimore, 1967), vol. 696.
88. M. Stacho *et al.*, A cortex-like canonical circuit in the avian forebrain. *Science* **369**, eabc5534 (2020).
89. E. D. Jarvis, "Evolution of the Pallium in Birds and Reptiles" in Encyclopedia of Neuroscience, M. D. Binder, N. Hirokawa, U. Windhorst, Eds. (Springer Berlin Heidelberg, Berlin, Heidelberg, 2009), 10.1007/978-3-540-29678-2_3165, pp. 1390-1400.
90. A. Reiner, E. Stern, C. Wilson, Physiology and morphology of intratelencephalically projecting corticostriatal-type neurons in pigeons as revealed by intracellular recording and cell filling. *Brain behavior and evolution* **58**, 101-114 (2001).
91. G. J. Beckers, J. van der Meij, J. A. Lesku, N. C. Rattenborg, Plumes of neuronal activity propagate in three dimensions through the nuclear avian brain. *BMc Biology* **12**, 1-11 (2014).
92. J. Szymczak, W. Kaiser, H. Helb, B. Beszczyńska, A study of sleep in the European blackbird. *Physiology & behavior* **60**, 1115-1120 (1996).
93. I. Tobler, A. A. Borbély, Sleep and EEG spectra in the pigeon (Columba livia) under baseline conditions and after sleep deprivation. *Journal of comparative Physiology A* **163**, 729-738 (1988).
94. D. MARTINEZ-GONZALEZ, J. A. Lesku, N. C. Rattenborg, Increased EEG spectral power density during sleep following short-term sleep deprivation in pigeons (Columba livia): evidence for avian sleep homeostasis. *Journal of Sleep Research* **17**, 140-153 (2008).
95. C. M. Constantinople, R. M. Bruno, Deep Cortical Layers Are Activated Directly by Thalamus. *Science* **340**, 1591-1594 (2013).
96. J. van der Meij, D. Martinez-Gonzalez, G. J. L. Beckers, N. C. Rattenborg, Intra-"cortical" activity during avian non-REM and REM sleep: variant and invariant traits between birds and mammals. *Sleep* **42** (2018).
97. C. H. Vanderwolf, Hippocampal electrical activity and voluntary movement in the rat. *Electroencephalography and clinical neurophysiology* **26**, 407-418 (1969).
98. G. Buzsáki, Hippocampal sharp wave-ripple: A cognitive biomarker for episodic memory and planning. *Hippocampus* **25**, 1073-1188 (2015).
99. H. L. Payne, G. F. Lynch, D. Aronov, Neural representations of space in the hippocampus of a food-caching bird. *Science* **373**, 343-348 (2021).
100. H. Yeganegi, H. Luksch, J. M. Ondracek, Hippocampal-like network dynamics underlie avian sharp wave-ripples. *bioRxiv*, 825075 (2019).
101. C. Montagnese, J. Krebs, G. Meyer, The dorsomedial and dorsolateral forebrain of the zebra finch, Taeniopygia guttata: a Golgi study. *Cell and tissue research* **283**, 263-282 (1996).
102. Y. Atoji, J. M. Wild, Anatomy of the avian hippocampal formation. *Reviews in the Neurosciences* **17**, 3-16 (2006).
103. T. Tömböl, D. Davies, A. Németh, T. Sebestény, A. Alpár, A comparative Golgi study of chicken (Gallus domesticus) and homing pigeon (Columba livia) hippocampus. *Anatomy and Embryology* **201**, 85-101 (2000).
104. D. Saucier, L. Astic, Polygraphic study of sleep in young chickens at hatching, evolution at third and fourth days. *Electroencephalography and Clinical Neurophysiology* **38**, 303-306 (1975).
105. J. A. Lesku *et al.*, Ostriches sleep like platypuses. *PloS one* **6**, e23203 (2011).

106. H. C. Heller, R. Graf, W. Rautenberg, Circadian and arousal state influences on thermoregulation in the pigeon. *American Journal of Physiology-Regulatory, Integrative and Comparative Physiology* **245**, R321-R328 (1983).
107. J.-E. Kang *et al.*, Amyloid-β Dynamics Are Regulated by Orexin and the Sleep-Wake Cycle. *Science* **326**, 1005-1007 (2009).
108. N. E. Fultz *et al.*, Coupled electrophysiological, hemodynamic, and cerebrospinal fluid oscillations in human sleep. *Science* **366**, 628-631 (2019).
109. G. Ungurean *et al.*, Wide-spread brain activation and reduced CSF flow during avian REM sleep. *Nature Communications* **14**, 3259 (2023).
110. N. C. Rattenborg *et al.*, Evidence that birds sleep in mid-flight. *Nature communications* **7**, 12468 (2016).
111. J. A. Lesku *et al.*, Adaptive sleep loss in polygynous pectoral sandpipers. *Science* **337**, 1654-1658 (2012).
112. M. G. Frank, H. C. Heller, The ontogeny of mammalian sleep: a reappraisal of alternative hypotheses. *Journal of sleep research* **12**, 25-34 (2003).
113. G. W. Vogel, P. Feng, G. G. Kinney, Ontogeny of REM sleep in rats: possible implications for endogenous depression. *Physiology & Behavior* **68**, 453-461 (2000).
114. G. A. Marks, J. P. Shaffery, A preliminary study of sleep in the ferret, Mustela putorius furo: a carnivore with an extremely high proportion of REM sleep. *Sleep* **19**, 83-93 (1996).
115. S. K. Jha, T. Coleman, M. G. Frank, Sleep and sleep regulation in the ferret (Mustela putorius furo). *Behavioural Brain Research* **172**, 106-113 (2006).
116. J. T. Szymczak, Distribution of sleep and wakefulness in 24-h light-dark cycles in the juvenile and adult magpie, Pica pica. *Chronobiologia* **14**, 277-287 (1987).
117. M. F. Scriba *et al.*, Linking melanism to brain development: expression of a melanism-related gene in barn owl feather follicles covaries with sleep ontogeny. *Frontiers in Zoology* **10**, 1-12 (2013).
118. M. E. Miletto Petrazzini, V. A. Sovrano, G. Vallortigara, A. Messina, Brain and Behavioral Asymmetry: A Lesson From Fish. *Frontiers in Neuroanatomy* **14** (2020).
119. I. C. McManus, *Handedness, cerebral lateralization, and the evolution of language* (Oxford University Press, 1999).
120. E. Drouin, Y. Péréon, Dax versus Broca. *The Lancet Neurology* **18**, 920 (2019).
121. F. Nottebohm, Neural lateralization of vocal control in a passerine bird. I. Song. *Journal of Experimental Zoology* **177**, 229-261 (1971).
122. F. Nottebohm, M. E. Nottebohm, Left hypoglossal dominance in the control of canary and white-crowned sparrow song. *Journal of Comparative Physiology* **108**, 171-192 (1976).
123. I. George, E. Hara, N. A. Hessler, Behavioral and neural lateralization of vision in courtship singing of the zebra finch. *Journal of neurobiology* **66**, 1164-1173 (2006).
124. R. Suthers, F. Goller, C. Pytte, The neuromuscular control of birdsong. *Philosophical Transactions of the Royal Society of London. Series B: Biological Sciences* **354**, 927-939 (1999).
125. D. Margoliash, Functional organization of forebrain pathways for song production and perception. *Journal of neurobiology* **33**, 671-693 (1997).
126. F. Nottebohm, T. M. Stokes, C. M. Leonard, Central control of song in the canary, Serinus canarius. *Journal of Comparative Neurology* **165**, 457-486 (1976).
127. J. Cynx, H. Williams, F. Nottebohm, Hemispheric differences in avian song discrimination. *Proceedings of the National Academy of Sciences* **89**, 1372-1375 (1992).
128. K. Okanoya, M. Ikebuchi, H. Uno, S. Watanabe, Left-side dominance for song discrimination in Bengalese finches (Lonchura striata var. domestica). *Animal cognition* **4**, 241-245 (2001).
129. Y. Orsher *et al.* (2023) Travelling waves or sequentially activated discrete modules: mapping the granularity of cortical propagation. (eLife Sciences Publications, Ltd).
130. E. Damaraju *et al.*, Functional connectivity in the developing brain: A longitudinal study from 4 to 9months of age. *NeuroImage* **84**, 169-180 (2014).

131. C. Kelly, F. X. Castellanos, Strengthening Connections: Functional Connectivity and Brain Plasticity. *Neuropsychology Review* **24**, 63-76 (2014).
132. K. Keunen, S. J. Counsell, M. J. N. L. Benders, The emergence of functional architecture during early brain development. *NeuroImage* **160**, 2-14 (2017).
133. H. Jasper, The 10-20 electrode system of the International Federation. *Electroencephalogr Clin Neuropysiol* **10**, 370-375 (1958).
134. M. Schabus *et al.*, Sleep spindle-related activity in the human EEG and its relation to general cognitive and learning abilities. *European Journal of Neuroscience* **23**, 1738-1746 (2006).
135. L. Marshall, H. Helgadóttir, M. Mölle, J. Born, Boosting slow oscillations during sleep potentiates memory. *Nature* **444**, 610-613 (2006).
136. B. P. Staresina, J. Niediek, V. Borger, R. Surges, F. Mormann, How coupled slow oscillations, spindles and ripples coordinate neuronal processing and communication during human sleep. *Nature Neuroscience* **26**, 1429-1437 (2023).
137. C. Roy, D. Joram van, B. Marieke de, M. T. Lucia, Slow Oscillations during Sleep Coordinate Interregional Communication in Cortical Networks. *The Journal of Neuroscience* **34**, 16890 (2014).
138. M. Massimini *et al.*, Breakdown of cortical effective connectivity during sleep. *Science* **309**, 2228-2232 (2005).
139. F. Ferrarelli *et al.*, Breakdown in cortical effective connectivity during midazolam-induced loss of consciousness. *Proceedings of the National Academy of Sciences* **107**, 2681-2686 (2010).
140. G. Vallortigara, R. Andrew, Lateralization of response by chicks to change in a model partner. *Animal Behaviour* **41**, 187-194 (1991).
141. J. Levy, The mammalian brain and the adaptive advantage of cerebral asymmetry. *Annals of the New York Academy of Sciences* **299**, 264-272 (1977).
142. L. J. Rogers, Evolution of side biases: Motor versus sensory lateralization. *Side bias: A neuropsychological perspective*, 3-40 (2000).
143. L. J. Rogers, Asymmetry of brain and behavior in animals: Its development, function, and human relevance. *genesis* **52**, 555-571 (2014).
144. M. Dadda, A. Bisazza, Does brain asymmetry allow efficient performance of simultaneous tasks? *Animal Behaviour* **72**, 523-529 (2006).
145. L. J. Rogers, P. Zucca, G. Vallortigara, Advantages of having a lateralized brain. *Proceedings of the Royal Society of London. Series B: Biological Sciences* **271**, S420-S422 (2004).
146. A.-L. Bibost, C. Brown, Laterality influences schooling position in rainbowfish, Melanotaenia spp. *PLoS One* **8**, e80907 (2013).
147. K. Hugdahl, L. Anderson, A Dichotic Listening Study of Differences in Cerebral Organization in Dextral and Sinistral Subjects. *Cortex* **20**, 135-141 (1984).
148. K. Hugdahl, Lateralization of cognitive processes in the brain. *Acta Psychologica* **105**, 211-235 (2000).
149. M. Hirnstein, K. Hugdahl, M. Hausmann, How brain asymmetry relates to performance–a large-scale dichotic listening study. *Frontiers in psychology* **4**, 997 (2014).
150. D. Ulrich, Sleep Spindles as Facilitators of Memory Formation and Learning. *Neural Plasticity* **2016**, 1796715 (2016).
151. C.-F. V. Latchoumane, H.-V. V. Ngo, J. Born, H.-S. Shin, Thalamic spindles promote memory formation during sleep through triple phase-locking of cortical, thalamic, and hippocampal rhythms. *Neuron* **95**, 424-435. e426 (2017).
152. L. N. Wüst *et al.*, Interrelations between delta waves, spindles and slow oscillations in human NREM sleep and their functional role in memory. *bioRxiv*, 2021.2009. 2003.458607 (2021).
153. B. P. Staresina *et al.*, Hierarchical nesting of slow oscillations, spindles and ripples in the human hippocampus during sleep. *Nature neuroscience* **18**, 1679-1686 (2015).
154. A. G. Siapas, M. A. Wilson, Coordinated interactions between hippocampal ripples and cortical spindles during slow-wave sleep. *Neuron* **21**, 1123-1128 (1998).
155. N. Maingret, G. Girardeau, R. Todorova, M. Goutierre, M. Zugaro, Hippocampo-cortical coupling mediates memory consolidation during sleep. *Nature neuroscience* **19**, 959-964 (2016).

156. S. Ruch *et al.*, Sleep stage II contributes to the consolidation of declarative memories. *Neuropsychologia* **50**, 2389-2396 (2012).
157. M. P. Walker, The role of slow wave sleep in memory processing. *Journal of Clinical Sleep Medicine* **5**, S20-S26 (2009).
158. M. Navarrete, M. Valderrama, P. A. Lewis, The role of slow-wave sleep rhythms in the cortical-hippocampal loop for memory consolidation. *Current Opinion in Behavioral Sciences* **32**, 102-110 (2020).
159. F. Ferrarelli *et al.*, An increase in sleep slow waves predicts better working memory performance in healthy individuals. *Neuroimage* **191**, 1-9 (2019).
160. V. Hinard *et al.*, Key Electrophysiological, Molecular, and Metabolic Signatures of Sleep and Wakefulness Revealed in Primary Cortical Cultures. *The Journal of Neuroscience* **32**, 12506-12517 (2012).
161. I. Colombi, F. Tinarelli, V. Pasquale, V. Tucci, M. Chiappalone, A Simplified In vitro Experimental Model Encompasses the Essential Features of Sleep. *Frontiers in Neuroscience* **10** (2016).
162. S. Deurveilher, K. Semba, Basal forebrain regulation of cortical activity and sleep-wake states: Roles of cholinergic and non-cholinergic neurons. *Sleep and Biological Rhythms* **9**, 65-70 (2011).
163. G. Girardeau, V. Lopes-dos-Santos, Brain neural patterns and the memory function of sleep. *Science* **374**, 560-564 (2021).
164. N. C. Rattenborg, J. Van der Meij, G. J. Beckers, J. A. Lesku, Local aspects of avian non-REM and REM sleep. *Frontiers in Neuroscience* **13**, 567 (2019).
165. J. M. Krueger, J. T. Nguyen, C. J. Dykstra-Aiello, P. Taishi, Local sleep. *Sleep Medicine Reviews* **43**, 14-21 (2019).
166. M. S. Blumberg, J. A. Lesku, P.-A. Libourel, M. H. Schmidt, N. C. Rattenborg, What Is REM Sleep? *Current Biology* **30**, R38-R49 (2020).
167. H. Norimoto *et al.*, A claustrum in reptiles and its role in slow-wave sleep. *Nature* **578**, 413-418 (2020).
168. J. Cabral, M. L. Kringelbach, G. Deco, Functional connectivity dynamically evolves on multiple time-scales over a static structural connectome: Models and mechanisms. *NeuroImage* **160**, 84-96 (2017).
169. J. A. Roberts *et al.*, Metastable brain waves. *Nature Communications* **10**, 1056 (2019).
170. J. Cabral *et al.*, Metastable oscillatory modes emerge from synchronization in the brain spacetime connectome. *Communications Physics* **5**, 184 (2022).
171. G. Deco, M. L. Kringelbach, Turbulent-like Dynamics in the Human Brain. *Cell Reports* **33** (2020).
172. R. Kato, H. Ishii, Cluster Synchronization of Kuramoto Oscillators and Brain Functional Connectivity. *arXiv e-prints*, arXiv: 2204.02627 (2022).
173. P.-A. Libourel *et al.*, Partial homologies between sleep states in lizards, mammals, and birds suggest a complex evolution of sleep states in amniotes. *PLOS Biology* **16**, e2005982 (2018).
174. M. G. Frank, R. H. Waldrop, M. Dumoulin, S. Aton, J. G. Boal, A preliminary analysis of sleep-like states in the cuttlefish Sepia officinalis. *PLoS One* **7**, e38125 (2012).
175. D. V. Meisel, R. A. Byrne, J. Mather, M. Kuba, Behavioral sleep in Octopus vulgaris. *Vie et Milieu* **61**, 185-190 (2011).
176. E. R. Brown, S. Piscopo, R. De Stefano, A. Giuditta, Brain and behavioural evidence for rest-activity cycles in Octopus vulgaris. *Behavioural brain research* **172**, 355-359 (2006).
177. S. d. S. Medeiros *et al.*, Cyclic alternation of quiet and active sleep states in the octopus. iScience 24. *102223, doi: 10.1016/j. isci* (2021).
178. D. C. Rößler *et al.*, Regularly occurring bouts of retinal movements suggest an REM sleep–like state in jumping spiders. *Proceedings of the National Academy of Sciences* **119**, e2204754119 (2022).
179. J. J. Vitti, Cephalopod Cognition in an Evolutionary Context: Implications for Ethology. *Biosemiotics* **6**, 393-401 (2013).

180. M. Shamir, Y. Bar-On, R. Phillips, R. Milo, SnapShot: timescales in cell biology. *Cell* **164**, 1302-1302. e1301 (2016).
181. D. R. Samson, C. L. Nunn, Sleep intensity and the evolution of human cognition. *Evolutionary Anthropology: Issues, News, and Reviews* **24**, 225-237 (2015).
182. C. L. Nunn, D. R. Samson, Sleep in a comparative context: investigating how human sleep differs from sleep in other primates. *American Journal of Physical Anthropology* **166**, 601-612 (2018).

# Acknowledgments

Janie took a significant risk in selecting me as her first Ph.D. student. It already took me almost six months to join the lab waiting for the bureaucratic procedures for coming to Germany. Throughout my Ph.D., we encountered both highs and lows, but Janie showed remarkable patience in dealing with all my naiveties. Janie, I extend my heartfelt gratitude to you for your patience and unwavering support. Clearly, you did an outstanding job convincing an engineer graduate to remain in science post-Ph.D.!

Ph.D. is a challenging journey! In my case, it transformed into a pleasurable experience thanks to my supportive and caring colleagues. I express my gratitude to Harald for his availability and immediate support, even amidst his hectic schedule. I want to thank my lab mates for fostering a joyful work environment. Special thanks to Lejla for her companionship and the leisurely 'coffee breaks'! Gianmarco, Francisco, Jan, and Ali, you're not just lab mates; you're excellent friends. From the moment I stepped into the lab, Birgit cared for me, earning a special place in my heart.

A significant part of my Ph.D. coincided with the Corona pandemic. At home, I had the honor of living with Ale, Luisa, and Claudia—fantastic people who became my cherished friends.

I extend my gratitude to my other TAC members, Prof. Jan Born, Dr. Daniela Vallentin, and Prof. Christian Leibold, for their availability and support. Their inspiration was truly uplifting. I also thank Dr. Thomas Fenzl, Dr. Mark Shein-Idelson, Dr. Nicolas Giret, and Prof. Anton Sirota for generously investing their time in providing feedback on my work. I am particularly thankful to Dr. Matthias Kreuzer and Dr. Lisa Fenk, who hired me directly after I left the Ph.D. lab.

I also wish to express my appreciation to everyone contributing to the GSN program. GSN played a pivotal role in my professional progress in neuroscience. Given my non-neuroscientific educational background, without the learning opportunities provided by GSN, envisioning myself as a neuroscientist by the end of my Ph.D. would have been impossible. It's hard to forget that I initially failed 'Fundamentals in Neuroscience I,' and later, worked as a neuroscience researcher at the Max Planck Institute!

Lastly, I want to thank my parents for instilling a passion for science in me since my childhood. I vividly recall my father holding my hand to buy new books as a present at the end of the school semesters and my mother, dramatically threatening to stop my schooling if I didn't achieve straight As! While not recommended, it worked in my case!

Lastly, this thesis is not my individual work. Science is a collaborative human endeavor. I want to acknowledge all the people whose work has been the ground for this thesis.

# List of publications

**Local sleep in songbirds: Different simultaneous sleep states across the avian pallium**

H Yeganegi, JM Ondracek, Journal of Sleep Research, e14344,2023

**Multi-channel recordings reveal age-related differences in the sleep of juvenile and adult zebra finches**

H Yeganegi, JM Ondracek, Scientific Reports 13 (1), 8607

# Author Contributions

**Study 1:** 'Multi-channel recordings reveal age-related differences in the sleep of juvenile and adult zebra finches'

Hamed Yeganegi and Janie M. Ondracek

Conceptualization, Janie M. Ondracek.; Methodology, Janie M. Ondracek. and Hamed Yeganegi; Software: Hamed Yeganegi and Janie M. Ondracek.; Validation, Janie M. Ondracek.; Formal Analysis, Hamed Yeganegi; Investigation, Hamed Yeganegi; Writing – Original Draft, Hamed Yeganegi; Writing – Review & Editing, Janie M. Ondracek; Funding Acquisition, Janie M. Ondracek; Resources, Janie M. Ondracek; Visualization, Hamed Yeganegi and Janie M. Ondracek; Supervision, Janie M. Ondracek; Project Administration, Janie M. Ondracek

**My contributions in detail**

I performed the animal surgeries and collected the electrophysiology data. I analyzed the data and created the initial figures. Final figures were created together with Janie Michelle Ondracek. I wrote the first draft, and worked together with Janie Michelle Ondracek on the reviewer comments from the publishing journal.

**Study 2:** 'Local sleep in songbirds: Different simultaneous sleep states across the avian pallium'

Hamed Yeganegi and Janie M. Ondracek

Hamed Yeganegi conducted the experiments, analyzed and visualized the data and wrote the initial draft. Janie M. Ondracek conceptualized and designed the experiments, secured the funding, supervised the project, assisted with data interpretation, and revised the initial draft.

**My contributions in detail**

I performed the animal surgeries and conducted the electrophysiology and sound recordings. I analyzed the data and created the initial figures. Final figures were created together with Janie Michelle Ondracek. I wrote the first draft.

# Affidavit

I hereby confirm that the dissertation "Avian Sleep: Examining Age-Related Variations and Local Sleep in Zebra Finches" is the result of my own work and that I have only used sources or materials listed and specified in the dissertation.

Hamed Yeganegi

02.10.2024

Munich

# CV

## Education

**Ph.D. Systems Neuroscience (2019-2024)**
Graduate School of Systemic Neurosciences (GSN), LMU, Munich, Germany
(conducted at Chair of Zoology, Technical University of Munich, Freising, Germany)
Thesis title: "Sleep and memory consolidation in songbirds"
Supervisors: Dr. Janie M. Ondracek, TUM

**M.Sc. Biomedical Engineering (2014-2017)**

Department of Electrical Engineering, Iran University of Science and Technology, Tehran, Iran
Thesis title: "Decoding hind limb position using spinal extracellular recordings in cat"
Supervisor: Prof. A. Erfanian, Iran Neural Technology Center

**B.Sc. Electrical Engineering (2010-2014)**

Department of Engineering, Shahrekord University, Shahrekord, Iran Thesis title: "Design and implementation of a USB data acquisition system using a PIC microcontroller"
Supervisor: Dr. G. R. Arab Markadeh

## Research Skills

**Laboratory:** animal handling, anesthesia, and surgical protocols, histology staining, extracellular recording (single-unit, LFP, EEG), in rodents, feline, small birds, and fruit flies, Human EEG

**Programming:** MATLAB and relevant data processing toolboxes (advanced)
Python, R, LabVIEW, Java, C family languages, Linux scripting (understanding)

**Analytical:** Advanced signal processing: time-frequency analysis, information theory, machine learning, nonlinear methods

## Job Experiences

### Professions

- Post-doctoral researcher, Max Planck Institute for Biological Intelligence, Active Sensing Group of Dr. Lisa Fenk (June 2023-June 2024)
- Research assistant, Klinikum rechts der Isar, Technical University of Munich, Clinic for Anesthesiology, Neuromonitoring group of Dr. Matthias Kreuzer (Oct 2022-June 2023)
- Scientific Representor, ScinceBeam Co., Tehran, Iran (2017-2018)

### Teaching Experience

Teacher assistant of three courses: Electromagnetics, Computer Architecture, Signals and Systems – Shahrekord University, Shahrekord, Iran

Teacher assistant for Neuroscience of Vision, Chair of Zoology, Technical University of Munich, Summer 2019

## Publications

Lorenz, C., Das, A., Centeno, E. G. Z., Yeganegi, .... (2024). Neural population dynamics during sleep in a songbird vocal circuit resemble sharp wave ripple activity. *bioRxiv*, 2024-09.

Yeganegi, H., & Ondracek, J. M. (2023). Local sleep in songbirds: Different simultaneous sleep states across the avian pallium. Journal of Sleep Research, e14344.

Yeganegi, H., & Ondracek, J. M. (2023). Multi-channel recordings reveal age-related differences in the sleep of juvenile and adult zebra finches. Scientific Reports, 13(1), 8607.

M. Shiri, H. Behnam, H. Yeganegi, Z. A. Sani, & N. Nematollahi (2022). Trackable-speckle detection using a dual-path convolutional neural network, accepted to be published in *Asian Journal Of Medical Technology*

Ondracek, J. M., Yeganegi, H., & Luksch, H. (2020). Hippocampal-like network dynamics underlie avian sharp wave-ripples. *bioRxiv*.

Yeganegi, H., Salami, P., & Daliri, M. R. (2020). A Template-Based Sequential Algorithm for Online Clustering of Spikes in Extracellular Recordings. *Cognitive Computation*, 1-11.

Sharifian, F. E., Bahrami, F., Yeganegi, H., & Afra, M. G. (2020). Alteration in REM sleep and sleep spindles' characteristics by a model of immobilization stress in rat. *Sleep and Biological Rhythms*.

Yeganegi, H., Fathi, Y., & Erfanian, A. (2018). Decoding hind limb kinematics from neuronal activity of the dorsal horn neurons using multiple level learning algorithm. *Scientific Reports*, *8*(1), 1-12.

## Conferences (Poster Presentation)

Hamed Yeganegi, Janie Ondracek, Local sleep in songbirds: Different simultaneous sleep stages in zebra finches, 15th International Congress of Neuroethology, Berlin, Jul. 28 - Aug. 2, Berlin

Hamed Yeganegi and Lisa Fenk, Unraveling the dynamics of eye movements during sleep in fruit fly: a research proposal, Scientific retreat of Bernstein Center for Computational Neuroscience, Tutzing, Germany, 29-30 June. 2023

Hamed Yeganegi and Janie M. Ondracek, Ontological changes in neural signature of sleep in an avian brain, Algarve, Portugal, 3-5 May 2023

Hamed Yeganegi and Janie M. Ondracek, Mammalian-like developmental changes are present in the neural signatures of avian sleep, 114th Annual Meeting of the German Zoological Society, Bonn, Germany, 13-16 Sept. 2022

Hamed Yeganegi and Janie M. Ondracek, Sleep structure in juvenile and adult zebra finches: broad differences in EEG oscillations and functional connectivity, FENS Forum 2022, Paris, France, 9-13 Jul. 2022

Hamed Yeganegi and Janie M. Ondracek, Compartmentalization of brain activity during sleep in an avian brain, 113th Annual Meeting of the German Zoological Society, online conference, 30 Aug.-03 Sep. 2021

Hamed Yeganegi, Janie M. Ondracek, Compartmentalization of brain activity during sleep in zebra finches, German Neuroscience Society, Goettingen, Germany, March 22, 2021

Hamed Yeganegi, Detection of Sharp Wave ripples in an avian brain, Neuro DoWo 2019, Wuerzburg, Germany, 28-31th Aug. 2019

Shiri, M., Gifani, P., Behnam, H., Sani, Z. A., Yeganegi, H., & Shojaeifard, M. (2019, April). A Color-Encoded Map to Facilitate the Identification of Abnormal Segments of the Left Ventricle by Novice Examiners. In *2019 27th Iranian Conference on Electrical Engineering (ICEE)* (pp. 1737-1741). IEEE.

Hamed Yeganegi, Milad Shiri, Mohammad Norizadeh Cherloo, A fast 3D segmentation of brain MRI using a modified fuzzy c-means clustering algorithm, ISBM2018, Tehran, Iran, 10-11th Oct. 2018

# Permission form Publishers regarding the cited illustrations

## Fig. 1

The figure is adapted from the following article:

*A. P. Vorster, J. Born, Sleep and memory in mammals, birds and invertebrates. Neuroscience & Biobehavioral Reviews 50, 103-119 (2015).*

As seen below, any adaptation of the content from this journal, for non-commercial purposes, such as its use in this thesis, is permitted.

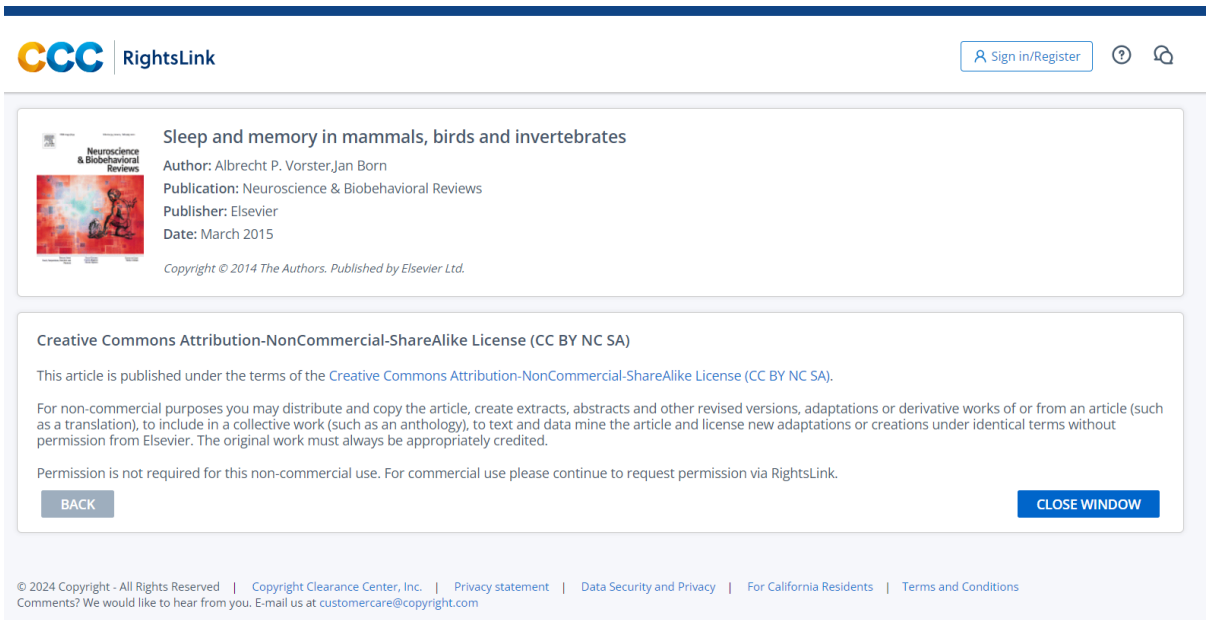

CCC RightsLink

Sign in/Register

Sleep and memory in mammals, birds and invertebrates

**Author:** Albrecht P. Vorster,Jan Born

**Publication:** Neuroscience & Biobehavioral Reviews

**Publisher:** Elsevier

**Date:** March 2015

*Copyright © 2014 The Authors. Published by Elsevier Ltd.*

Creative Commons Attribution-NonCommercial-ShareAlike License (CC BY NC SA)

This article is published under the terms of the Creative Commons Attribution-NonCommercial-ShareAlike License (CC BY NC SA).

For non-commercial purposes you may distribute and copy the article, create extracts, abstracts and other revised versions, adaptations or derivative works of or from an article (such as a translation), to include in a collective work (such as an anthology), to text and data mine the article and license new adaptations or creations under identical terms without permission from Elsevier. The original work must always be appropriately credited.

Permission is not required for this non-commercial use. For commercial use please continue to request permission via RightsLink.

BACK

CLOSE WINDOW

© 2024 Copyright - All Rights Reserved | Copyright Clearance Center, Inc. | Privacy statement | Data Security and Privacy | For California Residents | Terms and Conditions

Comments? We would like to hear from you. E-mail us at customercare@copyright.com

## Fig. 2

The figure is adapted from the following article:
*E. D. Jarvis, "Evolution of the Pallium in Birds and Reptiles" in Encyclopedia of Neuroscience, M. D. Binder, N. Hirokawa, U. Windhorst, Eds. (Springer Berlin Heidelberg, Berlin, Heidelberg, 2009), 10.1007/978-3-540-29678-2_3165, pp. 1390-1400.*
Permission was acquired as presented as seen below.

9/19/24, 12:08 PM RightsLink Printable License

SPRINGER NATURE LICENSE
TERMS AND CONDITIONS

Sep 19, 2024

---

This Agreement between Hamed Yeganegi ("You") and Springer Nature ("Springer Nature") consists of your license details and the terms and conditions provided by Springer Nature and Copyright Clearance Center.

| | |
|---|---|
| License Number | 5872430248314 |
| License date | Sep 19, 2024 |
| Licensed Content Publisher | Springer Nature |
| Licensed Content Publication | Springer eBook |
| Licensed Content Title | Evolution of the Pallium in Birds and Reptiles |
| Licensed Content Author | Erich D. Jarvis |
| Licensed Content Date | Jan 1, 2009 |
| Type of Use | Thesis/Dissertation |
| Requestor type | academic/university or research institute |
| Format | electronic |
| Portion | figures/tables/illustrations |
| Number of figures/tables/illustrations | 1 |

## Fig. 3

The figure is adapted from the following article:

*F. Nottebohm, Neural lateralization of vocal control in a passerine bird. I. Song. Journal of Experimental Zoology 177, 229-261 (1971).*

Permission was acquired as presented as seen below.

9/19/24, 12:18 PM RightsLink Printable License

JOHN WILEY AND SONS LICENSE
TERMS AND CONDITIONS

Sep 19, 2024

---

This Agreement between Hamed Yeganegi ("You") and John Wiley and Sons ("John Wiley and Sons") consists of your license details and the terms and conditions provided by John Wiley and Sons and Copyright Clearance Center.

| | |
|---|---|
| License Number | 5872430908988 |
| License date | Sep 19, 2024 |
| Licensed Content Publisher | John Wiley and Sons |
| Licensed Content Publication | JOURNAL OF EXPERIMENTAL ZOOLOGY PART A: ECOLOGICAL AND INTEGRATIVE PHYSIOLOGY |
| Licensed Content Title | Neural lateralization of vocal control in a passerine bird. I. Song |
| Licensed Content Author | Fernando Nottebohm |
| Licensed Content Date | May 9, 2005 |
| Licensed Content Volume | 177 |
| Licensed Content Issue | 2 |
| Licensed Content Pages | 33 |
| Type of use | Dissertation/Thesis |
| Requestor type | University/Academic |